

Understanding Progression in Primary
Progressive Multiple Sclerosis:
a longitudinal clinical and magnetic
resonance imaging study

Zhaleh Khaleeli

A thesis submitted to University College, London for the degree of

Doctor of Philosophy

February 2009

Department of Brain Repair and Rehabilitation
Institute of Neurology
Queen Square
London WC1N 3BG

Declaration

I, Zhaleh Khaleeli, confirm that the work presented in this thesis is my own. Where information has been derived from other sources, I confirm that this has been indicated in the thesis.

.....

Abstract

The work in this thesis applies magnetization transfer imaging (MTI) and conventional MRI measures (brain volume, T2 lesion load and enhancing lesions) to investigate the mechanisms underlying progression in primary progressive multiple sclerosis (PPMS), and identifies MR markers to predict and monitor progression.

First, we demonstrated that MTI was sensitive to change in the normal appearing brain tissues over one year, and that clinical progression over this period was predicted by baseline normal appearing white matter (NAWM) MT ratio (MTR). However, our second study showed that over three years, grey matter MTR became a better predictor of progression than any other MRI measure. Grey matter MTR and T2 lesion load changes reflected concurrent progression during this study.

To localize the baseline grey matter injury more precisely, we developed a voxel-based technique to identify areas of grey matter MTR reduction and volume loss in patients compared with controls. The regions of grey matter MTR reduction identified correlated with clinical function in anatomically related systems.

Finally, because our studies showed that lesion load influenced progression, we used contrast enhanced T1-weighted imaging to examine active focal inflammation. We found that while lesion activity declined over five years, levels of activity at the start of the study could influence mobility five years later.

The work presented in this thesis suggests that grey matter damage has a predilection for certain brain regions and is an important determinant of progression in early PPMS. In the white matter, changes in lesion volume and activity continue to influence progression, but NAWM injury may have a declining role. MTR is a sensitive and responsive tool for predicting, monitoring, and localizing clinically relevant brain injury in early PPMS.

Acknowledgements

This research was carried out in the Department of Brain Repair and Rehabilitation at the Institute of Neurology, and funded by the MS Society of Great Britain and Northern Ireland. The Department funded my attendance at conferences, and provided a well-equipped, supportive and friendly environment in which to work.

Many thanks to my principal supervisor, Professor Alan Thompson, who ensured I remained motivated and focused, and from whom I have learned a great deal. My second supervisor, Dr Olga Ciccarelli, was closely involved in every aspect of this thesis (as well as my life!) and I would like to thank her for all her kind support and encouragement.

My work would not have been possible without Dr Mara Cercignani, whose tireless enthusiasm for physics compensated for my inexperience. Many thanks to Dr Daniel Altmann, whose vast expertise and extreme patience led me to actually enjoy statistics. Thanks to Dr Gordon Ingle, who initiated this research project, and to Dr Jaume Sastre-Garriga, who passed it on to me, along with useful advice and encouragement. I am very grateful to the radiographers who contributed to this project, and kept both myself and the subjects cheerful during the long imaging protocols: Chris Benton, Ros Gordon, Karyn Chappell, Alaine Berry and Marios Yiannakas. My warmest gratitude is extended to the altruistic patients and controls who spent hours in the scanner in order for this research to be undertaken.

I am indebted to Drs Benedetta Bodini, Tom Jenkins, Gisele Caseiras and Francesco Manfredonia, and latterly Carmen Tur and Maria Aguirre-Gomozcorta, for making this an extremely enjoyable and fruitful period. They have taught me a great deal about MS, general neurology, Italian and seagulls. Finally, thank you to my parents for everything, to both my sisters for keeping me happy, and to my husband, Imran, for his patience and positivity.

Publications Associated with this Thesis

1. **Zhaleh Khaleeli**, Jaume Sastre-Garriga, Olga Ciccarelli, David Miller and Alan Thompson: Magnetisation Transfer Ratio in the Normal Appearing White Matter predicts change in walking ability over one year in early PPMS. *Journal of Neurology, Neurosurgery and Psychiatry*. 2007 Oct;78(10):1076-82.
2. **Zhaleh Khaleeli**, Mara Cercignani, Bertrand Audoin, Olga Ciccarelli, David Miller and Alan Thompson: Localized grey matter damage in early Primary Progressive Multiple Sclerosis contributes to disability. *Neuroimage*. 2007 Aug 1;37(1):253-61.
3. **Zhaleh Khaleeli**, Daniel Altmann, Mara Cercignani, Olga Ciccarelli, David H.Miller and Alan J.Thompson: Grey matter MTR: a potential surrogate marker for progression in early primary progressive MS. *Archives of Neurology*. 2008 Nov;65(11):1454-9.
4. **Zhaleh Khaleeli**, Olga Ciccarelli, Katherine Mizskiel, Daniel Altmann, David H.Miller and Alan J.Thompson: Lesion enhancement diminishes with time in PPMS (under submission)
5. Thomas M Jenkins, **Zhaleh Khaleeli** and Alan Thompson: Diagnosis and management of primary progressive multiple sclerosis. *Minerva Medica*. 2008 Apr;99(2):141-55.

Table of Contents

	Page
Title page	1
Declaration	2
Abstract	3
Acknowledgements	4
Publications associated with this thesis	5
Table of Contents	6
List of Tables	13
List of Figures	14
List of Abbreviations	15
Chapter 1 Introduction to primary progressive MS and Imaging	
1.1 Primary progressive MS (PPMS)	19
1.1.1 Epidemiology	19
1.1.2 Aetiology	20
1.1.3 Symptoms, Signs and Clinical Course	22
1.1.4 Pathology	24
1.1.4.1 White matter plaques	24
1.1.4.2 Diffuse white matter pathology	25
1.1.4.3 Grey matter pathology	25
1.1.4.4 Remyelination	26
1.1.5 Diagnosis	26
1.1.6 Investigations	27
1.1.7 The role of disease modifying treatment	28
1.2 Imaging and PPMS	30
1.2.1 Conventional measures	31
1.2.1.1 T2 and T1 lesions	30
1.2.1.2 Gadolinium enhancing lesions	31
1.2.1.3 Brain Atrophy	32
1.2.1.4 Spinal Cord Imaging	32

1.2.1.5 The Clinico-radiological Paradox	33
1.2.2 Non-conventional MRI measures	34
1.2.2.1 Spectroscopy	34
1.2.2.2 Diffusion Tensor Imaging	35
1.2.2.3 Magnetization transfer imaging	36
1.3 Conclusions	36
References	37

Chapter 2 Principles of MRI

2.1 Nuclear magnetic resonance	48
2.1.1 The NMR signal	50
2.2 Relaxation	50
2.2.1 T1 relaxation (spin-lattice relaxation)	50
2.2.2 T2 relaxation (spin-spin relaxation)	50
2.3 The spin echo	52
2.4 Image formation	53
2.4.1 Spatial encoding	53
2.4.1.1 Slice selection gradient	53
2.4.1.2 Phase encoding gradient	53
2.4.1.3 Frequency encoding gradient	54
2.4.2 k-space	55
2.4.3 The Fourier transformation	55
2.5 Sequences	56
2.5.1 Fast/turbo spin echo	56
2.5.2 Interleaved or multi-echo sequences	56
2.5.3 Gradient echo	57
2.5.4 Three-Dimensional Fast Spoiled Gradient Recalled Echo (FSPGR)	57
2.6 Use of Contrast agents	58
2.6.1 Gadolinium	58
2.7 Measuring brain volume	59

2.7.1 Segmentation-based techniques	60
2.7.2 Registration-based techniques	62
2.7.3 Voxel-based morphometry	63
2.8 Magnetization Transfer Imaging	64
2.8.1 MTR	65
2.8.2 Factors influencing MTR <i>in vivo</i>	65
2.8.2.1 Properties of the tissue	65
2.8.2.2 MR scanner parameters	65
2.8.3 MT sequence	66
2.8.4 Post-processing	66
2.8.4.1 Region of Interest (ROI) analysis	66
2.8.4.2 MTR Histogram analysis	67
2.8.4.3 Voxel-based MTR analysis	67
2.9 Conclusions	70
References	71

Chapter 3 Understanding progression: Magnetization Transfer Histograms and Atrophy

3.1 Detecting change and predicting progression over one year in early PPMS

3.1.1 Introduction	75
3.1.2 Methods	76
3.1.2.1 Subjects	76
3.1.2.2 MRI Acquisition	78
3.1.2.3 Image Post Processing	79
3.1.2.3.1 MTI	79
3.1.2.3.2 Atrophy	80
3.1.2.4 Statistical Analysis	81
3.1.2.4.1 Clinical data	81
3.1.2.4.2 Baseline MTR predictors	81

3.1.2.4.3 MTR change over one year in patients and controls	82
3.1.2.4.4 Relationship between MTR and atrophy	82
3.1.3 Results	83
3.1.3.1 Clinical changes	83
3.1.3.2. Predictive value of baseline MTR	83
3.1.3.3. MTR changes over one year	86
3.1.3.4. Correlations between MTR and volume changes	88
3.1.4 Discussion	89
3.1.4.1 MTR parameters predict clinical change	89
3.1.4.2 MTR decreases significantly over one year	90
3.1.4.3 MTR changes and progression of atrophy	91
<u>3.2 Monitoring and predicting clinical progression over three years in early PPMS</u>	
3.2.1 Introduction	92
3.2.2 Methods	93
3.2.2.1 Subjects	93
3.2.2.2 MRI Acquisition	95
3.2.2.3 Post-processing	96
3.2.2.4 Statistical Analysis	97
3.2.2.4.1 Clinical data	97
3.2.2.4.2 Piecewise mixed effect linear regression models	97
3.2.2.4.3 Rates of change in brain MTR, volume and T2 lesion load	98
3.2.2.4.4 Baseline MRI predictors of EDSS change	99
3.2.3 Results	100
3.2.3.1 Changes in EDSS and MRI parameters over three years	100
3.2.3.2 Surrogate MRI markers of clinical change	102
3.2.3.2.1 Markers of concurrent clinical progression	102
3.2.3.2.2 Baseline predictors of clinical progression	102
3.2.4 Discussion	105

3.2.4.1 MRI changes	105
3.2.4.2 Predicting progression	105
3.2.4.3 Monitoring progression	106
3.2.4.4 Limitations	107
3.3 Conclusions	108
References	109

Chapter 4 Localizing tissue injury: Voxel-based Analysis of MTR and Atrophy

4.1 Introduction	114
4.2 Methods	115
4.2.1 Subjects	115
4.2.2 Image acquisition and post-processing	116
4.2.2.1 Lesion masks creation	116
4.2.2.2 Co-registration of MTR and T1-weighted images	116
4.2.2.3 Segmentation of the T1-weighted images in native space	116
4.2.2.4 Normalization of segmented images	117
4.2.2.5 Normalization of the original T1-weighted images	117
4.2.2.6 Segmentation in stereotactic space	117
4.2.2.7 Production and application of grey matter mask	117
4.2.2.8 Smoothing	118
4.2.3 Location of Regions with abnormal MTR and grey matter volume	118
4.2.4 Correlations between MTR in abnormal regions and clinical measures	119
4.2.5 <i>Post hoc</i> analysis on the region in the left pre-central gyrus	120
4.3 Results	121
4.3.1 Location of regions of reduced MTR and atrophy	121
4.3.1.1 Cortical grey matter	121
4.3.1.2 Deep grey matter	121

4.3.2 Clinical correlations with MTR in abnormal regions after adjusting for atrophy	124
4.3.2.1 Motor function	124
4.3.2.2 Cognition	124
4.3.2.3 <i>Post hoc</i> Analysis	124
4.4 Discussion	126
4.4.1 Regions of reduced MTR and atrophy	126
4.4.1.1 Cortical regions	126
4.4.1.2 Deep Grey Matter Regions	126
4.4.1.3 Relationship between MTR reduction and Atrophy	127
4.4.1.4 Methodological considerations	128
4.4.2 Clinical correlations	129
4.4.2.1 Motor function	129
4.4.2.2 Cognition	129
4.5 Conclusions	130
References	131

Chapter 5 Enhancing Lesions: the role of inflammation in early PPMS

5.1 Introduction	135
5.2 Methods	136
5.2.1 Subjects	136
5.2.2 MRI Acquisition	138
5.2.3 MRI post-processing	139
5.2.4 Statistical Analysis	139
5.2.4.1 Clinical data	139
5.2.4.2 Gadolinium measures	139
5.2.4.3 Changes in enhancing lesions over five years	140
5.2.4.4 Predicting clinical changes over three and five years	140
5.2.4.5 Correlates of MRI change over three years	141
5.3 Results	141

5.3.1 Clinical progression	141
5.3.2 The proportion of patients with enhancing lesions decreased over five years	143
5.3.3 Enhancing lesions were modestly related to clinical progression	145
5.3.5 Enhancing lesions were related to T2 lesion load increase but not atrophy	146
5.5 Discussion	146
5.6 Conclusions	149
References	149
Conclusions and Future Directions	153
Mechanisms and measures of progression	153
Spinal Cord Studies	154
Understanding grey matter injury	154
Cognition	154
Understanding White matter injury	156
References	158

List of Tables

Chapter 1		Page
Table 1.A	Diagnosis of PPMS	28
Chapter 3		
Table 3.A	Clinical characteristics of patients at baseline and follow-up	78
Table 3.B	Baseline MTR parameters predict clinical change over one year	85
Table 3.C	Baseline NAWM mean MTR < 37 pu predicts worsening on EDSS over one year	86
Table 3.D	MTR changes over one year in patients and controls	87
Table 3.E	Correlation of change in MTR with change in intra-segmental volume over one year	88
Table 3.F	Baseline clinical and imaging characteristics of patients and controls	94
Table 3.G	Numbers of patients assessed at each time-point and reasons for non-attendance	95
Table 3.H	Summary of significant findings for MTR, volume and lesion load measurements in early PPMS	100
Table 3.I	Mean annual rates of change in grey and NAWM MTR in patients and controls	101
Chapter 4		
Table 4.A	Characteristics of patients and controls	115
Table 4.B	Regions with significantly reduced MTR and grey matter volume in patients compared to controls	123
Table 4.C	Correlation between mean MTR in abnormal regions found within the motor network and clinical measures of disability	125
Chapter 5		
Table 5.A	Patients attending at each time-point	138
Table 5.B	Clinical tests at baseline, three and five years, with separate data on patients completing all tests and study time-points	143
Table 5.C	The frequency of each number of enhancing lesions identified in the brain and spinal cord at each time-point	145

List of Figures

Chapter 1		Page
Figure 1a	Diffuse white matter injury in the brain in PPMS	25
Figure 1b	Brain and spinal cord atrophy in two patients with PPMS	33
Chapter 2		
Figure 2a	Precession of protons	49
Figure 2b	The exponential curve for T1 relaxation	51
Figure 2c	The exponential curve for T2 relaxation	52
Figure 2d	The spin echo pulse sequence	54
Figure 2e	T1-weighted image after injection with triple dose gadolinium	58
Figure 2f	Segmentation of FSPGR image in SPM2	62
Figure 2g	MTR image	67
Figure 2h	Histogram of the grey matter MTR in a patient with PPMS	69
Chapter 3		
Figure 3a	Baseline NAWM mean MTR predicts change in EDSS over one year	84
Figure 3b	Grey matter mean MTR decline by EDSS step change over three years	103
Figure 3c	Grey matter MTR (A) and grey matter PH MTR (B) at baseline in patients who remained stable and patients who progressed markedly over 3 years	104
Chapter 4		
Figure 4a	Regions of significantly reduced MTR and grey matter volume in patients compared to controls	122
Figure 4b	The abnormal region in the left pre-central gyrus translated back into native space and applied to the original PD-weighted MTR images	125
Chapter 5		
Figure 5a	Percentage of patients with gadolinium enhancing lesions at each time-point	145

List of Abbreviations

<	Less than
>	Greater than
>=	Greater than or equal to
μ T	Micro-Tesla
2D	Two dimensional
3D	Three dimensional
95%CI	95 percent confidence intervals
B_0	External magnetic field
BA	Brodmann area
BBSI	Brain boundary shift integral
BL	Baseline
BPF	Brain parenchymal fraction
Cr	Creatine
CSF	Cerbro-spinal fluid
DTI	Diffusion tensor imaging
DTPA	diethylenetriaminepenta-acetic acid
EBV	Epstein-Barr virus
EDSS	Expanded disability status scale
ETL	Echo train length
FDA	Food and drug administration
FE, G_{read} , G_x	Frequency encoding gradient
FID	Frequency induction decay
FLAIR	Fluid attenuated inversion recovery
fMRI	Functional magnetic resonance imaging
FOV	Field of view
FSPGR	Fast spoiled gradient recoil
FU	Follow-up
FWHM	Full width half maximum
GMF	Grey matter fraction
GMV	Grey matter volume
Hz	Herz

i	Inverse
kHz	KiloHerz
LV	Lesion volume
M	Net magnetization
M_0	PD-weighted signal in the absence of a saturation pulse
ml	Millilitres
mm	Millimetres
mmol/l	Millimoles per litre
MNI	Montreal Neurological Institute
MRI	Magnetic resonance imaging
ms	Milliseconds
MS	Multiple sclerosis
M_s	PD-weighted signal in the presence of a saturation pulse
MSFC	Multiple sclerosis functional composite
MTI	Magnetization transfer imaging
mTm^{-1}	Milli-Tesla per minute
MTR	Magnetization transfer ratio
NAA	N-acetyl-aspartate
NABT	Normal appearing brain tissue
NAWM	Normal appearing white matter
NAGM	Normal appearing grey matter
NAWMF	Normal appearing white matter fraction
NEX	Number of excitations
NHPT	Nine hole peg test
NMR	Nuclear magnetic resonance
NWM	Normal white matter
OR	Odds ratio
PASAT	Paced auditory serial addition test
PD	Proton density
PE, G_{phase}, Gy	Phase encoding gradient
PGMF	Percentage grey matter fraction
PH	Peak height

PL	Peak location
PNAWMF	Percentage normal appearing white matter fraction
PNAGMF	Percentage normal appearing grey matter fraction
PPMS	Primary progressive multiple sclerosis
pu	Per cent units
RARE	Rapid acquisition relaxation enhancement
RF	Radiofrequency
ROI	Region of interest
RRMS	Relapsing remitting multiple sclerosis
SD	Standard deviation
SIENA(X)	Structural image evaluation, using normalization, of atrophy (cross-sectional)
SPM	Statistical parametric mapping
SPMS	Secondary progressive multiple sclerosis
SPSS	Statistical package for the social sciences
SS, G_{slice}, G_z	Slice selection gradient
TE	Echo time
TIV	Total intra-cranial volume
TR	Relaxation time
TWT	Timed walk test
VBM	Voxel-based morphometry
VEP	Visual evoked potential
WB	Whole brain
z	z-score
γ	Gyromagnetic ratio
ω_0	Larmor frequency

Introduction to Primary Progressive MS and Imaging

CHAPTER 1

The chapter begins with an overview of the clinical features of primary progressive multiple sclerosis (PPMS), and current knowledge of the pathological processes underlying it. In contrast to other MS subtypes, no disease modifying treatments are available for PPMS, and the particular challenges for clinical trials in this group are outlined. The second half of the chapter explores the application and limitations of MRI for investigating the disease process in PPMS, summarizing research findings to date.

1.1 Primary progressive Multiple Sclerosis

Multiple sclerosis (MS) is a chronic inflammatory disease of the central nervous system, and it is the commonest cause of neurological disability in young adults in the UK. Patients typically follow a *relapsing-remitting* disease course (RRMS), presenting with acute neurological dysfunction (a relapse) followed by some degree of recovery and a period of indefinite remission, before further relapses. After some years a proportion of patients show a gradual functional deterioration, independent of relapse activity, which is called secondary progression (Lublin 1996). A minority of patients with MS progress from onset without relapses, and are described as having *primary progressive* MS (PPMS).

1.1.1 Epidemiology

MS has a prevalence of 97-184/100 000 (Pugliatti 2006), and an incidence of 5.5/100 000 (Alonso 2007) in the UK. Northern European populations are particularly affected, and incidence remains higher in these groups in North America, Canada and Australia (Ebers 2008). However, MS has been diagnosed worldwide (Cheng 2007, Alter 2006, Cabre 2001, Kantarci 1998).

Detailed information regarding PPMS is more difficult to collect, but three epidemiological reports from Asia (Yamout 2008, Maghzi 2007, Wasay 2007) and one from Africa (Modi 2008) specifically mention PPMS. In a European epidemiological review, estimates of PPMS prevalence ranged from 4 to 35% of all MS cases (Pugliatti 2006). This probably reflects the difficulty of categorizing

patients before definitive diagnostic criteria were set out in 2000 (Thompson 2000). It is generally accepted, from natural history studies in MS cohorts, that PPMS constitutes 10-15% of all MS cases (Tremlett 2005, Thompson 2004, Confavreux 2000, Runmarker 1993). In contrast to RRMS, where there is a female preponderance, PPMS has an equal sex distribution. The age of onset is usually in the fourth or fifth decade (Tremlett 2005, Cottrell 1999), roughly ten years later than in RRMS (Compston 2002); similar to the onset of secondary progression (Confavreux 2006b, Ebers 2004). PPMS in children is extremely unusual, but has been described (Renoux 2007, Boiko 2002).

1.1.2 Aetiology

Genetic susceptibility to PPMS has been mapped to the same region as RRMS: the HLA class II region of the MHC molecule on the short arm of chromosome 6, specifically the HLA-DR2 allele DRB1*1501. HLA alleles do not appear to influence the age of onset or severity of the disease (Barcellos 2006). More recently, single nucleotide polymorphisms at IL7R and IL2R have been implicated in MS susceptibility, in large scale genome-wide association studies, which have included patients with PPMS (Hafler 2007). Australian studies postulate that there is under-expression of the IL7R alpha chain mRNA, CD127, in PPMS in particular, and that this affects the T cell response (McKay 2008). Thus there are some indications that genetic factors may have some influence on disease subtype. Another study in 1083 families with MS suggested a slight concordance for a primary progressive clinical course among siblings ($\kappa < 0.2$); however, concordance was not observed among parent-child groups (Hensiek 2007). A French study recently found that the DRB1*15 allele was more frequent in patients developing SPMS, compared to both PPMS patients and RRMS patients who had not converted after 12-15 years (Cournu-Rebeix 2008).

The recurrence rate in monozygotic twins for all types of MS taken together is just over one third (Ebers 2008), suggesting that environmental factors also play a role in disease causation. This phenomenon can not be identified at an individual level, but can be seen in large cohorts at a population level (Sawcer 2008). Although

there is no specific data for PPMS, studies in genetically homogenous populations suggest that MS incidence increases with latitude (Vukusic 2007), although this pattern appears increasingly complex and could be changing (Ascherio 2007). For example, east-west geographic variations also exist, with some irregularity, and countries at the same latitude do not all have the same incidence (Ebers 2008). Migration studies also provide evidence of a complex environmental influence. While child migrants take on the risk profile of their host community, those who migrate later in life maintain the risk associated with their country of origin (Dean 1997). Similarly, second generation African and Asian immigrants have a higher risk than their parents (Elian 1990). Furthermore, the specific environmental agents which trigger MS in susceptible individuals remain unidentified. One hypothesis centres on sunlight exposure, which varies with latitude and is the principal inducer of vitamin D production: studies have suggested that vitamin D is an immune modulator (Smolders 2008), and that higher vitamin D levels protect against MS (Munger 2006). Diet may be another significant element in modulating individual responses to other risk factors (Ebers 2008). Finally, a large number of infectious agents, particularly viruses, have been implicated in MS, although no causal association has been proved. The strongest candidate at present is the Epstein-Barr virus (EBV). Almost all patients with MS are sero-positive for EBV, compared to 90% in the general population (Giovannoni 2007).

Regarding PPMS in particular, there is little information available on specific environmental risk factors. Smoking may be a risk factor for PPMS (Hernan 2005), although it has no effect on age of onset or disability accrual (Koch 2007). While there is evidence that Spring births increase the risk of RRMS (Willer 2005), timing of birth does not seem to influence PPMS susceptibility (Sadovnick 2007). A recent study suggests that the immune response to EBV may be related to disease subtype (Farrell 2009), but it remains to be established whether this is a cause or a consequence of phenotypic differences.

1.1.2 Symptoms, Signs and Clinical Course

The clinical onset of PPMS tends to be insidious, with a gradual functional deterioration over months and years. While symptoms may fluctuate through the year, and sometimes remain stable for long periods, accumulated disability is irreversible. The majority of patients present with a progressive spinal cord syndrome, usually leg weakness and stiffness progressing to spasms. Initially, weakness may be evident only after exercise, and is often asymmetrical. Urinary urgency and constipation are common, and erectile dysfunction may be a feature. More rarely sphincter disturbance manifests as faecal urgency. Sensory symptoms, though less prominent than in RRMS, may be distressing and include pins and needles, numbness and pain. Less commonly, patients present with poor balance and tremor or hemiplegia, and very rarely with progressive visual or cognitive decline. Examination may reveal a spastic para- or hemi-paresis, cerebellar signs, and sensory loss which tends to be patchy rather than describing a definite sensory level.

Cognitive impairment occurs in all MS subtypes. A study in 24 PPMS patients, with a mean disease duration of 5.4 years, emphasized information processing speed as the most markedly affected domain in comparison to healthy controls, and the only domain markedly declining over 3 years. Verbal memory was also impaired, and age had a significant impact on performance (Denney 2008). A larger group of 99 PPMS patients with more advanced disease demonstrated wide heterogeneity in cognitive decline over two years; roughly one third deteriorated on individual tests (Camp 2005). Several studies have compared cognitive decline in PP and SPMS (Bergendal 2007, Wachowius 2005, Foong 1997, Comi 1995). There is no consensus as to which subtype, matched for age and disease duration, shows greater cognitive impairment, and while some studies indicate qualitative differences between the impaired domains (Kraus 2005, Gaudino 2001), others do not (de Sonneville 2002). It is possible that wide variations within subtypes (Kraus 2005) have made differences harder to detect in these studies, all of which are limited in cohort size.

Gradual progression of the presenting syndrome is typical. In severe cases paraparesis progresses to quadriparesis, cerebellar involvement and, at an advanced stage, brainstem dysfunction with dysphagia and dysarthria.

The rate and character of progression is broadly similar to the secondary progressive phase in patients with RRMS (Kremenchutzky 2006, Confavreux 2006a, Confavreux 2000). Indeed, in secondary progressive MS the previous relapse history appears to have minimal influence on eventual disability (Ebers 2004, Confavreux 2003, Confavreux 2000).

However, the rate of disability accrual varies widely between individuals in PPMS. In a large natural history study from Canada, 25% of patients required a walking aid seven years after onset, but 25% were still walking independently at twenty-five years (Tremlett 2005). The mean time to reach EDSS 6 (the patient requires a cane to walk) was 13.3 years. Studies in other cohorts have identified a worse prognosis, ranging from 6 to 8.5 years (Confavreux 2000, Cottrell 1999, Andersson 1999, Runmarker 1993).

At present, clinical indicators of future prognosis are uncertain. In the London, Ontario cohort, the small number of patients presenting with involvement of more than three systems had a worse prognosis (Cottrell 1999). A study from British Columbia indicated that involvement of the brainstem and cerebellum at presentation may adversely affect prognosis, and these symptoms were more common in men (Tremlett 2005). Both the London Ontario and Lyons cohorts describe a poorer prognosis in men (Confavreux 2006a, Cottrell 1999), but this is not a feature of all studies (Andersson 1999). Finally, both the Canadian studies suggest that the rate of initial progression is an important indicator of future prognosis (Tremlett 2005, Cottrell 1999).

1.1.4 Pathology

1.1.4.1 White matter plaques

The MS plaque is an area of demyelination, axonal loss and oligodendrocyte death on a background of inflammation (Bruck 2002). Plaques typically occur in the white matter, but are also abundant in grey matter (Peterson 2001). They are thought to result from a breach in the blood brain barrier, which allows the infiltration of macrophages, T cells and plasma cells into the central nervous system, and activates resident microglia (Frohman 2006). The inflammatory T cells attack myelin and oligodendrocytes in the central nervous system, creating a focus of inflammatory activity (Frohman 2006). Gradually, inflammation gives way to fibrillary gliosis, with fewer macrophages, loss of oligodendrocytes, and a decrease in axonal density, particularly at the lesion centre (Lucchinetti 2004).

Post mortem investigations have demonstrated fewer inflammatory cells in PP compared to SPMS lesions (Revesz 1994), and specifically a reduction in T cells and macrophages has been described (Lucchinetti 2004). Magliozzi and colleagues found less meningeal inflammation in PP compared to SPMS, with fewer B cells seen in perivascular cuffs. The ectopic B cell meningeal follicles which they identified in SPMS, which may have produced a locally sustained B cell inflammatory response, were absent in PPMS (Magliozzi 2007). Finally, both PP and SPMS plaques tend to demonstrate a tendency to slow radial expansion, with a lower percentage of classical active lesions, when compared to RRMS (Kutzelnigg 2005, Prineas 2001).

Some investigators have postulated inter-patient lesion heterogeneity in MS, with intra-patient homogeneity. Four lesion types with different mechanisms of myelin injury were identified, and pattern IV, demonstrating oligodendrocyte dystrophy without remyelination, was found exclusively in PPMS (Lucchinetti 2000). However, this concept was challenged in 2004 (Barnett 2004), and more recently another study found acute lesions to be homogeneous, and oligodendrocyte apoptosis to be rare (Breij 2008).

1.1.4.2 Diffuse white matter pathology

The relevance of white matter pathology outside defined plaques has been increasingly recognized over the last two decades (Trapp 1999). Damage to the healthy-appearing white matter is most pronounced in progressive MS (see Figure 1a), and involves widespread reduction in myelin and axon density on a background of parenchymal, perivascular and meningeal inflammation. Inflammation is less marked in PP compared to SPMS cases (Kutzelnigg 2005). The relatively normal appearance of the white matter may be preserved by the persistence of some myelin sheaths despite Wallerian degeneration of associated axons secondary to transection in lesions (Dutta 2007). There is no obvious correlation between NAWM injury and white matter lesion load, suggesting that diffuse white matter injury may be independent of lesion pathology (Kutzelnigg 2005).

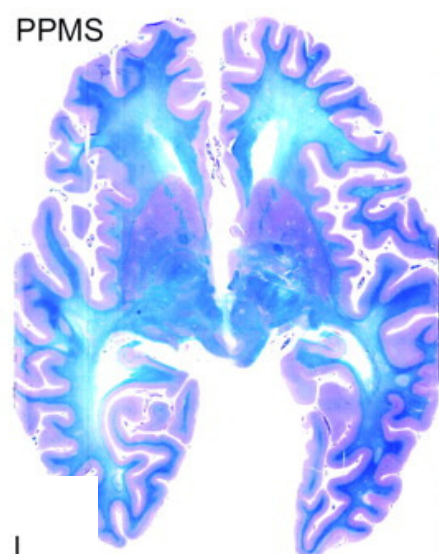


Figure 1a: Diffuse white matter injury in the brain in PPMS

Only the subcortical myelin is intact, and there are few focal demyelinated plaques
Luxol fast blue stain, x0.5

(adapted from Kutzelnigg *et al*, *Brain* 2005)

1.1.4.3 Grey matter pathology

Although grey matter demyelination was identified in the nineteenth century, it is only recently that its true extent has been appreciated. This is partly because the conventional lipid stains, used in the past for histo-pathological studies, were not sensitive enough to detect it (Stadelmann 2008). More recent studies, using

immunohistochemical techniques, have shown that lesions in the cortex and deep grey matter are prominent in progressive MS (Kutzelnigg 2007) and three types of cortical lesion have been identified (Peterson 2001): leukocortical lesions (type I), small cortical lesions, often perivascular (type II), and the commonest type, subpial lesions which can extend into layers III and IV of the cortex (type III). There are fewer inflammatory cells in grey matter lesions compared to white matter lesions (Pirko 2007, Peterson 2001), and marked neuro-axonal injury and neuronal apoptosis have been identified (Dutta 2007, Kutzelnigg 2005, Peterson 2001). Some neuronal damage may be ascribed to Wallerian and retrograde degeneration following white matter axonal injury, but the lack of association between focal white matter and grey matter injury suggest that the latter is a largely independent process (Lassmann 2007, Bo 2007). Extensive grey matter demyelination has also been demonstrated in the spinal cord, in patients with progressive MS (Gilmore 2006).

1.1.4.4 Remyelination

There is evidence that some lesions seek to repair themselves. Oligodendrocyte numbers are increased in such lesions, known as *shadow plaques*, and myelin density is intermediate between fully demyelinated lesions and healthy brain tissue. Remyelination occurs in all MS subtypes (Patrikios 2006), does not diminish with disease duration (Patani 2007), and appears to be most extensive in the cortex (Albert 2007). In the white matter, remyelination is more often seen in deep and subcortical compared to periventricular lesions (Patrikios 2006).

In summary, the pathology of progressive MS is distinct from RRMS in the relative preponderance of injury to the grey and NAWM. The pathology of PPMS is distinct from RRMS in the relative paucity of active focal inflammation, and from SPMS in the relative reduction of diffuse and focal inflammation.

1.1.5 Diagnosis

Multiple sclerosis remains a primarily clinical diagnosis. Diagnostic criteria based

on evidence of dissemination in time and space were formalized by the Poser Committee in 1983 (Poser 1983), and for the first time evoked potential or MRI evidence of a second lesion was accepted *in lieu* of clinical evidence. To achieve a *laboratory supported* diagnosis, it was necessary to demonstrate intrathecal synthesis of IgG on CSF analysis. However, these criteria were inappropriate for PPMS, by definition a slowly evolving deficit, often in a single system. This was addressed by Thompson in 2000 (Thompson 2000) who established three levels of diagnostic certainty (definite, probable and possible). The criteria were based on clinical information and supportive investigations (CSF, MRI, VEPs), for application to patients who had progressed for one year and in whom alternative diagnoses had been appropriately excluded. The identification of intrathecal IgG synthesis was mandatory for a definite diagnosis. These criteria were largely adopted in the international diagnostic criteria for MS in 2001 (McDonald 2001). In 2005, the criteria were simplified (Polman 2005), and, in the light of evidence put forward from the PROMiSe trial (Wolinsky 2003), a positive CSF analysis is no longer essential for diagnosis (see Table 1.A).

1.1.6 Investigations

MRI of both the brain and spinal cord is recommended, as the majority of patients present with a spastic paraparesis, and because lesions in the spinal cord may, rarely, be present in the absence of brain lesions (Thorpe 1996). In addition, age-related non-specific white matter lesions are rare in the spinal cord, and therefore lesions identified at this site are more suggestive of MS (Kidd 1993). CSF analysis reveals increased intrathecal synthesis of IgG or the presence of oligoclonal IgG bands which are absent in the serum, in about 80% of PPMS cases (Wolinsky 2004, Andersson 1999). Visual evoked potentials demonstrating a preserved waveform with a prolonged P100 latency can be taken as evidence of demyelination in the optic nerve (Thompson 2000). However, symptomatic optic neuritis is unusual in PPMS, and there is little data regarding the frequency of VEP abnormalities in this group. In a small study including 14 patients with PPMS it was suggested that VEP abnormalities may be less common than in SPMS, but of

similar frequency to RRMS (Rot 2006). Motor and somatosensory evoked potentials may also be delayed in PPMS.

Table 1.A Diagnosis of PPMS

Original McDonald Criteria	2005 Revisions
1. Positive CSF <i>and</i>	1. One year of disease progression (retrospectively or prospectively determined)
2. Dissemination in <i>space</i> by MRI evidence of nine or more T2 brain lesions <i>or</i>	2. <i>Plus</i> two of the following: a. Positive brain MRI (nine T2 lesions or four or more T2 lesions with positive VEP) b. Positive spinal cord MRI (two focal T2 lesions) c. Positive CSF (isoelectric focusing evidence of oligoclonal IgG bands or increased IgG index or both).
Two or more cord lesions <i>or</i>	
Four to eight brain lesions and one cord lesion <i>or</i>	
Positive VEP with four to eight MRI lesions <i>or</i>	
Positive VEP with less than four brain lesions plus one cord lesion <i>and</i>	
3. Dissemination in <i>time</i> by MRI <i>or</i> Continued progression for 1 year	

(taken from Polman *et al*, *Annals of Neurology* 2005)

1.1.7 The role of disease modifying treatments

The disease modifying treatments used in RRMS are anti-inflammatory drugs which target relapses. The inflammatory component of PPMS implies a potential to respond to these treatments. The studies which have investigated this possibility are discussed in the next part of this section. However, disease modifying agents have proven largely ineffective in PPMS. Management has therefore focused on symptomatic control and rehabilitation (Jenkins 2008), with the hope that future treatment strategies aimed at neuro-axonal protection and repair will be more productive (Leary 2005).

The largest randomized study in PPMS is the PROMiSe trial of glatiramer acetate, in which 943 patients with PPMS were randomised to placebo or glatiramer acetate for 3 years. Unfortunately, a lack of progression in both arms studied made it

impossible to identify a treatment effect, and the study was terminated early (Wolinsky 2007). Beta interferons are widely used to treat RRMS and SPMS with relapses, and two small placebo controlled trials have been performed in PPMS. The first, on interferon beta-1a, found no reduction in disability accumulation, brain or spinal cord atrophy (Leary 2003). However, patients on the drug had a lower rate of T2 lesion accumulation. In the second study, testing interferon 1-beta *versus* placebo in 73 patients, a favourable effect was demonstrated on the MSFC in the treated group. T2 lesion load accumulation was reduced, although brain and spinal cord atrophy were not (Montalban 2004). Mitoxantrone has been studied in a small placebo controlled trial in 61 patients with PPMS (Stuve 2004), but preliminary results have not been positive (Miller 2007). Further, retrospective analysis of 163 patients with PPMS showed that those taking mitoxantrone continued to progress (Debouverie 2007). A randomised control trial investigating monthly intravenous immunoglobulin infusions suggested that progression was delayed in eight patients with PPMS, though there was no significant effect in the much larger group of SPMS patients (Pohlau 2007). A randomised controlled study of the monoclonal antibody Rituximab is underway (Miller 2007) following a report of successful B cell depletion in patients with PPMS (Monson 2005). Open label studies in perfenidone, an immune modulating oral medication (Bowen 2003), and cyclophosphamide (Zephir 2004) have appeared to demonstrate stabilization of PPMS patients, but interpretation is limited by study design. Studies in methotrexate (Goodkin 1995), azathioprine (British and Dutch Multiple Sclerosis Azathioprine Trial Group 1988) and cladribine (Rice 2000) have included PPMS, but no benefit was demonstrated. A retrospective study of haematopoietic stem cell transplantation reported benefit in a proportion of PPMS patients, but mortality was considerable (Fassas 2002).

From the point of view of neuro-protection, riluzole has shown some promise in preliminary studies (Kalkers 2002), and an unblinded pilot study in high dose recombinant erythropoietin showed some improvement in motor function over 24 weeks (Ehrenreich 2007). Intravenous methylprednisolone, used in RRMS to shorten relapse duration, may sometimes be used for subacute functional deterioration in PPMS patients (Miller 2007). However, there have been calls to

investigate steroids as neuro-protective agents in progressive MS, following retrospective reports of longer term clinical benefit (Pirko 2004).

Many of these studies highlight the difficulties of performing clinical trials in PPMS. Firstly, PPMS is a relatively uncommon MS subtype, which limits cohort sizes. This can only be addressed by large multi-centre collaborations. Secondly, in the absence of prognostic markers for progression, recruitment is unselected. Thus some study patients may progress very gradually, making treatment effects difficult to identify over short periods of time. Finally, while MRI outcome measures such as T2 lesion load have responded to treatment in some studies, the uncertain relationship between these measures and disease progression in PPMS makes the findings difficult to interpret. For this reason reliable, responsive surrogate outcome measures, which accurately reflect concurrent and future clinical progression, are needed to facilitate clinical trials in PPMS. MRI studies have tried to address some of these issues, and are discussed in the next section as part of a brief overview of MRI in PPMS.

1.2 Imaging and PPMS

1.2.1 Conventional MRI measures

1.2.1.2 T2 and T1 lesions

White matter plaques are best visualized on proton density-, T2-weighted and fluid attenuated inversion recovery (FLAIR) imaging. Lesions are usually less than 1cm in diameter and rounded in shape, but adjacent lesions may coalesce.

T2 lesions are pathologically heterogeneous, showing wide variations in levels of demyelination, inflammatory activity and axonal loss (Fisher 2007). In PPMS, lesions are fewer and smaller than in other MS subtypes (Thompson 1990), and increases in T2 lesion load are largely due to expansion of existing lesions rather than to the formation of new ones (Stevenson 2000). Recent work suggests that the smaller T2 lesions occurring in PPMS are more persistent and destructive than larger lesions in RRMS (Meier 2007). This may contribute to the poor correlation between T2 lesion load and disability in PPMS. In addition, grey matter lesions

tend not to be visible on T2-weighted images. They have a signal intensity close to the normal grey matter, and are rarely seen on MRI even at higher field strengths (Geurts 2008). This may further limit the ability of T2 lesion loads to reflect the disease burden in PPMS.

T2 lesions which develop into areas of hypo-intensity on T1-weighted images are called 'T1 black holes'. In progressive MS a greater proportion of T2 lesions develop in this way compared to RRMS (Wolinsky 2004, van Walderveen 2001). Some of the black holes persist indefinitely, representing focal areas of irreversible matrix destruction and axonal loss (van Walderveen 1998). There is some indication that T1 lesion load correlates better than T2 with disability in SPMS (Truyen 1996), but this has not been demonstrated in PPMS.

1.2.1.2 Gadolinium enhancing lesions

It is not possible to demonstrate the age or activity of a lesion on unprocessed unenhanced T1 and T2 imaging. Gadolinium, an intravenous contrast agent, penetrates the blood brain barrier in areas of active inflammation causing enhancement of active lesions on T1-weighted images (Bruck 1997). While the majority of T2 lesions show some gadolinium enhancement, a minority do not; it has been suggested that these lesions, which are often peri-ventricular, may arise from mechanisms other than BBB breakdown, such as Wallerian degeneration or the coalescence of two smaller lesions (Lee 1999). Lesions may enhance uniformly or inhomogeneously. Some demonstrate ring enhancement, possibly representing the concentric pattern of lesion recovery (Meier 2007). Lesions which have ceased to enhance may reactivate and start to enhance again (Bruck 1997). Enhancement continues for a variable amount of time, but usually lasts less than 2 months (Ciccarelli 1999), and there have been suggestions that lesions which enhance for longer are more destructive (Silver 1999). Enhancing lesions may develop into T1 black holes, remain as T2 hyper-intensities, or resolve completely, and this varies both between subjects and in different lesions within a subject (Minneboo 2005, Ciccarelli 1999).

Patients with established PPMS demonstrate fewer gadolinium enhancing lesions

on MRI compared to SPMS (Thompson 1991); only 14% of the PPMS patients entering the PROMiSe trial had gadolinium enhancing lesions (Wolinsky 2004). However, a study in patients with early PPMS have demonstrated a higher level of gadolinium enhancement, albeit using triple dose gadolinium (Ingle 2005), suggesting the possibility of an early inflammatory phase. This may have implications for the potential of anti-inflammatory disease modifying therapies during the early stages of PPMS.

1.2.1.3 Brain Atrophy

Atrophy is a putative marker for axonal loss, but other pathological processes affect tissue volume including gliosis, axonal swelling, inflammation, and demyelination (Fisher 2007, Kezele 2007, Simon 2006). In addition, the temporal relationship between loss of axons and subsequent volume loss is not clearly established (Simon 2006). Brain volume has been correlated with clinical function in cross-sectional studies in established PPMS (Nijeholt 1998). In longitudinal studies, atrophy does not correlate with accumulation of disability in the short term (Ingle 2002, Stevenson 2000), but an association is evident over five years (Ingle 2003b). Brain atrophy on an initial scan can also predict long term clinical outcome (Sastre-Garriga 2005b, Ingle 2003a). In early PPMS, atrophy is already present in both grey and NAWM, and a correlation between NAWM volume and clinical function has been identified (Sastre-Garriga 2004).

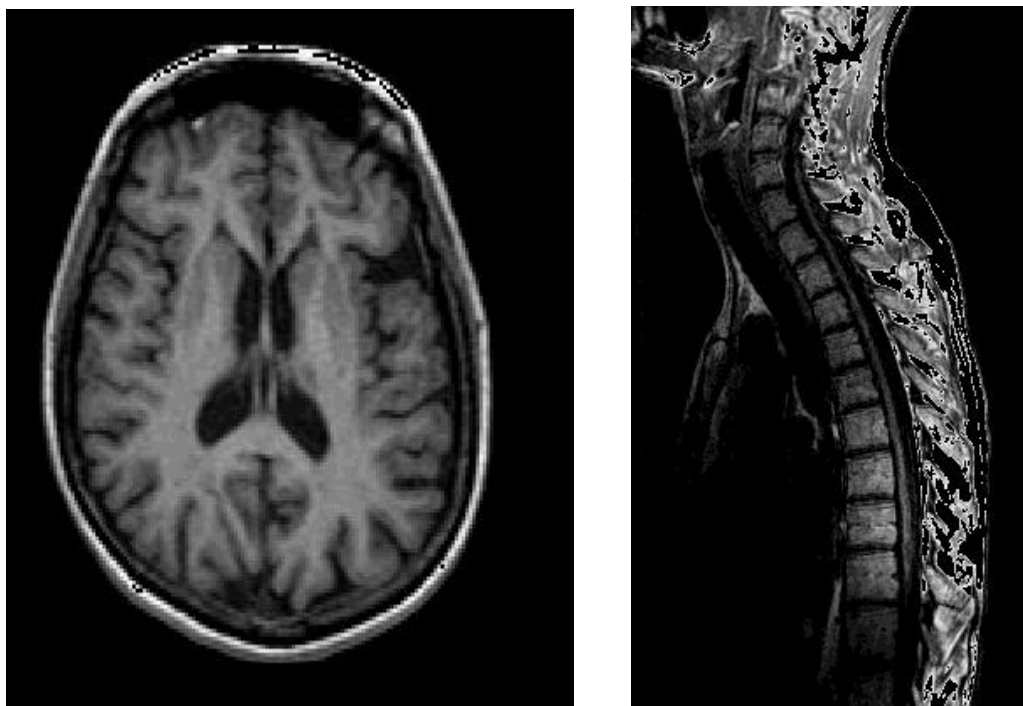
1.2.1.4 Spinal cord imaging

Spinal cord lesions are less likely than brain lesions to demonstrate enhancement, or to develop into T1 lesions (Neema 2007). In PPMS, there are fewer lesions in the spinal cord, with less enhancement, than in other MS subtypes. In addition, a diffuse T2-weighted signal abnormality, shown to represent demyelination on histological studies (Bergers 2002), may be visible in PPMS. Spinal cord lesions have not shown strong correlations with disability in PPMS (Nijeholt 1998). Spinal cord volume is reduced in PPMS, although not as much as it is in SPMS. Compared with brain imaging parameters, spinal cord atrophy was found to be the best way of separating early PPMS and early RRMS (Bieniek 2006). Cord atrophy particularly affects the cervical spine (Losseff 1996). Spinal cord atrophy correlates

with clinical measures in cross-sectional studies in PPMS (Stevenson 1998), and loss of cord volume over two years has been correlated with disability accrual over five years (Ingle 2003b).

Figure 1b: Brain and spinal cord atrophy in two patients with PPMS

T1-weighted FSPGR sequences showing marked volume loss in the brain and spinal cord



1.2.1.5 The Clinico-radiological Paradox

The relationship between abnormalities identified on conventional imaging and disability has been surprisingly limited (Barkhof 2002), particularly in PPMS (Stevenson 1999). Longitudinally, the modest correlation between changes in clinical and MR measures may become apparent only after several years (Ingle 2003b, Ingle 2002). A number of explanations for this have been suggested. Firstly, clinical outcome measures used in MRI studies, usually the EDSS (Kurtzke 1983) and MSFC (Cutter 1999), have been widely criticized. Several studies, some in patients with PPMS (Kragt 2008), have demonstrated that the scales are unresponsive to disability accrual, and distinguish poorly between individuals (Hobart 2000, Sharrack 1999). These issues may be addressed in part by

examining patients early in their disease course, within five years of symptom onset. Clinical rating scales tend to be most responsive in less disabled individuals (Kragt 2006), and epidemiological studies suggest that early progression rates may give an indication of future course (Cottrell 1999). A second problem is that although patients usually present with a paraparesis, relatively little attention has been devoted to spinal cord imaging. Thirdly, repair, remyelination, and functional reorganization may obscure the relationship between measures of brain injury and disability. Finally, the pathological processes driving disability accrual in PPMS may occur in areas which appear normal on conventional MRI: the *normal appearing brain tissues* (NABT). In recent years quantitative MRI techniques have been developed to address some of these problems. Although their application in the spinal cord was initially limited, technical improvements have led to a recent expansion in research into spinal cord injury in PPMS. Quantitative techniques are better able to reflect the balance of damage and repair in MS lesions, as confirmed by correlation with pathological studies. Most importantly, they have extended our understanding of the disease process in PPMS by allowing examination of the NABT.

1.2.2 Non-conventional MRI measures

Widespread abnormalities have been demonstrated in the grey and normal appearing white matter (NAWM) and in lesions in PPMS using non-conventional quantitative techniques, including spectroscopy, diffusion tensor imaging (DTI), and magnetization transfer imaging (MTI). Each of these modalities provides information about tissue damage, although their specificity for pathological processes is limited. In this section each technique is briefly described, and findings in the NABT, lesions and spinal cord in PPMS are summarized. Finally the findings in early PPMS are delineated.

1.2.2.1 Spectroscopy

Of the quantitative techniques, spectroscopy provides the most direct measure of tissue injury. Four major resonances are seen on proton MR spectra: N-acetylaspartate (NAA), choline, lactate, and creatinine (Cr) (Filippi 2004). NAA is a

putative marker of axonal integrity, and choline and lactate reflect demyelination and inflammation; however these relationships may be more complex, as demonstrated by studies in PPMS and other subtypes (Cader 2007, Sijens 2005). In PPMS, data from the PROMiSe trial analyzed by Narayana and colleagues showed NAA/Cr ratio reduction in both the NABT and in lesions (Narayana 2004). The indices did not correlate with disability or change over three years (Sajja 2008). Another study, examining specific brain compartments in PPMS and SPMS, identified marked NAA reduction in the grey matter, with a less striking reduction in the NAWM (Sijens 2006). In early PPMS, NAA reduction has also been observed in both grey and NAWM; grey matter NAA changes correlated with disability (Sastre-Garriga 2005a).

1.2.2.2 Diffusion Tensor Imaging (DTI)

In DTI, the properties of water diffusion are used to examine tissue microstructure. The micro-architecture of a tissue limits and directs water motion, and tissue injury disrupts this architecture, allowing diffusion to occur freely in all directions. In DTI, a three dimensional tensor is constructed, and the magnitude of diffusion (mean diffusivity, MD) and degree of anisotropy (fractional anisotropy, FA) is measured (Filippi 2004). In a cohort including PPMS patients, Ciccarelli and colleagues identified widespread NAWM FA reduction, indicating tissue injury, and found that diffusion measures in the cerebral peduncles correlated with EDSS score. No difference in diffusion measures emerged between MS subtypes (Ciccarelli 2001). In another study, patients with progressive MS (including 54 PPMS patients) demonstrated tissue injury in the grey, NAWM and lesions, indicated by increased MD (Rovaris 2005). In 52 of these PPMS patients, followed up after 15 months, MD increased further in grey matter and lesions. Higher grey matter MD at baseline predicted clinical worsening at five years (Rovaris 2006). Reduction in FA and increase in MD has also been observed in the cervical cord in PPMS (Agosta 2005). When MS subtypes were compared, PPMS patients demonstrated marked FA reduction in the cervical cord over two and a half years compared to RR and SPMS; in contrast, changes in cord MD and volume were comparable in the three groups (Agosta 2007).

1.2.2.3 Magnetization transfer imaging

MTI is a particularly promising quantitative technique for the study of PPMS, because it is sensitive to the subtle pathological processes which cause tissue injury in the NABT. MT ratio (MTR) measures are derived from the MT images, and reflect the efficiency of magnetization exchange between macromolecules and tissue water (see section 2.8). MTR is altered by processes which affect the balance between macromolecules, most often related to myelin, and brain water. Animal and *post mortem* studies have shown that these processes include oedema, inflammation, and gliosis, but that MTR particularly reflects demyelination and axonal loss (Schmierer 2004, van Waesberghe 1999, Brochet 1999). In MS, MTR reduction has been shown to precede the appearance of lesions on T2-weighted imaging (Filippi 1998), and MTR provides an accurate quantitative measure of the extent of demyelination and repair within lesions (Chen 2007, Filippi 1999). In established PPMS, widespread clinically eloquent MTR reduction has been demonstrated in the NABT (Rovaris 2008) and also in the spinal cord (Nijeholt 2000). In early PPMS, MTR reduction is evident in the grey and NAWM, and correlates with disability (Ramio-Torrenta 2006) .

1.3 Conclusions

PPMS patients seldom experience relapses, and provide a relatively pure model for the study of progression in MS. This is reflected pathologically by comparatively modest focal inflammation and marked NABT injury. There are no effective disease modifying treatments for PPMS, and there are a number of challenges which impede clinical trials. MRI studies allow investigation of the disease process *in vivo*; however, correlation between conventional MRI parameters and clinical function are modest. Clinico-radiological correlation may be improved using quantitative techniques which assess disease burden more sensitively, through the inclusion of the NABT. Furthermore, targeting PPMS at the earliest stage, when disability accrual appears to influence future deterioration, may further augment clinico-radiological correlation. To date, studies in early PPMS have demonstrated marked, clinically eloquent injury to the NABT, as well as a surprisingly high proportion of active inflammatory lesions.

References

1. Double-masked trial of azathioprine in multiple sclerosis. British and Dutch Multiple Sclerosis Azathioprine Trial Group. *Lancet* 1988; 2: 179-183.
2. Agosta F, Absinta M, Sormani MP *et al.* In vivo assessment of cervical cord damage in MS patients: a longitudinal diffusion tensor MRI study. *Brain* 2007; 130: 2211-2219.
3. Agosta F, Benedetti B, Rocca MA *et al.* Quantification of cervical cord pathology in primary progressive MS using diffusion tensor MRI. *Neurology* 2005; 64: 631-635.
4. Albert M, Antel J, Bruck W, Stadelmann C. Extensive cortical remyelination in patients with chronic multiple sclerosis. *Brain Pathol.* 2007; 17: 129-138.
5. Alonso A, Jick SS, Olek MJ, Hernan MA. Incidence of multiple sclerosis in the United Kingdom : Findings from a population-based cohort. *J.Neurol.* 2007; 254: 1736-1741.
6. Alter M, Kahana E, Zilber N, Miller A. Multiple sclerosis frequency in Israel's diverse populations. *Neurology* 2006; 66: 1061-1066.
7. Andersson PB, Waubant E, Gee L, Goodkin DE. Multiple sclerosis that is progressive from the time of onset: clinical characteristics and progression of disability. *Arch.Neurol.* 1999; 56: 1138-1142.
8. Ascherio A, Munger KL. Environmental risk factors for multiple sclerosis. Part I: the role of infection. *Ann.Neurol.* 2007; 61: 288-299.
9. Barcellos LF, Sawcer S, Ramsay PP *et al.* Heterogeneity at the HLA-DRB1 locus and risk for multiple sclerosis. *Hum.Mol.Genet.* 2006; 15: 2813-2824.
10. Barkhof F. The clinico-radiological paradox in multiple sclerosis revisited. *Curr Opin Neurol* 2002; 15: 239-245.
11. Barnett MH, Prineas JW. Relapsing and remitting multiple sclerosis: pathology of the newly forming lesion. *Ann Neurol* 2004; 55: 458-468.
12. Bergendal G, Fredrikson S, Almkvist O. Selective decline in information processing in subgroups of multiple sclerosis: an 8-year longitudinal study. *Eur Neurol* 2007; 57: 193-202.
13. Bergers E, Bot JC, van d, V *et al.* Diffuse signal abnormalities in the spinal cord in multiple sclerosis: direct postmortem in situ magnetic resonance imaging correlated with in vitro high-resolution magnetic resonance imaging and histopathology. *Ann Neurol* 2002; 51: 652-656.
14. Bieniek M, Altmann DR, Davies GR *et al.* Cord atrophy separates early primary progressive and relapsing remitting multiple sclerosis. *J Neurol Neurosurg Psychiatry* 2006; 77: 1036-1039.
15. Bo L, Geurts JJ, van d, V, Polman C, Barkhof F. Lack of correlation between cortical demyelination and white matter pathologic changes in multiple sclerosis. *Arch Neurol* 2007; 64: 76-80.
16. Boiko A, Vorobeychik G, Paty D, Devonshire V, Sadovnick D. Early onset multiple sclerosis: a longitudinal study. *Neurology* 2002; 59: 1006-1010.

17. Bowen JD, Maravilla K, Margolin SB. Open-label study of pirfenidone in patients with progressive forms of multiple sclerosis. *Mult Scler* 2003; 9: 280-283.
18. Breij EC, Brink BP, Veerhuis R *et al.* Homogeneity of active demyelinating lesions in established multiple sclerosis. *Ann.Neurol.* 2008; 63: 16-25.
19. Brochet B, Dousset V. Pathological correlates of magnetization transfer imaging abnormalities in animal models and humans with multiple sclerosis. *Neurology* 1999; 53: S12-S17.
20. Bruck W, Bitsch A, Kolenda H, Bruck Y, Stiefel M, Lassmann H. Inflammatory central nervous system demyelination: correlation of magnetic resonance imaging findings with lesion pathology. *Ann Neurol* 1997; 42: 783-793.
21. Bruck W, Lucchinetti C, Lassmann H. The pathology of primary progressive multiple sclerosis. *Mult.Scler.* 2002; 8: 93-97.
22. Cabre P, Heinzlef O, Merle H *et al.* MS and neuromyelitis optica in Martinique (French West Indies). *Neurology* 2001; 56: 507-514.
23. Cader S, Johansen-Berg H, Wylezinska M *et al.* Discordant white matter N-acetylaspartate and diffusion MRI measures suggest that chronic metabolic dysfunction contributes to axonal pathology in multiple sclerosis. *Neuroimage* 2007; 36: 19-27.
24. Camp SJ, Stevenson VL, Thompson AJ *et al.* A longitudinal study of cognition in primary progressive multiple sclerosis. *Brain* 2005; 128: 2891-2898.
25. Chen JT, Kuhlmann T, Jansen GH *et al.* Voxel-based analysis of the evolution of magnetization transfer ratio to quantify remyelination and demyelination with histopathological validation in a multiple sclerosis lesion. *Neuroimage* 2007; 36: 1152-1158.
26. Cheng Q, Miao L, Zhang J *et al.* A population-based survey of multiple sclerosis in Shanghai, China. *Neurology* 2007; 68: 1495-1500.
27. Ciccarelli O, Giugni E, Paolillo A *et al.* Magnetic resonance outcome of new enhancing lesions in patients with relapsing-remitting multiple sclerosis. *Eur J Neurol* 1999; 6: 455-459.
28. Ciccarelli O, Werring DJ, Wheeler-Kingshott CA *et al.* Investigation of MS normal-appearing brain using diffusion tensor MRI with clinical correlations. *Neurology* 2001; 56: 926-933.
29. Comi G, Filippi M, Martinelli V *et al.* Brain MRI correlates of cognitive impairment in primary and secondary progressive multiple sclerosis. *J Neurol Sci* 1995; 132: 222-227.
30. Compston A, Coles A. Multiple sclerosis. *Lancet* 2002; 359: 1221-1231.
31. Confavreux C, Vukusic S. Age at disability milestones in multiple sclerosis. *Brain* 2006b; 129: 595-605.
32. Confavreux C, Vukusic S. Natural history of multiple sclerosis: a unifying concept. *Brain* 2006a; 129: 606-616.
33. Confavreux C, Vukusic S, Adeleine P. Early clinical predictors and progression of irreversible disability in multiple sclerosis: an amnesic process. *Brain* 2003; 126: 770-782.
34. Confavreux C, Vukusic S, Moreau T, Adeleine P. Relapses and progression of disability in multiple sclerosis. *N.Engl.J.Med.* 2000; 343: 1430-1438.

35. Cottrell DA, Kremenchutzky M, Rice GP *et al.* The natural history of multiple sclerosis: a geographically based study. 5. The clinical features and natural history of primary progressive multiple sclerosis. *Brain* 1999; 122 (Pt 4): 625-639.
36. Cournu-Rebeix I, Genin E, Leray E *et al.* HLA-DRB1(*)15 allele influences the later course of relapsing remitting multiple sclerosis. *Genes Immun.* 2008.
37. Cutter GR, Baier ML, Rudick RA *et al.* Development of a multiple sclerosis functional composite as a clinical trial outcome measure. *Brain* 1999; 122 (Pt 5): 871-882.
38. de Sonneville LM, Boringa JB, Reuling IE, Lazeron RH, Ader HJ, Polman CH. Information processing characteristics in subtypes of multiple sclerosis. *Neuropsychologia* 2002; 40: 1751-1765.
39. Dean G, Elian M. Age at immigration to England of Asian and Caribbean immigrants and the risk of developing multiple sclerosis. *J.Neurol.Neurosurg.Psychiatry* 1997; 63: 565-568.
40. Debouverie M, Taillandier L, Pittion-Vouyovitch S, Louis S, Vespignani H. Clinical follow-up of 304 patients with multiple sclerosis three years after mitoxantrone treatment. *Mult Scler* 2007; 13: 626-631.
41. Denney DR, Lynch SG, Parmenter BA. A 3-year longitudinal study of cognitive impairment in patients with primary progressive multiple sclerosis: Speed matters. *J Neurol Sci* 2008; 267: 129-136.
42. Dutta R, Trapp BD. Pathogenesis of axonal and neuronal damage in multiple sclerosis. *Neurology* 2007; 68: S22-S31.
43. Ebers GC. Natural history of primary progressive multiple sclerosis. *Mult.Scler.* 2004; 10 Suppl 1: S8-13.
44. Ebers GC. Environmental factors and multiple sclerosis. *Lancet Neurol.* 2008; 7: 268-277.
45. Ehrenreich H, Fischer B, Norra C *et al.* Exploring recombinant human erythropoietin in chronic progressive multiple sclerosis. *Brain* 2007; 130: 2577-2588.
46. Elian M, Nightingale S, Dean G. Multiple sclerosis among United Kingdom-born children of immigrants from the Indian subcontinent, Africa and the West Indies. *J.Neurol.Neurosurg.Psychiatry* 1990; 53: 906-911.
47. Farrell RA, Antony D, Wall GR *et al.* Humoral immune response to EBV in multiple sclerosis is associated with disease activity on MRI. *Neurology* 2009; 73: 32-38.
48. Fassas A, Passweg JR, Anagnostopoulos A *et al.* Hematopoietic stem cell transplantation for multiple sclerosis. A retrospective multicenter study. *J Neurol* 2002; 249: 1088-1097.
49. Filippi M. Magnetization transfer imaging to monitor the evolution of individual multiple sclerosis lesions. *Neurology* 1999; 53: S18-S22.
50. Filippi M, Rocca MA, Martino G, Horsfield MA, Comi G. Magnetization transfer changes in the normal appearing white matter precede the appearance of enhancing lesions in patients with multiple sclerosis. *Ann.Neurol.* 1998; 43: 809-814.
51. Filippi M, Rovaris M, Rocca MA. Imaging primary progressive multiple sclerosis: the contribution of structural, metabolic, and functional MRI techniques. *Mult Scler* 2004; 10 Suppl 1: S36-S44.

52. Fisher E, Chang A, Fox RJ *et al.* Imaging correlates of axonal swelling in chronic multiple sclerosis brains. *Ann.Neurol.* 2007; 62: 219-228.
53. Foong J, Rozewicz L, Quaghebeur G *et al.* Executive function in multiple sclerosis. The role of frontal lobe pathology. *Brain* 1997; 120 (Pt 1): 15-26.
54. Frohman EM, Racke MK, Raine CS. Multiple sclerosis--the plaque and its pathogenesis. *N.Engl.J.Med.* 2006; 354: 942-955.
55. Gaudino EA, Chiaravalloti ND, DeLuca J, Diamond BJ. A comparison of memory performance in relapsing-remitting, primary progressive and secondary progressive, multiple sclerosis. *Neuropsychiatry Neuropsychol.Behav.Neurol* 2001; 14: 32-44.
56. Geurts JJ, Blezer EL, Vrenken H *et al.* Does high-field MR imaging improve cortical lesion detection in multiple sclerosis? *J.Neurol.* 2008; 255: 183-191.
57. Gilmore CP, Bo L, Owens T, Lowe J, Esiri MM, Evangelou N. Spinal cord gray matter demyelination in multiple sclerosis-a novel pattern of residual plaque morphology. *Brain Pathol* 2006; 16: 202-208.
58. Giovannoni G, Ebers G. Multiple sclerosis: the environment and causation. *Curr.Opin.Neurol.* 2007; 20: 261-268.
59. Goodkin DE, Rudick RA, VanderBrug MS *et al.* Low-dose (7.5 mg) oral methotrexate reduces the rate of progression in chronic progressive multiple sclerosis. *Ann Neurol* 1995; 37: 30-40.
60. Hafler DA, Compston A, Sawcer S *et al.* Risk alleles for multiple sclerosis identified by a genomewide study. *N Engl J Med* 2007; 357: 851-862.
61. Hensiek AE, Seaman SR, Barcellos LF *et al.* Familial effects on the clinical course of multiple sclerosis. *Neurology* 2007; 68: 376-383.
62. Hernan MA, Jick SS, Logroscino G, Olek MJ, Ascherio A, Jick H. Cigarette smoking and the progression of multiple sclerosis. *Brain* 2005; 128: 1461-1465.
63. Hobart J, Freeman J, Thompson A. Kurtzke scales revisited: the application of psychometric methods to clinical intuition. *Brain* 2000; 123 (Pt 5): 1027-1040.
64. Ingle GT, Sastre-Garriga J, Miller DH, Thompson AJ. Is inflammation important in early PPMS? a longitudinal MRI study. *J.Neurol.Neurosurg.Psychiatry* 2005; 76: 1255-1258.
65. Ingle GT, Stevenson VL, Miller DH *et al.* Two-year follow-up study of primary and transitional progressive multiple sclerosis. *Mult.Scler.* 2002; 8: 108-114.
66. Ingle GT, Stevenson VL, Miller DH, Thompson AJ. Primary progressive multiple sclerosis: a 5-year clinical and MR study. *Brain* 2003b; 126: 2528-2536.
67. Ingle GT, Stevenson VL, Miller DH, Thompson AJ. Primary progressive multiple sclerosis: a 5-year clinical and MR study. *Brain* 2003a; 126: 2528-2536.
68. Jenkins TM, Khaleeli Z, Thompson AJ. Diagnosis and management of primary progressive multiple sclerosis. *Minerva Med* 2008; 99: 141-155.
69. Kalkers NF, Barkhof F, Bergers E, van SR, Polman CH. The effect of the neuroprotective agent riluzole on MRI parameters in primary progressive multiple sclerosis: a pilot study. *Mult Scler* 2002; 8: 532-533.

70. Kantarci O, Siva A, Eraksoy M *et al.* Survival and predictors of disability in Turkish MS patients. Turkish Multiple Sclerosis Study Group (TUMSSG). *Neurology* 1998; 51: 765-772.
71. Kezele IB, Chen JT, Arnold DL, Collins DL. The relation of focal white matter signal abnormality and focal volume loss in multiple sclerosis. *Mult.Scler.* 2007; 13: 809-813.
72. Kidd D, Thorpe JW, Thompson AJ *et al.* Spinal cord MRI using multi-array coils and fast spin echo. II. Findings in multiple sclerosis. *Neurology* 1993; 43: 2632-2637.
73. Koch M, van HA, Uyttenboogaart M, De KJ. Cigarette smoking and progression in multiple sclerosis. *Neurology* 2007; 69: 1515-1520.
74. Kragt JJ, Nielsen IM, van der Linden FA, Uitdehaag BM, Polman CH. How similar are commonly combined criteria for EDSS progression in multiple sclerosis? *Mult.Scler.* 2006; 12: 782-786.
75. Kragt JJ, Thompson AJ, Montalban X *et al.* Responsiveness and predictive value of EDSS and MSFC in primary progressive MS. *Neurology* 2008.
76. Kraus JA, Schutze C, Brokate B, Kroger B, Schwendemann G, Hildebrandt H. Discriminant analysis of the cognitive performance profile of MS patients differentiates their clinical course. *J Neurol* 2005; 252: 808-813.
77. Kremenchutzky M, Rice GP, Baskerville J, Wingerchuk DM, Ebers GC. The natural history of multiple sclerosis: a geographically based study 9: observations on the progressive phase of the disease. *Brain* 2006; 129: 584-594.
78. Kurtzke JF. Rating neurologic impairment in multiple sclerosis: an expanded disability status scale (EDSS). *Neurology* 1983; 33: 1444-1452.
79. Kutzelnigg A, Faber-Rod JC, Bauer J *et al.* Widespread demyelination in the cerebellar cortex in multiple sclerosis. *Brain Pathol.* 2007; 17: 38-44.
80. Kutzelnigg A, Lucchinetti CF, Stadelmann C *et al.* Cortical demyelination and diffuse white matter injury in multiple sclerosis. *Brain* 2005; 128: 2705-2712.
81. Lassmann H, Bruck W, Lucchinetti CF. The immunopathology of multiple sclerosis: an overview. *Brain Pathol* 2007; 17: 210-218.
82. Leary SM, Miller DH, Stevenson VL, Brex PA, Chard DT, Thompson AJ. Interferon beta-1a in primary progressive MS: an exploratory, randomized, controlled trial. *Neurology* 2003; 60: 44-51.
83. Leary SM, Thompson AJ. Primary progressive multiple sclerosis : current and future treatment options. *CNS.Drugs* 2005; 19: 369-376.
84. Lee MA, Smith S, Palace J *et al.* Spatial mapping of T2 and gadolinium-enhancing T1 lesion volumes in multiple sclerosis: evidence for distinct mechanisms of lesion genesis? *Brain* 1999; 122 (Pt 7): 1261-1270.
85. Losseff NA, Webb SL, O'Riordan JI *et al.* Spinal cord atrophy and disability in multiple sclerosis. A new reproducible and sensitive MRI method with potential to monitor disease progression. *Brain* 1996; 119 (Pt 3): 701-708.
86. Lublin FD, Reingold SC. Defining the clinical course of multiple sclerosis: results of an international survey. National Multiple Sclerosis Society (USA) Advisory Committee on Clinical Trials of New Agents in Multiple Sclerosis. *Neurology* 1996; 46: 907-911.

87. Lucchinetti C, Bruck W. The pathology of primary progressive multiple sclerosis. *Mult Scler* 2004; 10 Suppl 1: S23-S30.
88. Lucchinetti C, Bruck W, Parisi J, Scheithauer B, Rodriguez M, Lassmann H. Heterogeneity of multiple sclerosis lesions: implications for the pathogenesis of demyelination. *Ann.Neurol.* 2000; 47: 707-717.
89. Maghzi AH, Etemadifar M, Saadatnia M. Clinical and demographical characteristics of primary progressive multiple sclerosis in Isfahan, Iran. *Eur.J.Neurol.* 2007; 14: 403-407.
90. Magliozzi R, Howell O, Vora A *et al.* Meningeal B-cell follicles in secondary progressive multiple sclerosis associate with early onset of disease and severe cortical pathology. *Brain* 2007; 130: 1089-1104.
91. McDonald WI, Compston A, Edan G *et al.* Recommended diagnostic criteria for multiple sclerosis: guidelines from the International Panel on the diagnosis of multiple sclerosis. *Ann.Neurol.* 2001; 50: 121-127.
92. McKay FC, Swain LI, Schibeci SD *et al.* Haplotypes of the interleukin 7 receptor alpha gene are correlated with altered expression in whole blood cells in multiple sclerosis. *Genes Immun.* 2008; 9: 1-6.
93. Meier DS, Weiner HL, Guttman CR. MR imaging intensity modeling of damage and repair in multiple sclerosis: relationship of short-term lesion recovery to progression and disability. *AJNR Am J Neuroradiol* 2007; 28: 1956-1963.
94. Miller DH, Leary SM. Primary-progressive multiple sclerosis. *Lancet Neurol* 2007; 6: 903-912.
95. Minneboo A, Uitdehaag BM, Ader HJ, Barkhof F, Polman CH, Castelijns JA. Patterns of enhancing lesion evolution in multiple sclerosis are uniform within patients. *Neurology* 2005; 65: 56-61.
96. Modi G, Mochan A, du TM, Stander I. Multiple sclerosis in South Africa. *S Afr.Med J* 2008; 98: 391-393.
97. Monson NL, Cravens PD, Frohman EM, Hawker K, Racke MK. Effect of rituximab on the peripheral blood and cerebrospinal fluid B cells in patients with primary progressive multiple sclerosis. *Arch Neurol* 2005; 62: 258-264.
98. Montalban X. Overview of European pilot study of interferon beta-1b in primary progressive multiple sclerosis. *Mult Scler* 2004; 10 Suppl 1: S62-S64.
99. Munger KL, Levin LI, Hollis BW, Howard NS, Ascherio A. Serum 25-hydroxyvitamin D levels and risk of multiple sclerosis. *JAMA* 2006; 296: 2832-2838.
100. Narayana PA, Wolinsky JS, Rao SB, He R, Mehta M. Multicentre proton magnetic resonance spectroscopy imaging of primary progressive multiple sclerosis. *Mult.Scler.* 2004; 10 Suppl 1: S73-S78.
101. Neema M, Stankiewicz J, Arora A, Guss ZD, Bakshi R. MRI in multiple sclerosis: what's inside the toolbox? *Neurotherapeutics.* 2007; 4: 602-617.
102. Nijeholt GJ, Castelijns JA, Lazeron RH *et al.* Magnetization transfer ratio of the spinal cord in multiple sclerosis: relationship to atrophy and neurologic disability. *J Neuroimaging* 2000; 10: 67-72.

103. Nijeholt GJ, van Walderveen MA, Castelijns JA *et al.* Brain and spinal cord abnormalities in multiple sclerosis. Correlation between MRI parameters, clinical subtypes and symptoms. *Brain* 1998; 121 (Pt 4): 687-697.
104. Patani R, Balaratnam M, Vora A, Reynolds R. Remyelination can be extensive in multiple sclerosis despite a long disease course. *Neuropathol.Appl.Neurobiol.* 2007; 33: 277-287.
105. Patrikios P, Stadelmann C, Kutzelnigg A *et al.* Remyelination is extensive in a subset of multiple sclerosis patients. *Brain* 2006; 129: 3165-3172.
106. Peterson JW, Bo L, Mork S, Chang A, Trapp BD. Transected neurites, apoptotic neurons, and reduced inflammation in cortical multiple sclerosis lesions. *Ann.Neurol.* 2001; 50: 389-400.
107. Pirko I, Lucchinetti CF, Sriram S, Bakshi R. Gray matter involvement in multiple sclerosis. *Neurology* 2007; 68: 634-642.
108. Pirko I, Rodriguez M. Pulsed intravenous methylprednisolone therapy in progressive multiple sclerosis: need for a controlled trial. *Arch Neurol* 2004; 61: 1148-1149.
109. Pohlau D, Przuntek H, Sailer M *et al.* Intravenous immunoglobulin in primary and secondary chronic progressive multiple sclerosis: a randomized placebo controlled multicentre study. *Mult Scler* 2007; 13: 1107-1117.
110. Polman CH, Reingold SC, Edan G *et al.* Diagnostic criteria for multiple sclerosis: 2005 revisions to the "McDonald Criteria". *Ann.Neurol.* 2005; 58: 840-846.
111. Poser CM, Paty DW, Scheinberg L *et al.* New diagnostic criteria for multiple sclerosis: guidelines for research protocols. *Ann.Neurol.* 1983; 13: 227-231.
112. Prineas JW, Kwon EE, Cho ES *et al.* Immunopathology of secondary-progressive multiple sclerosis. *Ann Neurol* 2001; 50: 646-657.
113. Pugliatti M, Rosati G, Carton H *et al.* The epidemiology of multiple sclerosis in Europe. *Eur.J.Neurol.* 2006; 13: 700-722.
114. Ramio-Torrenta L, Sastre-Garriga J, Ingle GT *et al.* Abnormalities in normal appearing tissues in early primary progressive multiple sclerosis and their relation to disability: a tissue specific magnetisation transfer study. *J.Neurol.Neurosurg.Psychiatry* 2006; 77: 40-45.
115. Renoux C, Vukusic S, Mikaeloff Y *et al.* Natural history of multiple sclerosis with childhood onset. *N.Engl.J.Med.* 2007; 356: 2603-2613.
116. Revesz T, Kidd D, Thompson AJ, Barnard RO, McDonald WI. A comparison of the pathology of primary and secondary progressive multiple sclerosis. *Brain* 1994; 117 (Pt 4): 759-765.
117. Rice GP, Filippi M, Comi G. Cladribine and progressive MS: clinical and MRI outcomes of a multicenter controlled trial. Cladribine MRI Study Group. *Neurology* 2000; 54: 1145-1155.
118. Rot U, Mesec A. Clinical, MRI, CSF and electrophysiological findings in different stages of multiple sclerosis. *Clin Neurol Neurosurg* 2006; 108: 271-274.
119. Rovaris M, Gallo A, Valsasina P *et al.* Short-term accrual of gray matter pathology in patients with progressive multiple sclerosis: an in vivo study using diffusion tensor MRI. *Neuroimage.* 2005; 24: 1139-1146.

120. Rovaris M, Judica E, Gallo A *et al.* Grey matter damage predicts the evolution of primary progressive multiple sclerosis at 5 years. *Brain* 2006; 129: 2628-2634.
121. Rovaris M, Judica E, Sastre-Garriga J *et al.* Large-scale, multicentre, quantitative MRI study of brain and cord damage in primary progressive multiple sclerosis. *Mult Scler* 2008.
122. Runmarker B, Andersen O. Prognostic factors in a multiple sclerosis incidence cohort with twenty-five years of follow-up. *Brain* 1993; 116 (Pt 1): 117-134.
123. Sadovnick AD, Duquette P, Herrera B, Yee IM, Ebers GC. A timing-of-birth effect on multiple sclerosis clinical phenotype. *Neurology* 2007; 69: 60-62.
124. Sajja BR, Narayana PA, Wolinsky JS, Ahn CW. Longitudinal magnetic resonance spectroscopic imaging of primary progressive multiple sclerosis patients treated with glatiramer acetate: multicenter study. *Mult Scler* 2008; 14: 73-80.
125. Sastre-Garriga J, Ingle GT, Chard DT *et al.* Metabolite changes in normal-appearing gray and white matter are linked with disability in early primary progressive multiple sclerosis. *Arch.Neurol.* 2005a; 62: 569-573.
126. Sastre-Garriga J, Ingle GT, Chard DT, Ramio-Torrenta L, Miller DH, Thompson AJ. Grey and white matter atrophy in early clinical stages of primary progressive multiple sclerosis. *Neuroimage.* 2004; 22: 353-359.
127. Sastre-Garriga J, Ingle GT, Rovaris M *et al.* Long-term clinical outcome of primary progressive MS: predictive value of clinical and MRI data. *Neurology* 2005b; 65: 633-635.
128. Sawcer S. The complex genetics of multiple sclerosis: pitfalls and prospects. *Brain* 2008; 131: 3118-3131.
129. Schmierer K, Scaravilli F, Altmann DR, Barker GJ, Miller DH. Magnetization transfer ratio and myelin in postmortem multiple sclerosis brain. *Ann.Neurol.* 2004; 56: 407-415.
130. Sharrack B, Hughes RA, Soudain S, Dunn G. The psychometric properties of clinical rating scales used in multiple sclerosis. *Brain* 1999; 122 (Pt 1): 141-159.
131. Sijens PE, Irwan R, Potze JH, Mostert JP, De KJ, Oudkerk M. Analysis of the human brain in primary progressive multiple sclerosis with mapping of the spatial distributions using 1H MR spectroscopy and diffusion tensor imaging. *Eur Radiol* 2005; 15: 1686-1693.
132. Sijens PE, Mostert JP, Oudkerk M, De KJ. (1)H MR spectroscopy of the brain in multiple sclerosis subtypes with analysis of the metabolite concentrations in gray and white matter: initial findings. *Eur Radiol* 2006; 16: 489-495.
133. Silver N, Lai M, Symms M, Barker G, McDonald I, Miller D. Serial gadolinium-enhanced and magnetization transfer imaging to investigate the relationship between the duration of blood-brain barrier disruption and extent of demyelination in new multiple sclerosis lesions. *J Neurol* 1999; 246: 728-730.
134. Simon JH. Brain atrophy in multiple sclerosis: what we know and would like to know. *Mult.Scler.* 2006; 12: 679-687.
135. Smolders J, Menheere P, Kessels A, Damoiseaux J, Hupperts R. Association of vitamin D metabolite levels with relapse rate and disability in multiple sclerosis. *Mult.Scler.* 2008; 14: 1220-1224.
136. Stadelmann C, Albert M, Wegner C, Bruck W. Cortical pathology in multiple sclerosis. *Curr Opin Neurol* 2008; 21: 229-234.

137. Stevenson VL, Leary SM, Losseff NA *et al.* Spinal cord atrophy and disability in MS: a longitudinal study. *Neurology* 1998; 51: 234-238.
138. Stevenson VL, Miller DH, Leary SM *et al.* One year follow up study of primary and transitional progressive multiple sclerosis. *J.Neurol.Neurosurg.Psychiatry* 2000; 68: 713-718.
139. Stevenson VL, Miller DH, Rovaris M *et al.* Primary and transitional progressive MS: a clinical and MRI cross-sectional study. *Neurology* 1999; 52: 839-845.
140. Stuve O, Kita M, Pelletier D *et al.* Mitoxantrone as a potential therapy for primary progressive multiple sclerosis. *Mult Scler* 2004; 10 Suppl 1: S58-S61.
141. Thompson A. Overview of primary progressive multiple sclerosis (PPMS): similarities and differences from other forms of MS, diagnostic criteria, pros and cons of progressive diagnosis. *Mult.Scler.* 2004; 10 Suppl 1: S2-S7.
142. Thompson AJ, Kermod AG, MacManus DG *et al.* Patterns of disease activity in multiple sclerosis: clinical and magnetic resonance imaging study. *BMJ* 1990; 300: 631-634.
143. Thompson AJ, Kermod AG, Wicks D *et al.* Major differences in the dynamics of primary and secondary progressive multiple sclerosis. *Ann.Neurol.* 1991; 29: 53-62.
144. Thompson AJ, Montalban X, Barkhof F *et al.* Diagnostic criteria for primary progressive multiple sclerosis: a position paper. *Ann.Neurol.* 2000; 47: 831-835.
145. Thorpe JW, Kidd D, Moseley IF *et al.* Spinal MRI in patients with suspected multiple sclerosis and negative brain MRI. *Brain* 1996; 119 (Pt 3): 709-714.
146. Trapp BD, Ransohoff R, Rudick R. Axonal pathology in multiple sclerosis: relationship to neurologic disability. *Curr.Opin.Neurol.* 1999; 12: 295-302.
147. Tremlett H, Paty D, Devonshire V. The natural history of primary progressive MS in British Columbia, Canada. *Neurology* 2005; 65: 1919-1923.
148. Truyen L, van Waesberghe JH, van Walderveen MA *et al.* Accumulation of hypointense lesions ("black holes") on T1 spin-echo MRI correlates with disease progression in multiple sclerosis. *Neurology* 1996; 47: 1469-1476.
149. van Waesberghe JH, Kamphorst W, De Groot CJ *et al.* Axonal loss in multiple sclerosis lesions: magnetic resonance imaging insights into substrates of disability. *Ann.Neurol.* 1999; 46: 747-754.
150. van Walderveen MA, Kamphorst W, Scheltens P *et al.* Histopathologic correlate of hypointense lesions on T1-weighted spin-echo MRI in multiple sclerosis. *Neurology* 1998; 50: 1282-1288.
151. van Walderveen MA, Lycklama ANG, Ader HJ *et al.* Hypointense lesions on T1-weighted spin-echo magnetic resonance imaging: relation to clinical characteristics in subgroups of patients with multiple sclerosis. *Arch.Neurol.* 2001; 58: 76-81.
152. Vukusic S, Van B, V, Gosselin S, Confavreux C. Regional variations in the prevalence of multiple sclerosis in French farmers. *J.Neurol.Neurosurg.Psychiatry* 2007; 78: 707-709.
153. Wachowius U, Talley M, Silver N, Heinze HJ, Sailer M. Cognitive impairment in primary and secondary progressive multiple sclerosis. *J Clin Exp Neuropsychol.* 2005; 27: 65-77.

154. Wasay M, Ali S, Khatri IA *et al.* Multiple sclerosis in Pakistan. *Mult.Scler.* 2007; 13: 668-669.
155. Willer CJ, Dyment DA, Sadovnick AD, Rothwell PM, Murray TJ, Ebers GC. Timing of birth and risk of multiple sclerosis: population based study. *BMJ* 2005; 330: 120.
156. Wolinsky JS. The diagnosis of primary progressive multiple sclerosis. *J Neurol Sci* 2003; 206: 145-152.
157. Wolinsky JS. The PROMiSe trial: baseline data review and progress report. *Mult Scler* 2004; 10 Suppl 1: S65-S71.
158. Wolinsky JS, Narayana PA, O'Connor P *et al.* Glatiramer acetate in primary progressive multiple sclerosis: results of a multinational, multicenter, double-blind, placebo-controlled trial. *Ann.Neurol.* 2007; 61: 14-24.
159. Yamout B, Barada W, Tohme RA, Mehio-Sibai A, Khalifeh R, El-Hajj T. Clinical characteristics of multiple sclerosis in Lebanon. *J Neurol Sci* 2008; 270: 88-93.
160. Zephir H, de SJ, Duhamel A *et al.* Treatment of progressive forms of multiple sclerosis by cyclophosphamide: a cohort study of 490 patients. *J Neurol Sci* 2004; 218: 73-77.

Principles of MRI

CHAPTER 2

Magnetic resonance imaging (MRI) is a non-invasive technique used to image tissues in the human body *in vivo*. The first part of this chapter provides an overview of the basic principles of MRI; a full discussion of this complex subject necessitates an understanding of quantum mechanics, and is beyond the scope of this thesis. The latter part of the chapter discusses the sequences and post-processing techniques employed in the studies described in this thesis.

2.1 Nuclear magnetic resonance

Atomic nuclei contain protons, which are positively charged particles, and neutrons, which have no charge. Nuclei with an odd number of protons exhibit nuclear magnetism, a form of paramagnetism. Materials with this property do not generate a net magnetic field, but are able to interact with an external magnetic field. This interaction is the basis of nuclear magnetic resonance (McRobbie 2003).

The hydrogen atom has a nucleus consisting of a single proton. It is the most abundant atom in the human body and the most relevant paramagnetic nucleus for MR imaging studies. When it is placed in an external magnetic field (\mathbf{B}_0) it spins around its own axis, and thus exhibits a *magnetic dipole moment* or *spin*. At thermal equilibrium, the magnetic moment of each hydrogen nucleus is either aligned with \mathbf{B}_0 , in a low energy state, or at 180° to \mathbf{B}_0 in a high energy state. There is a very slight excess of protons aligned in the low energy state, which gives the 'bulk' or 'net' magnetization (\mathbf{M}) in the direction of \mathbf{B}_0 . The application of the external magnetic field causes the protons to rotate, or 'precess', around it, similar to the way a compass oscillates about the earth's magnetic field (see Figure 2a).

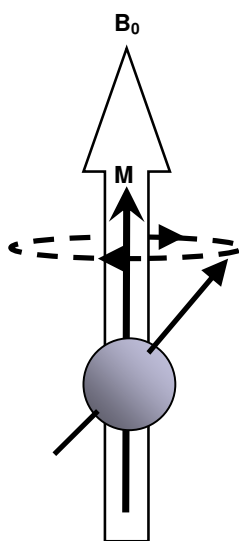


Figure 2a: Precession of protons

The external magnetic field, \mathbf{B}_0 , is depicted as a large arrow behind the proton. The magnetic dipole moment of the proton aligns towards this, in the low energy state, giving a bulk magnetization vector of \mathbf{M} , in the direction of \mathbf{B}_0 . The proton precesses around \mathbf{B}_0 , along the dashed line. In a substance with many protons, some protons will be in the low energy state, aligned towards \mathbf{B}_0 , and some in the high energy state, aligned in the opposite direction. \mathbf{M} is the sum of all the individual dipole moments, divided by the volume of the substance. At equilibrium there is a small excess of protons in the low energy state, so \mathbf{M} is aligned towards \mathbf{B}_0 .

The frequency at which the protons precess is called the Larmor frequency. It depends upon the strength of the external magnetic field, and a constant intrinsic to the nucleus, called the gyromagnetic ratio:

Larmor frequency (ω_0) = gyromagnetic ratio (γ) * external magnetic field (\mathbf{B}_0)

ω_0 is described in Herz (Hz) and \mathbf{B}_0 in Tesla. The stronger the magnetic field, the higher the Larmor frequency. For a hydrogen proton in a standard 1.5 Tesla scanner, the Larmor frequency is 64MHz.

An external radio-frequency (RF) pulse is described as being *on resonance* if it oscillates at the Larmor frequency. It is able to transfer energy to, or *excite*, the hydrogen nuclei because it is oscillating at the same frequency at which they precess. This excitation increases the number of magnetic moments which are in a high energy state, and tilts the direction of net magnetization (\mathbf{M}) away from \mathbf{B}_0 .

2.1.1 The NMR signal

The angle at which \mathbf{M} is rotated away from \mathbf{B}_0 , or the longitudinal axis, is called the *flip angle*, and it depends on the amplitude and the duration of the RF pulse. For example, a RF pulse applied orthogonally to \mathbf{B}_0 with a 90° flip angle converts all the longitudinal magnetization into transverse magnetization, with \mathbf{M} lying at 90° to \mathbf{B}_0 . The RF pulse also produces *phase coherence*, so that all the nuclei precess together in the transverse plane.

The presence of a component of magnetization in the transverse plane induces a voltage in the MR scanner's receiver coil, according to Faraday's laws of induction. This is the NMR signal, and its magnitude depends on the *magnetization vector*, or the amount of magnetization in the transverse plane.

2.2 Relaxation

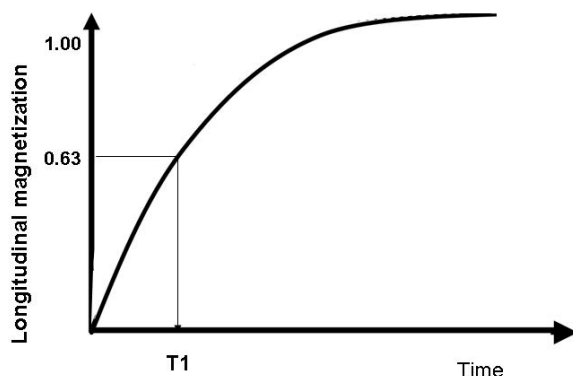
When the RF pulse is switched off, the protons lose energy and gradually return to thermal equilibrium, and the net magnetization returns towards \mathbf{B}_0 . The signal observed during this *relaxation* process is called free induction decay (FID). Relaxation is achieved through two concomitant and independent processes: protons regain longitudinal magnetization (T1 relaxation) and lose transverse magnetization (T2 relaxation).

2.2.1 T1 Relaxation (spin-lattice relaxation)

When the RF pulse is turned off, nuclei lose energy to their surroundings, or *lattice*. Many of them return to a low energy state, so that \mathbf{M} is once more aligned with \mathbf{B}_0 , and longitudinal magnetization is regained. The time that this takes depends on the intrinsic properties of the tissue, and it is an exponential process. It is described by the time constant T1, or the time taken for 63% of the spins to regain longitudinal magnetization (see Figure 2b). This time constant is used to describe the exponential process.

Figure 2b: The exponential curve for T1 relaxation

At time T1, 63% of the longitudinal magnetization has been regained.

2.2.2 T2 relaxation (spin-spin relaxation)

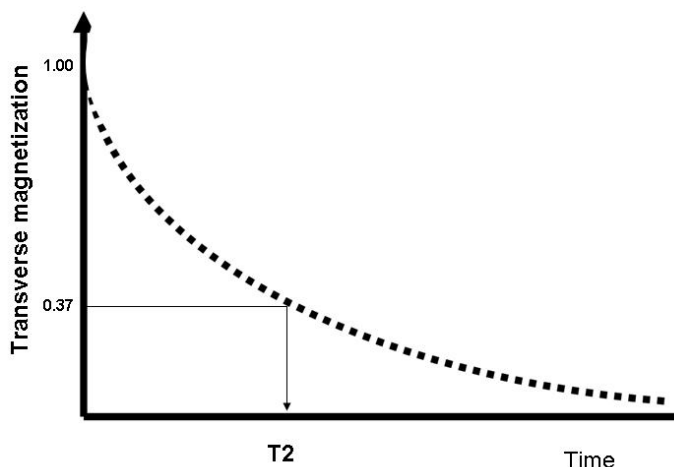
After the RF pulse has been turned off, the protons gradually lose energy to their neighbouring nuclei, as their magnetic fields interact. This causes variations in the precession frequency of each individual nucleus, and so reduces phase coherence and thus transverse magnetization. This exponential process is governed by a time constant T2, which is the time at which only 37% of the transverse magnetization remains (see Figure 2c).

Substances such as water are highly mobile with high inherent energy, while large molecules, such as fat, have a low inherent energy. Energy transfer is more efficient in larger molecules, and T1 relaxation time is therefore shorter in fat than water. There are greater spin-spin interactions when molecules are more tightly packed, thus protons in fats de-phase more rapidly and have a shorter T2 relaxation time than those in water, where the spins are farther apart. However, the magnetic field inside a scanner is distorted by imperfections in the magnetic coil, and variations in the sample itself, so that it is not truly homogeneous. Therefore protons lose phase coherence faster than expected from T2 effects, at a rate described by the time constant T2*. T2* describes both the T2

relaxation intrinsic to a tissue, and the relaxation effects of the magnetic field inhomogeneities extrinsic to the tissue.

Figure 2c: The exponential curve for T2 relaxation

At time T2 the signal has fallen to 37%.



2.3 The spin echo

It is not possible to reverse the loss of phase coherence due to the intrinsic effect of neighbouring spins in a specific tissue (T2 effects). It is, however, possible to reverse the loss of phase coherence which is due to main field inhomogeneities. One method is the application of a second RF pulse, with a 180° flip angle, to the de-phased nuclei. This has the effect of flipping the magnetic moments, so that those 'further back' along the precessional path are now 'at the front', and *vice-versa*. Precession continues at the same speed, so the nuclei which were precessing faster, and now find themselves 'further back', are able to 'catch up' with those at the front. This puts the nuclei back in phase (after an interval matching the time between the first and the second RF pulse) so that the NMR signal increases again, and is described as a *spin echo*. The total time between the first RF pulse and the formation of the echo is called echo time, or TE.

2.4 Image Formation

2.4.1 Spatial encoding

In order to obtain an MR image from the signal in the receiver coil, it is necessary to be able to locate where the NMR signal is coming from. This is achieved using linear magnetic field gradients. There are two ways of obtaining MR images of a three dimensional (3D) object: two dimensional (2D) spatial encoding, and 3D spatial encoding. To create a 2 dimensional image, the sample is divided into slices (through slice-selection), each of which is then further differentiated by applying frequency encoding in one dimension, and phase encoding in another (see below). For 3D images, frequency encoding is applied in one dimension and phase encoding in the remaining two.

2.4.1.1. Slice selection gradient (SS, G_{slice} , G_z)

The slice-selection direction is often indicated with 'z', although it does not necessarily coincide with the direction of \mathbf{B}_0 . A linear gradient is applied along the direction orthogonal to the planes to be imaged, so that the magnetic field changes strength at different locations along it. Thus at each location protons will precess at a different frequency to the rest of the sample. A RF pulse can therefore be applied at a frequency which is equal to the Larmor frequency of the protons at a specific location. In this way a specific *slice* of the sample can be selectively excited.

2.4.1.2. Phase encoding gradient (PE, G_{phase} , G_y)

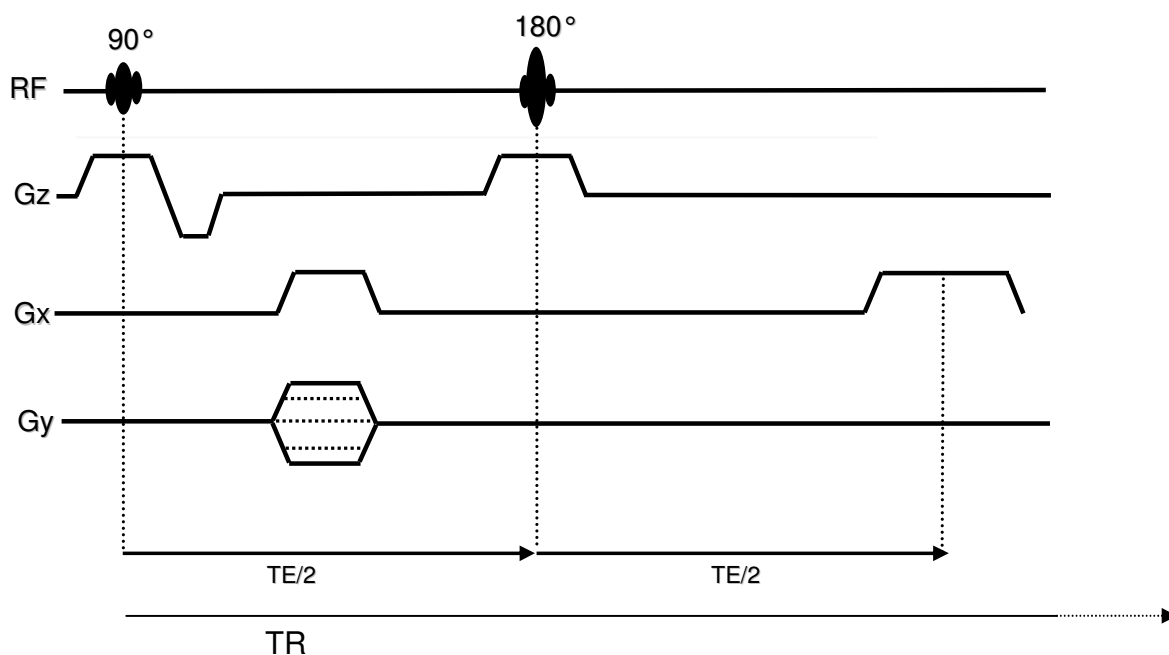
The phase encoding gradient is applied along the direction conventionally indicated as 'y', prior to sampling, and alters the magnetic field strength at different points. This changes the precessional frequency of the protons at each point, so that nuclei along the gradient lose phase coherence. This makes the phase of the protons dependent on their position along the gradient. This allows protons to be located within a slice, and the greater the PE gradient the finer the detail of information obtained. This process is repeated a number of times N , which determines the number of phase-encoding steps.

2.4.1.3. Frequency encoding gradient (FE , G_{read} , G_x)

A magnetic field gradient is applied in a direction orthogonal to the phase encoding gradient (the 'x' direction) during the measurement of the NMR signal. The frequency of the spins varies with the gradient, and so the signal changes with position along the gradient.

Figure 2d demonstrates how these steps are employed in a spin echo sequence. At the echo time, TE , the signal is received. The next excitation pulse follows after the repetition time, TR , has elapsed.

Figure 2d: The spin echo pulse sequence



A RF pulse is applied at 90° , with a slice select gradient. This is followed by the frequency encoding and phase encoding gradients, and a rephasing pulse at $TE/2$. At time TE the signal is produced. Time TR is the time between one excitation and the next.

By varying the TR and TE, different contrasts in intensity can be achieved, to help differentiate between tissues. Shortening the TR helps differentiate tissues on the basis of their longitudinal relaxation (T1-weighting), because those with a long T1 will not have had time to fully regain longitudinal magnetization before the next pulse. This reduces the transverse magnetization produced after the subsequent excitation, resulting in a smaller signal. Conversely, lengthening the TE helps to differentiate tissues on the basis of their T2-relaxation times (T2-weighting). It follows that a long TR and short TE minimises both T1 and T2 effects. In this case signal depends largely on the density of protons in the tissue (proton density [PD] weighting).

2.4.2 k-space

The receiver coil in the MR scanner receives information in the form of the NMR signal, and converts it into digits. Each digit represents the phase and frequency of signal at a specific point in time during scanning, and they are stored in an information matrix known as k-space. The order in which these data points are collected into k-space can be varied, but most often it is filled at regular intervals along the x and y directions. However, the trajectory always begins at the centre of k-space. The phase encoding gradient moves the trajectory vertically, along k_y , and the larger the gradient the further away from the origin. Similarly, the frequency gradient moves the trajectory horizontally, along k_x . Application of the 180° pulse will cause the trajectory to flip to the diametrically opposite position on the matrix. Low frequency, high amplitude data are recorded at the centre of k-space. They describe most aspects of the MR image, in particular the overall shape and contrast. High frequency, low amplitude data are recorded at the periphery of k-space. They define areas of rapid spatial variation (such as edges), and therefore contain information about the finer details of the image.

2.4.3 The Fourier Transformation

To convert the information stored in k-space into an image, each data point undergoes a mathematical process known as the Fourier transform. It changes the

data from the time to the frequency domain. Each pixel in the image can then be allocated a colour on the grayscale corresponding to the amplitude of the frequencies, or signal intensity, recorded at that location.

2.5 Sequences

There are many ways in which the spin echo acquisition sequence can be altered, so that scanning time can be reduced and different types of contrast obtained. Below I will describe the acquisitions which have been used for the studies in this thesis.

2.5.1 Fast/Turbo spin echo

(also known as RARE (Hennig 1986), rapid acquisition with relaxation enhancement)

In this sequence the 180° rephasing pulse is repeated, resulting in the formation of further spin echoes. The number of 180° pulses applied during TR is called the echo train length (ETL). After each new rephasing pulse, the phase encoding gradient is varied so that a different line of k-space can be filled for that slice. The scan time is decreased because the number of acquisitions necessary to fill k-space is reduced by a factor equivalent to the ETL. However, the use of large ETL's can result in image artefacts. Furthermore, it is necessary to control image contrast because each echo is acquired at a different TE, and therefore shows a different degree of T2-weighting. Image contrast is adjusted by assigning the echoes collected at the TE of interest to the low frequency signals, at the centre of k-space, where they have more influence on the image contrast. Those echoes collected at different TE's are assigned to the edge of k-space.

2.5.2 Interleaved or multi-echo sequences

Images with different contrasts can be gathered at the same time by using different echoes in the echo train to fill the k-space for different images. For example, in a

dual-echo sequence the first image is obtained at short TE. The second image is then obtained after a further 180° pulse, so the TE is longer and the image is more T2-weighted. The phase encoding gradient is kept the same, so that the same line of k-space is filled in both images. In this way interleaved PD and T2 images of the same slice can be obtained at almost the same time, without increasing acquisition length. It is also possible to employ longer echo trains, where the first part of the echo train produces the PD image, and the second part the T2 image, but several lines of k-space are sampled in each TR. In the studies described in this thesis, we have used an interleaved sequence to acquire co-registered PD and T2-weighted images as part of the magnetization transfer sequence (see section 2.8.3).

2.5.3 Gradient echo

Gradient echo sequences differ from the spin echo because the excitation pulse is applied at a flip angle which is typically less than 90° . This means that not all the longitudinal magnetization is converted to transverse magnetization, and TR and TE are reduced. In addition a gradient is used to rephase the protons instead of a 180° pulse, which reduces the TE. Although the sequence is faster, it can not compensate for magnetic field inhomogeneities and is susceptible to artefacts.

2.5.4 Three-Dimensional Fast Spoiled Gradient Recalled Echo (3D-FSPGR)

In this 3-D T1-weighted acquisition, the third dimension is provided by an additional phase encoding gradient, applied in the same direction as the slice selection gradient. For each slab excited by the slice-select gradients, there is a given number of phase-encodings. Thus the slice thickness is the slab thickness divided by the number of phase encodings, and it can be reduced by increasing the number of partitions per slab, without limiting the RF amplitude. To produce T1-weighting, the sequence can be preceded by an inversion RF pulse at 180° , which flips the longitudinal magnetization. Tissues begin their T1 relaxation from full saturation, so that the differences in their T1 relaxation times have greater influence on the signal produced. An RF excitation pulse is applied at a flip angle lower than 90° (typically of the order of 20°), and a bipolar readout gradient is used

to create an echo, as described above. However, because the TR is short, some transverse magnetization may remain when the next excitation occurs. This is destroyed using a *spoiler* gradient, which de-phases the spins. This acquisition has a high resolution and good differentiation between tissues. It is useful for examining brain structure and volume, and in our studies we have used it to measure brain atrophy (see section 2.7.1).

2.6 Use of Contrast agents

Altering acquisition parameters changes the contrast for the whole image. To specifically improve contrast in certain tissues, for example to differentiate between normal tissues and pathology, contrast agents are used to decrease T1 or T2 relaxation times.

2.6.1 Gadolinium

Gadolinium is a trivalent lanthanide metal with seven unpaired electrons. Following intravenous injection, it extravasates from the cerebral circulation in areas where the blood-brain barrier is damaged by inflammation. It has a large magnetic moment which causes a fluctuation in the local magnetic field. This reduces T1 relaxation time in the surrounding water molecules (McRobbie 2003), and produces a brighter signal on T1-weighted images (see Figure2e).

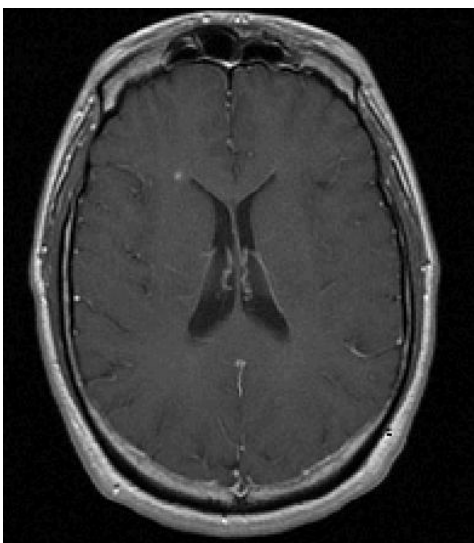


Figure 2e: T1-weighted image after injection with triple dose gadolinium

A gadolinium enhancing lesion is seen adjacent to the left frontal horn

In MS, gadolinium enhancement produces high signal in active inflammatory lesions, and most new lesions visible on T2 imaging enhance initially (Lee 1999). A number of studies have investigated how best to maximize the detection of new, active lesions. Imaging patients regularly (Tortorella 1999); including the spinal cord in the imaging protocol (Kidd 1993); imaging thirty minutes after injection rather than the standard five to seven minutes (Filippi 1995); using an MR sequence with thinner slices; using magnetization contrast for the images (Silver 1997), and using high field MR (Sicotte 2003) all increase the number of enhancing lesions detected in MS. The most useful adaptation identified to increase sensitivity in RRMS, however, has been an increase in the gadolinium dose from single (0.1mm/kg) to triple (0.3mmol/kg) (Filippi 2000). In PPMS, relatively few studies have been performed and it has not been established whether triple dose gadolinium increases sensitivity. In one small study, triple dose gadolinium increased sensitivity to lesion enhancement (Filippi 1995), but in another it conferred no benefit (Silver 1997).

To prevent toxic accumulation in body tissues, gadolinium is chelated with DTPA (forming gadolinium-diethylenetriaminepenta-acetic acid), so that it can be safely excreted by the kidneys. However, recent case reports of nephrogenic systemic fibrosis developing in patients with renal impairment have resulted in Food and drug administration (FDA) recommendations that renal function is always tested before gadolinium administration. There is a small risk of anaphylaxis, and the drug should only be given under medical supervision with resuscitation equipment and drugs to hand. Patients should be fully informed of the reasons for contrast administration, and the potential risks, prior to imaging.

2.7 Measuring brain volume

There are a wide variety of rapidly evolving techniques available to measure brain volume and atrophy from MRI. This section briefly discusses some of the techniques most commonly employed in multiple sclerosis imaging studies.

Specific areas of interest, or indeed the whole brain, may be outlined manually in two dimensions, and measured. In MS, the corpus callosum has often been studied in this way (Paolillo 2000), as a site of particular disease predilection. The technique is straightforward but time consuming, and limited by problems of intra- and inter-observer reproducibility. The use of simple individual measurements of ventricular dimension, which can be used as markers for atrophy, has also been explored (Butzkueven 2008).

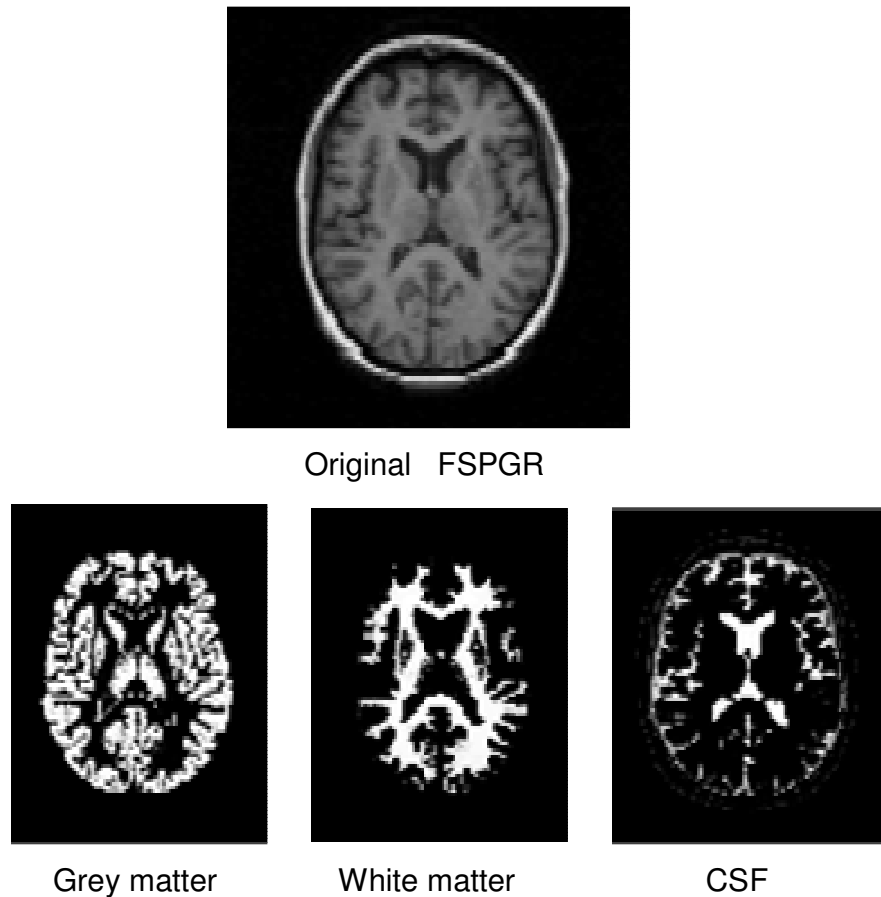
2.7.1 Segmentation-based techniques

This type of analysis involves separating segments of the brain from surrounding structures, and then measuring the volume of tissue within them. Segmentation on serial MRI allows measurement of the rate of atrophy. A semi-automated technique to measure central cerebral volume (Losseff 1996) has been widely used in PPMS (Stevenson 1999). This technique concentrates on between four and six axial slices (depending on slice thickness) at the centre of the brain, a common site for peri-ventricular lesions which is particularly vulnerable to atrophy. The brain is segmented from the relevant image slices using an optimum intensity threshold that removes non-brain structures. Manual editing may be necessary, which limits reproducibility, and the accuracy of the technique is very dependent on slice thickness and patient positioning within the scanner. SIENAX (Structural Image Evaluation, using Normalization, of Atrophy cross-sectional) is an alternative segmentation-based package (Smith 2002), in which the brain is extracted from the image using a tessellated mesh to model the surface, followed by application of a brain mask in stereotactic space to remove extra-cerebral tissue. Further grey matter, white matter and CSF segmentation is carried out on this extracted brain image in order to determine brain volume. This technique also includes an estimation of partial volume effects, and therefore greater volumetric accuracy, as well as automatically normalizing the brain volume for head-size thereby making cross-sectional analyses more sensitive. Manual editing may improve accuracy, and does not compromise the high inter-centre reproducibility (Jasperse 2007). MIDAS, a semi-automated intensity thresholding technique (Freeborough 1997),

identifies the brain/CSF boundary in order to segment the whole brain, or CSF in order to calculate ventricular volume (Dalton 2006).

In the work described in this thesis, the SPM99 and SPM2 packages (Statistical Parametric Mapping; Wellcome Department of Cognitive Neurology, London, UK)(Ashburner 1997) have been applied to segment 3-D FSPGR images (see section 2.5.4). All images are normalized to a template, based on the Montreal Neurological Institute template, and extra-cranial tissues are removed. Intensity inhomogeneities are corrected. Segmentation proceeds according to an *a priori* template derived from a database of normal brain images, in addition to information from individual pixel intensities. A probability map is produced, wherein each voxel is assigned a probability of belonging to a specific tissue class (see Figure 2f). The use of normal brain templates may pose problems when pathology markedly alters subjects' brain morphology, for example in brains with severe atrophy or a very high lesion load. Another problem for MS studies is that white matter lesions may be erroneously classified as grey matter (Anderson 2006). This problem is addressed by applying a lesion mask following segmentation, which overrides local tissue classifications in order to remove lesions from the volume measurement.

A recent study compared three brain volumetry methods for measuring grey and white matter: FAST, the segmentation tool from the FSL library (<http://www.fmrib.ox.ac.uk/fsl>); Freesurfer, an automated surface reconstruction tool for measuring cortical thickness (Fischl 2002), which also contains an automated segmentation algorithm; and SPM5, an updated version of SPM2. SPM5 was most consistent in measuring segment volumes longitudinally; however, maximum deviations of 3% occurred even with this technique, indicating the current limitations of sequential atrophy measurements (Klauschen 2008).

Figure 2f: Segmentation of FSPGR image in SPM2

The 3-D FSPGR image is segmented into grey matter, white matter and CSF using SPM2. Note the inclusion of peri-ventricular lesions, around the posterior horn of the lateral ventricle, in the grey matter segment; these are later removed by lesion masking.

2.7.2 Registration-based techniques

These methods provide a direct measure of brain volume *change* between serial images by matching the position of, or registering, the images. This may address the limitations for sequential segmentation-based measures described above. For example, SIENA (Structural Image Evaluation, using Normalization, of Atrophy) uses a tessellated mesh to model the edge of the brain surface, and shifts in this edge are measured over time (Smith 2001). BBSI (Brain Boundary shift integral) is

a technique which measures atrophy based on the difference in brain voxel intensities between registered images at the brain/CSF boundaries (Fox 1997). However, although these techniques may be more precise than segmentation-based approaches in assessing whole brain volume change over time (Anderson 2007), they can not examine specific brain segments, and lesions can not be removed from the analysis.

2.7.3 Voxel-based morphometry (VBM)

This fully automated technique localizes atrophy without an *a priori* hypothesis, providing an unbiased survey of the whole brain, or more usually the grey matter. Information about localized atrophy is lost using the whole-brain techniques described above, because areas of atrophy may be counterbalanced by relatively normal areas. In VBM, all images are registered to a template, so that the tissue concentration (or density) at each voxel can be compared between subject groups (Ashburner 2000). Areas where the tissue concentration in one group significantly differs from that in the other group are highlighted. Thus only regions where a significant proportion of the subjects have atrophy are identified, and there is less sensitivity to changes between groups in areas of high natural variance (Anderson 2006). In addition this method does not provide absolute measures of volume or atrophy for individual subjects.

There have been concerns that changes identified on VBM may be due to mis-registration, patient positioning or other artefacts rather than to actual differences in brain volume (Bookstein 2001), and that localizing changes on normalized, smoothed images may be misleading (Smith 2006). In addition, methodological variations such as the size of the smoothing kernel may have considerable impact on results (Jones 2005). Particular challenges in multiple sclerosis studies include the normalization of images after lesions have been removed (Audoin 2004). In the VBM study described in Chapter 4, we have attempted to address uncertainties regarding the accuracy of localization by performing a *post-hoc* analysis of our results. As we have confined our analysis to the grey matter, removal of visible T2 lesions has minimal impact on normalization; in addition, the application of a zero-

weighted lesion mask meant that voxels classified as containing lesions were not considered during the normalization. However, the strengths and limitations of this novel technique must be borne in mind when interpreting the results (see section 4.4.1.4). In this study we also applied a voxel-based approach to the analysis of MTR images, as discussed in the next section.

2.8 Magnetization Transfer Imaging (MTI)

Much of the work described in this thesis is based on the use of magnetization transfer imaging (MTI), a semi-quantitative MRI technique based on cross-relaxation and chemical exchange between protons in free water and those bound to macromolecules. Bound protons are often associated with proteins, such as myelin, and are restricted in their movement by the chemical environment. The proximity of other protons increases spin-spin interactions and reduces their T2 relaxation time, so that they are far less visible than free water protons on most MR sequences. However, using MTI the properties of the bound proton pool can be indirectly explored.

2.8.1 MTR

Protons in the bound pool are constantly exchanging magnetization with the free proton pool. They tend to have a very broad spectrum of precessional frequencies due to their varying molecular structures and to the local interaction with neighbouring spins. In contrast, free water protons all precess at similar frequencies. This makes bound protons sensitive to *off-resonance* radiation, at frequencies other than the Larmor frequency, and allows a preparatory off-resonance RF pulse to saturate (reduce to zero) the magnetization of bound protons with minimal direct effect on free protons. However, the bound protons then transfer magnetization to the free pool, via cross relaxation and chemical exchange. This reduces the PD-weighted signal (M_s) obtained in areas where there are bound protons, because the transverse magnetization of the free water protons has been reduced. The signal is then measured again in the absence of the

saturation pulse (M_0), and the difference between the two signals in each voxel gives the MTR:

$$\text{MTR} = 100 (M_0 - M_s / M_0) \text{ per cent units (pu)}$$

The MTR of a voxel is thus an indication of the size of the bound proton pool in that voxel, and is higher when the bound proton pool is larger. In the brain CSF, like free water, has an MTR value close to zero. White matter is abundant in myelin, so the bound proton pool is large and the MTR high. In the grey matter, there are fewer bound protons than white matter, but more than in CSF, and the MTR is intermediate.

2.8.2 Factors influencing MTR *in vivo*

There are several considerations which reduce the accuracy and applicability of this model in clinical practice. These relate to either the tissues themselves or the MR scanner.

2.8.2.1 Properties of the tissue

Essentially, MTR is determined by the exchange rate between the free and bound proton pools, and the size of the bound proton pool, but it is also influenced by the T1 relaxation time of the free water. Magnetization destruction is determined by the magnetization exchange rate multiplied by the size of the bound pool, and magnetization recovery by the inverse of the free water T1 relaxation time. This means that where there is pathology MTR may lose some sensitivity. For example, in an MS lesion, there is a reduction in myelin and therefore a reduction in the bound proton pool. However, there is a concomitant increase in T1 relaxation which counteracts this effect, resulting in only a very small change in the overall MTR. Thus the MTR reduction does not reflect the full extent of demyelination (Tofts 2004). However, the T1 effect is relatively small, and is minimized in our studies using a PD rather than T1-weighted acquisition sequence (McGowan 1999). Another consideration is that some direct saturation of the free pool is difficult to avoid, and total saturation of the bound proton pool can not be achieved

safely *in vivo*. However, it has been shown that greater saturation of the bound pool is not necessarily optimal for studying pathology in MS (Graham 1999) .

2.8.2.2 MR scanner parameters

The MTR is also affected by the offset frequency selected, the bandwidth, amplitude and duration of the MT pulse (Tofts 2006). Typically, the MT pulse is Gaussian or sinc, with a bandwidth of a few 100Hz, delivered at 1-5kHz off the frequency of the mobile water. Care must also be taken to accurately set the flip angle and to minimise transmit field non-uniformity, for example by using body coil excitation, to achieve a reproducible MTR (Tofts 2006).

In the work presented in this thesis, the considerations above are addressed because MTR is always compared between patients and normal controls, and all scans are performed on the same scanner, using the same parameters at each acquisition.

2.8.3 MT sequence

The MT sequence described in this thesis is an interleaved acquisition, producing inherently co-registered saturated and unsaturated PD-weighted MT images, a PD image, and a T2 image, for each slice (Barker 1996). Using an interleaved spin echo acquisition is relatively slow. To speed the acquisition, the saturated images for multiple slices are collected during one sequence, and then the unsaturated images. The TR is also reduced to speed up the acquisition, and this may increase T1-weighting. However, the production of co-registered images of different modalities is extremely helpful for lesion identification and marking, and the creation of accurate lesion masks.

2.8.4 Post-processing

Once the MTR for each voxel has been calculated according to the formula described above, an MTR map is created (see Fig 2g), which can be processed and analyzed in different ways.

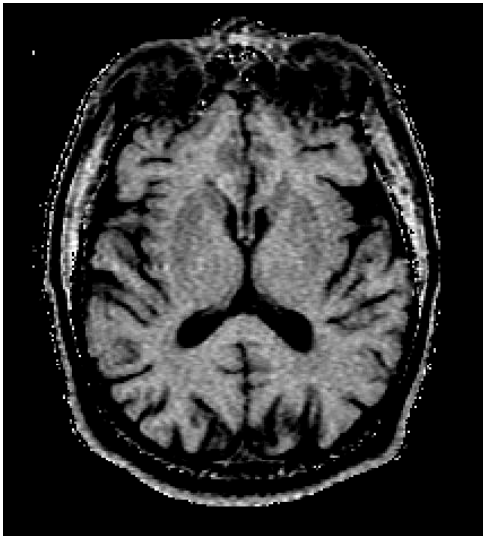


Figure 2g: MTR image

The image is derived from the saturated and unsaturated PD-weighted MT images

2.8.4.1 Region of Interest (ROI) Analysis

This process necessitates the *a priori* selection of a region for study, which is contoured on a suitable co-registered image and applied as a mask to the MTR map, to extract the MTR in specific voxels. The ROI contouring may be manual or partly automated, depending on the structure to be examined, and this introduces a margin for error. Alternatively, the ROI may be represented by a box placed at specific co-ordinates in the brain; in this case, accurate ROI placement may be particularly problematic in serial studies. Only a limited number of areas may be examined in this way; too many comparisons necessitate Bonferroni corrections and thus lose sensitivity (Tofts 2004). In MS, an ROI approach was initially employed to examine the normal appearing brain tissues (Leary 2000); however, this application has been superseded by more robust techniques, allowing unbiased examination of the whole NABT.

2.8.4.2 MTR Histogram Analysis

This technique is fully automated, relatively fast, and highly reproducible (van Buchem 1999). It involves the creation of a frequency distribution from the values in the MTR map, and allows modelling of the whole brain without an *a priori* hypothesis. If required, lesions can be masked and removed, and tissues can be segmented using automated algorithms, to obtain the MTR of the whole grey or NAWM.

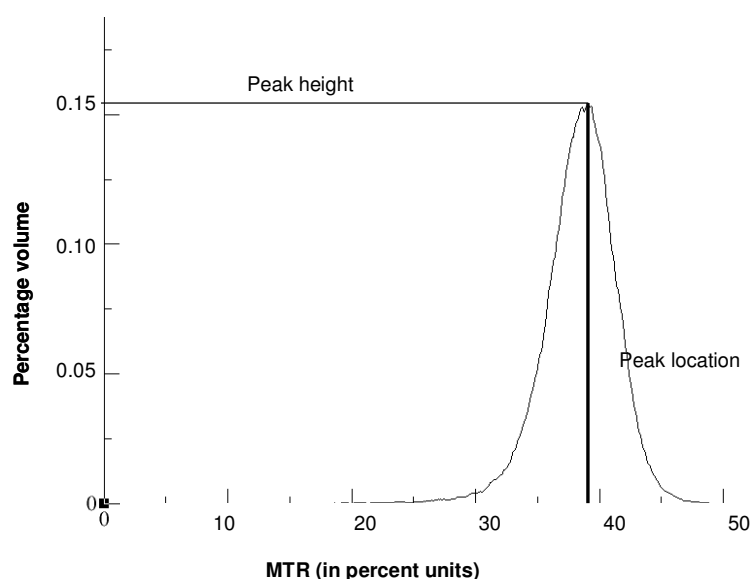
The MTR histogram obtained from a normal brain demonstrates a single peak with a fairly narrow range of values (van Buchem 1997). Several considerations are involved in creating histograms. The values included in the histogram are often integers, because images tend to be stored as integers to limit the amount of memory required, and so continuous intensity values have been rounded up or down. This produces spikes in the histogram, which can be smoothed by the addition of random noise to the intensity value before conversion into MTR, called a *pseudo-continuous* distribution (Tozer 2003). The intervals into which MTR values are divided in a histogram is called the bin width, and in the studies described in this thesis we have chosen a bin width of 0.1 pu (see Chapter 3 section 3.1.2.3). This is a trade-off between wider bin sizes, which can smooth away accurate localization and measurement of the peak, and the excess noise produced by very narrow bins (Tofts 2004). Initially, the area under the histogram curve gives the total number of voxels, so that the tissue volume is calculated by multiplying by the volume of one voxel. However, due to the wide variation in brain sizes, histograms are normalized to make them comparable. Each histogram value is divided by the sum of all the values and by the bin width, so that the area below the histogram becomes unity. The normalized histogram therefore shows the fraction of total brain volume lying at each MTR interval.

Specific parameters which describe the histogram can be extracted (see Figure 2h) and in our studies we have used peak height (PH), peak location (PL) and mean values. Histogram PH appears to be the most sensitive to decline in MS (van Buchem 1996, Zhou 2004), indicating a reduction in voxels at the most popular MTR value of the normal range. For this reason it has been claimed that histogram PH represents the amount of 'normal' brain parenchyma remaining in the segment (van Buchem 1996). However, PH also tends to be the most variable parameter as it is vulnerable to artefact; for this reason it may not be the best parameter to distinguish between patients and controls (Zhou 2004). The mean MTR is closely related to the PH, but it is less sensitive to change as more voxels at lower MTR are needed to shift the mean value of the whole histogram. The peak location (PL), which is the mode of the values, is closely related to the mean, and moves to the

left after considerable increase in voxels with a lower MTR. Some studies have included features which further describe the shape of the histogram, giving more information about pixels at lower values, such as the 25th and 75th centiles (Ramio-Torrenta 2006). Zhou *et al* proposed using the area under the histogram at a width of 2/3 the histogram height, to encompass a wider variety of information about the histogram peak and distribution (Zhou 2004), and McGowan *et al* proposed using the mean \pm standard deviation (SD) (McGowan 2000). Attempts have also been made to use more complex analyses which represent the features of the histogram more completely, such as principle component analysis (Dehmeshki 2001) and more recently analysis of skew (Hayton 2009).

Histograms are very sensitive to subtle diffuse change, because an average is taken from a large number of voxels, thus reducing the effect of noise. For this reason they are not ideal for analyzing small tissue volumes, such as lesions. They can be created from larger ROIs, but are extremely sensitive to slight changes in ROI positioning. In addition, the sensitivity of histogram analysis for the detection of very localized pathology is limited, because changes may be compensated for by normal areas. Generalized information about the segment under study is provided; all information about location is lost (Tofts 2004).

Figure 2h: Histogram of the grey matter MTR in a patient with PPMS



2.8.4.3 Voxel-based MTR Analysis

MTR changes can be localized using a voxel-based approach, as described in section 2.7.4. A mask of the area under study, for example the grey matter, may be created and applied to the MTR image (see Chapter 4), or the MTR image itself may be segmented (Audoin 2006). The MTR in each voxel can then be compared between groups. It is important to consider partial volume voxels, particularly in areas of localized atrophy. These occur when a voxel contains tissue from outside the segment under study; for example, some NAWM or CSF may contaminate a grey matter voxel and alter its MTR. In the study described in Chapter 4, we have addressed this issue by applying a 75% likelihood threshold to the grey matter mask, so that all voxels included are more than 75% likely to contain grey matter (see section 4.4.1.4). Other investigators have employed an erosion step, where the outer grey matter voxels are removed (Mesaros 2008); we avoided this because it indiscriminately reduces the number of grey matter voxels studied.

2.9 Conclusions

MRI exploits the paramagnetic properties of tissues by applying a radiofrequency pulse in the presence of an external magnetic field. Images are encoded using linear magnetic field gradients and recorded in k-space. Variations in acquisition can be used to manipulate image contrast. Contrast within an image can be altered using contrast agents such as gadolinium. The brain volume measurements performed in later chapters are calculated from 3-D FSPGR images using SPM2. The MT sequence used is an interleaved acquisition producing inherently co-registered PD- and T2-weighted images.

References

1. Anderson VM, Fernando KT, Davies GR *et al.* Cerebral atrophy measurement in clinically isolated syndromes and relapsing remitting multiple sclerosis: a comparison of registration-based methods. *J Neuroimaging* 2007; 17: 61-68.
2. Anderson VM, Fox NC, Miller DH. Magnetic resonance imaging measures of brain atrophy in multiple sclerosis. *J Magn Reson Imaging* 2006; 23: 605-618.
3. Ashburner J, Friston K. Multimodal image coregistration and partitioning--a unified framework. *Neuroimage*. 1997; 6: 209-217.
4. Ashburner J, Friston KJ. Voxel-based morphometry--the methods. *Neuroimage*. 2000; 11: 805-821.
5. Audoin B, Fernando KT, Swanton JK, Thompson AJ, Plant GT, Miller DH. Selective magnetization transfer ratio decrease in the visual cortex following optic neuritis. *Brain* 2006; 129: 1031-1039.
6. Audoin B, Ranjeva JP, Au Duong MV *et al.* Voxel-based analysis of MTR images: a method to locate gray matter abnormalities in patients at the earliest stage of multiple sclerosis. *J Magn Reson Imaging* 2004; 20: 765-771.
7. Barker GJ, Tofts PS, Gass A. An interleaved sequence for accurate and reproducible clinical measurement of magnetization transfer ratio. *Magn Reson Imaging* 1996; 14: 403-411.
8. Bookstein FL. "Voxel-based morphometry" should not be used with imperfectly registered images. *Neuroimage*. 2001; 14: 1454-1462.
9. Butzkueven H, Kolbe SC, Jolley DJ *et al.* Validation of linear cerebral atrophy markers in multiple sclerosis. *J Clin Neurosci* 2008; 15: 130-137.
10. Dalton CM, Miszkiewski KA, O'Connor PW, Plant GT, Rice GP, Miller DH. Ventricular enlargement in MS: one-year change at various stages of disease. *Neurology* 2006; 66: 693-698.
11. Dehmeshki J, Ruto AC, Arridge S, Silver NC, Miller DH, Tofts PS. Analysis of MTR histograms in multiple sclerosis using principal components and multiple discriminant analysis. *Magn Reson Med* 2001; 46: 600-609.
12. Filippi M. Enhanced magnetic resonance imaging in multiple sclerosis. *Mult Scler* 2000; 6: 320-326.
13. Filippi M, Campi A, Martinelli V *et al.* Comparison of triple dose versus standard dose gadolinium-DTPA for detection of MRI enhancing lesions in patients with primary progressive multiple sclerosis. *J Neurol Neurosurg Psychiatry* 1995; 59: 540-544.
14. Fischl B, Salat DH, Busa E *et al.* Whole brain segmentation: automated labeling of neuroanatomical structures in the human brain. *Neuron* 2002; 33: 341-355.
15. Fox NC, Freeborough PA. Brain atrophy progression measured from registered serial MRI: validation and application to Alzheimer's disease. *J Magn Reson Imaging* 1997; 7: 1069-1075.

16. Freeborough PA, Fox NC, Kitney RI. Interactive algorithms for the segmentation and quantitation of 3-D MRI brain scans. *Comput Methods Programs Biomed* 1997; 53: 15-25.
17. Graham SJ, Henkelman RM. Pulsed magnetization transfer imaging: evaluation of technique. *Radiology* 1999; 212: 903-910.
18. Hayton, T., Furby, J., Smith, K. J., Altmann, D., Brenner, R., Chattaway, J., Fisniku, L., Fox, N., Hughes, R. A. C., Hunter, K., Tozer, T., Khaleeli, Z., Miller, D. H., and Kapoor, R. Magnetization transfer ratio histogram skew in secondary progressive multiple sclerosis. 2009.
Ref Type: Unpublished Work
19. Hennig J, Nauerth A, Friedburg H. RARE imaging: a fast imaging method for clinical MR. *Magn Reson Med* 1986; 3: 823-833.
20. Jasperse B, Valsasina P, Neacsu V *et al.* Intercenter agreement of brain atrophy measurement in multiple sclerosis patients using manually-edited SIENA and SIENAX. *J Magn Reson Imaging* 2007; 26: 881-885.
21. Jones DK, Symms MR, Cercignani M, Howard RJ. The effect of filter size on VBM analyses of DT-MRI data. *Neuroimage*. 2005; 26: 546-554.
22. Kidd D, Thorpe JW, Thompson AJ *et al.* Spinal cord MRI using multi-array coils and fast spin echo. II. Findings in multiple sclerosis. *Neurology* 1993; 43: 2632-2637.
23. Klauschen F, Goldman A, Barra V, Meyer-Lindenberg A, Lundervold A. Evaluation of automated brain MR image segmentation and volumetry methods. *Hum Brain Mapp*. 2008.
24. Leary SM, Brex PA, MacManus DG *et al.* A (1)H magnetic resonance spectroscopy study of aging in parietal white matter: implications for trials in multiple sclerosis. *Magn Reson Imaging* 2000; 18: 455-459.
25. Lee MA, Smith S, Palace J *et al.* Spatial mapping of T2 and gadolinium-enhancing T1 lesion volumes in multiple sclerosis: evidence for distinct mechanisms of lesion genesis? *Brain* 1999; 122 (Pt 7): 1261-1270.
26. Losseff NA, Wang L, Lai HM *et al.* Progressive cerebral atrophy in multiple sclerosis. A serial MRI study. *Brain* 1996; 119 (Pt 6): 2009-2019.
27. McGowan JC. The physical basis of magnetization transfer imaging. *Neurology* 1999; 53: S3-S7.
28. McGowan JC, Berman JI, Ford JC, Lavi E, Hackney DB. Characterization of experimental spinal cord injury with magnetization transfer ratio histograms. *J Magn Reson Imaging* 2000; 12: 247-254.
29. McRobbie DW, Moore EA, Graves MJ, Prince MR. *MRI From Picture to Proton*. Cambridge University Press, 2003.
30. Mesaros S, Rocca MA, Absinta M *et al.* Evidence of thalamic gray matter loss in pediatric multiple sclerosis. *Neurology* 2008; 70: 1107-1112.
31. Paolillo A, Pozzilli C, Gasperini C *et al.* Brain atrophy in relapsing-remitting multiple sclerosis: relationship with 'black holes', disease duration and clinical disability. *J Neurol Sci* 2000; 174: 85-91.

32. Ramio-Torrenta L, Sastre-Garriga J, Ingle GT *et al.* Abnormalities in normal appearing tissues in early primary progressive multiple sclerosis and their relation to disability: a tissue specific magnetisation transfer study. *J.Neurol.Neurosurg.Psychiatry* 2006; 77: 40-45.
33. Sicotte NL, Voskuhl RR, Bouvier S, Klutch R, Cohen MS, Mazziotta JC. Comparison of multiple sclerosis lesions at 1.5 and 3.0 Tesla. *Invest Radiol* 2003; 38: 423-427.
34. Silver NC, Good CD, Barker GJ *et al.* Sensitivity of contrast enhanced MRI in multiple sclerosis. Effects of gadolinium dose, magnetization transfer contrast and delayed imaging. *Brain* 1997; 120 (Pt 7): 1149-1161.
35. Smith SM, De SN, Jenkinson M, Matthews PM. Normalized accurate measurement of longitudinal brain change. *J Comput Assist Tomogr* 2001; 25: 466-475.
36. Smith SM, Jenkinson M, Johansen-Berg H *et al.* Tract-based spatial statistics: voxelwise analysis of multi-subject diffusion data. *Neuroimage.* 2006; 31: 1487-1505.
37. Smith SM, Zhang Y, Jenkinson M *et al.* Accurate, robust, and automated longitudinal and cross-sectional brain change analysis. *Neuroimage.* 2002; 17: 479-489.
38. Stevenson VL, Miller DH, Rovaris M *et al.* Primary and transitional progressive MS: a clinical and MRI cross-sectional study. *Neurology* 1999; 52: 839-845.
39. Tofts P. *Quantitative MRI of the Brain.* Chichester: John Wiley & Sons, 2004.
40. Tofts PS, Steens SC, Cercignani M *et al.* Sources of variation in multi-centre brain MTR histogram studies: body-coil transmission eliminates inter-centre differences. *MAGMA.* 2006; 19: 209-222.
41. Tortorella C, Codella M, Rocca MA *et al.* Disease activity in multiple sclerosis studied by weekly triple-dose magnetic resonance imaging. *J Neurol* 1999; 246: 689-692.
42. Tozer DJ, Tofts PS. Removing spikes caused by quantization noise from high-resolution histograms. *Magn Reson Med* 2003; 50: 649-653.
43. van Buchem MA, McGowan JC, Grossman RI. Magnetization transfer histogram methodology: its clinical and neuropsychological correlates. *Neurology* 1999; 53: S23-S28.
44. van Buchem MA, McGowan JC, Kolson DL, Polansky M, Grossman RI. Quantitative volumetric magnetization transfer analysis in multiple sclerosis: estimation of macroscopic and microscopic disease burden. *Magn Reson Med* 1996; 36: 632-636.
45. van Buchem MA, Udupa JK, McGowan JC *et al.* Global volumetric estimation of disease burden in multiple sclerosis based on magnetization transfer imaging. *AJNR Am J Neuroradiol* 1997; 18: 1287-1290.
46. Zhou LQ, Zhu YM, Grimaud J, Hermier M, Rovaris M, Filippi M. A new method for analyzing histograms of brain magnetization transfer ratios: comparison with existing techniques. *AJNR Am J Neuroradiol* 2004; 25: 1234-1241.

**Understanding progression:
Magnetization Transfer Histograms
and Atrophy**

CHAPTER 3

This chapter contains two longitudinal studies which investigate progression in PPMS using MTR histograms. The first explores the sensitivity of MTR histograms for detecting short term changes in the brain over one year, and the potential for baseline MTR histograms to predict short term progression. The second study investigates whether the predictive value of MTR histograms is maintained over a longer period of three years, and whether MTR histogram parameters change concurrently with clinical measures during the study. In both sections, brain atrophy is also considered, both for its capacity to affect MTR measurements and its potential relevance to disease progression.

3.1 Detecting change and predicting progression over one year in early PPMS

3.1.1 Introduction

Magnetization transfer imaging quantifies injury in the NABT and in lesions by measuring the MTR. A reduction in MTR is thought to reflect demyelination and axonal loss (Schmierer 2004), thus the technique is particularly suited for exploring the disease processes driving clinical progression in PPMS. The basis of the MTR measurement is fully discussed in section 2.8. Diffuse abnormalities, reflected by reduction in MTR, have been identified in the NABT of subjects with PPMS (Dehmeshki 2003, Gass 1994). Some studies suggest that the changes are less profound than those seen in SPMS (Vrenken 2007, Rovaris 2000), but others have described an equivalent amount of damage (Dehmeshki 2001). Initially, correlations between MTR and clinical indices in established PPMS appeared weaker than in other MS subtypes (Dehmeshki 2001, Filippi 2000a), and short-term longitudinal studies did not demonstrate MTR changes despite concurrent increase in T2 lesion load (Filippi 2000b). However, a cross-sectional study in early PPMS demonstrated a correlation between MTR reduction (in both grey and NAWM) and clinical function (Ramio-Torrenta 2006), suggesting that MTI may be sensitive to longitudinal changes in this group.

Brain atrophy represents irreversible tissue damage, and is thought to be a reflection of axonal loss (Simon 2006). Brain atrophy is already evident in patients with early PPMS, in both the grey and NAWM segments (Sastre-Garriga 2004), and the extent of volume loss correlates with clinical function. Any investigation of MTI in PPMS must also consider brain atrophy, for two reasons. Firstly, volume loss interferes with MTR measurement by increasing 'partial volume' voxels: voxels which only partly contain either grey or NAWM. Voxels containing both tissue types would generate an MTR intermediate to that of a purely grey or NAWM voxel, and those containing NAWM and CSF together would have a markedly reduced MTR. For this reason, care must be taken in post-processing to minimize partial volume voxels, and statistical correction for atrophy may also be necessary to ensure that any remaining contribution of volume loss to the MTR measurement is taken into account. Secondly, MTR reduction is thought to reflect both reversible processes (principally demyelination, but also gliosis and inflammation) and irreversible processes (particularly axonal loss), although there is some indication that the former may be more directly related to MTR (Schmierer 2004). Thus models taking full account of concurrent volume change when measuring MTR may be more likely to highlight the contribution made by reversible processes, potentially gaining complementary information to that obtained from volume measurements.

The only previous longitudinal MTR study in PPMS examined nine patients with PPMS as part of a mixed MS cohort, using NAWM MTR histograms over one year. No change in MTR parameters was observed, despite an increase in T2 lesion load over the same period (Filippi 2000b). In this study we explored the value of baseline MTR to predict clinical progression in the short-term, and investigated whether MTI was sensitive enough to detect changes over one year in early PPMS, independently of any contribution from brain atrophy.

3.1.2 Methods

3.1.2.1 Subjects

The participants in this study were recruited as part of a cohort of fifty patients with definite or probable PPMS (Thompson 2000), within five years of symptom onset, who were participants in a longitudinal study comprising six monthly

radiological and clinical assessments. For this study we examined data obtained at baseline and after one year. One patient did not complete the baseline protocol, and two patients were excluded after baseline: one developed claustrophobia and one withdrew. Eleven patients did not attend at one year, the reasons were as follows: death, not MS related (1), illness unrelated to MS (2), personal commitments (6; in these cases patients were away from London or prevented from attending their appointment due to prior commitments). Two patients missed their one year time-point due to the scanner upgrade. In addition, three patients were scanned after the scanner upgrade, and excluded from this study, and two patients had not yet reached their one year time-point. Finally, one patient was excluded because all images were of sub-optimal quality (see section 3.1.2.3). Thus the subgroup for this study was composed of 30 patients (17 male, 13 female, mean age 42.1 years [range 25-63]). Patient characteristics are given in Table 3.A. None of the patients were taking disease modifying medications, but one patient was taking regular courses of oral steroids every three months. Patients were recruited from clinics at the National Hospital for Neurology and Neurosurgery and other hospitals in Southeast England. Written and informed consent was obtained from all participants. The study was approved by the Joint Medical Ethics Committee of the National Hospital for Neurology and Neurosurgery and the Institute of Neurology, London.

Patients underwent neurological examination at baseline and one year. They were scored on Kurtzke's Expanded Disability Status Scale (EDSS) (Kurtzke 1983) . The Multiple Sclerosis Functional Composite (MSFC) (Cutter 1999) and its subtests (Paced Auditory Serial Addition Test [PASAT], Nine Hole Peg Test [NHPT], and Timed Walk Test [TWT]) were performed for the first time at baseline (without previous practice sessions) and on 22 of the patients at one year (12 male, 10 female, mean age 41.9 years [range 25-63]). There was no significant difference in baseline EDSS, MSFC, T2 lesion load or brain parenchymal fraction (BPF), or in one year EDSS, T2 lesion load, or BPF between those patients scored for MSFC at one year and those who were not.

Fifteen healthy controls (9 male, 6 female, mean age 35.4 years [range 27-52]), were also scanned at baseline and one year. The difference in age between patients and controls was adjusted for in the statistical analysis.

Table 3.A Clinical characteristics of patients at baseline and follow-up

Characteristics	Baseline	One year	P value
Number male / female	17/13	-	-
Mean age in years (range)	42.06 (25-63)	-	-
Mean disease duration in years (range)	2.9 (1-5)	-	-
Presentation: cord/non-cord symptoms	23 / 7	-	-
Median EDSS (range)	4.0 (1.5-7)	4.75 (2-7.5)	p=0.02
Mean MSFC (SD)	0.05 (0.84)	0.02 (1.07)	p=0.8
Mean PASAT (range)	43.0 (0-60)	46.0 (3-60)	p=0.3
Mean NHPT (range)	34.3 (17.1-96.2)	40.9 (18.0-165.8)	p=0.2
Mean TWT (range)	17.6 (3.65-180)	23.9 (3.70-180)	p=0.4

P values were obtained from Wilcoxon rank tests (EDSS) and paired t-tests (all other variables) to compare baseline and follow-up values. *EDSS=Expanded disability status scale, MSFC= Multiple sclerosis functional composite, PASAT= Paced auditory serial addition test, NHPT=Nine hole peg test, TWT=Timed walk test, BL=Baseline, FU=follow-up, SD=Standard deviation.*

3.1.2.2 MRI Acquisition

All scans were performed at baseline and after one year on a 1.5 Tesla GE Signa scanner (General Electric Co, Milwaukee, Wisconsin, USA). The mean and median separation of baseline and one year scans were both 12.3 months (range 10.1 - 15.2 months).

MTI was acquired using a 2D interleaved spin echo sequence described by Barker *et al* (Barker 1996), comprising 28 contiguous axial slices, slice thickness 5mm, repetition time (TR) 1720ms (milliseconds), echo time (TE) 30/80 ms, number of excitations (NEX) 0.75, acquired matrix 256x128, reconstructed matrix 256x256 and field of view (FOV) 240x240mm. Proton density (PD)-weighted images were acquired in the presence and absence of a Hamming-apodised three lobe sinc MT pulse (duration 16ms, peak amplitude 23.2 μ T[micro-Tesla], bandwidth 250 Hz [Herz], 1kHz [kilo-Herz] off-water resonance). These saturated and unsaturated PD MT sequences were co-registered and interleaved with simultaneously acquired PD and T2-weighted images.

All subjects also underwent a 3D inversion-prepared fast spoiled gradient recall (3D FSPGR) sequence of the brain, comprising 124 contiguous axial slices, slice thickness 1.5mm, TR 13.3 ms, TE 4.2ms, inversion time 450 ms, matrix 256x160 [reconstructed matrix 256x256, final in plane resolution 1.17x1.17 mm] and FOV 300 x 225mm.

3.1.2.3 Image Post Processing

Images were displayed on a Sun workstation (Sun Microsystems, Mountain View, CA, USA) using DisplImage software (DisplImage, D. Plummer, Department of Medical Physics and Bioengineering, UCL, UK). Lesions were delineated with a semi-automated contour thresholding technique (Plummer 1992) on the unsaturated PD images, with reference to the co-registered T2 images, and used to create a binary lesion mask (setting the signal inside the lesion boundary to 0, and the rest to 1).

3.1.2.3.1 MTI

The pixel MTR was calculated from the pre- (Mo) and post- (Ms) saturation PD-weighted images using the formula $[(Mo-Ms)/Mo] \times 100$ percent units (pu), to produce MTR maps for each subject. These images were chosen because the resulting map has higher signal-to-noise ratio than that from the 80ms echo. The T2 images were segmented in SPM99 (Statistical Parametric Mapping 1999, Wellcome Department of Cognitive Neurology, London, England) using an algorithm based on cluster analysis combined with *a priori* knowledge of tissue distribution (see section 2.7.1) (Ashburner 2000), which assigns voxels to white matter, gray matter or CSF. We used SPM99 so that our results would be comparable to those from a previous cross-sectional study in our cohort (Ramio-Torrenta 2006). Non-brain tissue, whole brain (WB), white matter and grey matter probability maps were produced, and used to create WB, grey and white matter masks, which were then applied to the calculated MTR map in each subject to produce WB, grey and white matter MTR maps. To minimise partial volume voxels, we employed a 10pu threshold, and eroded the outer and inner layer of voxels twice in the white matter, and once in the grey (the cortical grey matter was too thin to support further erosions). The segmentation of the MTR images was checked manually in all subjects. One patient's scans were incorrectly segmented, with white matter accidentally included in the grey matter

segment due to a very high lesion load. This patient was excluded from the analysis.

The T2 lesion masks were then applied to the WB, grey and white matter MTR maps to produce grey and NAWM probability maps. We have avoided the term normal appearing grey matter because while all visible T2 lesions were removed, grey matter lesions are not visible on T2-weighted images at 1.5 Tesla (Geurts 2005b). To obtain the lesion MTR map, the lesion mask was reversed (setting the signal inside the lesion boundary to 1, and the rest to 0), applied to the grey and white matter probability maps to produce a lesion probability map, and then to the MTR images to produce a lesion MTR map. In the case of controls, where no lesions were found, segmentation produced normal white matter (NWM) and grey matter maps. MTR histograms were obtained for the grey, NAWM and lesions in patients, and grey matter and NWM in controls. To allow us to compare MTR histograms between subjects, the MTR histograms of each segment were normalized to the volume of that segment. The histograms had a bin width of 0.1 pu and a smoothing window of 0.3 pu. Mean, peak height (PH) and peak location (PL) MTR measures were taken from each individual histogram.

3.1.2.3.2 Atrophy

At each time-point lesions were contoured on the individual FSPGR scans using the software described above, to create a T1-weighted lesion mask. The observer was blinded to the clinical details. FSPGR images were segmented into white matter, grey matter and CSF using SPM99, and the volume of each segment calculated as described by Chard *et al* (Chard 2002b). The lesion mask was then subtracted from the white matter and grey matter T1 images and separate NAWM, grey matter and lesion segments were obtained, with their volumes in ml. Volume estimations were made using a caudal cut-off at the last slice containing cerebellum. The total intracranial volume (TIV), BPF, normal appearing white matter fraction (NAWMF) and grey matter fraction (GMF) were calculated as follows:

$$\text{TIV} = \text{lesion volume (LV)} + \text{NAWM volume (NAWMV)} + \text{GM volume (GMV)} + \text{CSF volume}$$

$$\text{BPF} = (\text{LV} + \text{NAWMV} + \text{GMV}) / \text{TIV}$$

$$\text{NAWMF} = \text{NAWMV} / \text{TIV}$$

$$\text{GMF} = \text{GMV} / \text{TIV}$$

3.1.2.4 Statistical Analysis

Analysis was carried out using SPSS 10.0 (Statistical package for the Social Sciences, Chicago, IL, USA). Statistical significance is reported at the 5% level. Significant values for correlation coefficients are reported without correction for multiple comparisons to avoid type II errors (Perneger 1998).

3.1.2.4.1 Clinical data

In analyzing the change in EDSS scores, a one step deterioration on the scale was defined as an increase of one if the baseline EDSS was less than or equal to five or an increase of 0.5 if it was greater than five (Ellison 1994). This gives greater weight to change in more disabled patients, in whom deterioration is harder to detect on the EDSS scale, and these steps have been regarded as equivalent in clinical trials (Hoogervorst 2003). Z-scores (z) were derived for the MSFC subtests using our own baseline sample as reference, and used to calculate the MSFC. One patient at baseline and two at one year were too disabled to complete the TWT, and were scored with the maximum time allowed for the TWT (180 seconds), as described by Hoogervorst *et al* (Hoogervorst 2002).

3.1.2.4.2 Baseline MTR predictors

To find whether baseline MTR in patients predicted clinical change, multiple linear regression analyses were performed for each clinical test and subtest, and each MTR parameter in each segment. Clinical score at one year was the dependent variable, and clinical score at baseline and baseline MTR parameters were independent variables, so that any relationship identified between baseline MTR variables and change in clinical score would be independent of any relationship between baseline MTR variables and baseline clinical score. Models were adjusted for age, gender and baseline intra-segmental volume *ie* WB analysis was adjusted for baseline BPF, NAWM for

NAWMF and grey matter for GMF. Where significant correlations were found between baseline MTR parameters and clinical change, the strength of the association was assessed using partial correlations adjusted for age, gender and intra-segmental volume.

To investigate further the utility of baseline MTR measures in predicting clinical change, patients were divided into two groups: those with a stable EDSS score at one year, and those who had worsened. The MTR parameter that most strongly predicted EDSS changes was chosen. A cut-off value for this MTR parameter, which was below the lowest value in controls, was chosen. Patients were divided into a further two subgroups depending on whether their MTR was below or above this value. A two by two table was constructed, showing the number of patients with low and normal MTR against those who were stable or worsened on EDSS. The sensitivity, specificity, positive and negative predictive values, and overall accuracy of using this MTR parameter to predict clinical worsening were calculated according to standard methods (Greenhalgh 1997).

3.1.2.4.3 MTR change over one year in patients and controls

To determine MTR change over one year, paired t-tests were used to compare MTR at baseline and one year within patient and control groups. Multiple linear regression analysis was then used to compare changes in each segmental MTR parameter between patient and control groups, adjusting for age and gender.

3.1.2.4.4 Relationship between MTR and atrophy

Pearson's correlations were performed to establish the relationship between change in MTR and brain volume in each segment. Grey matter damage is also related to white matter changes (Audoin 2006, Chard 2002a), therefore the correlation between grey matter MTR decrease and change in NAWMF was also examined.

3.1.3 Results

3.1.3.1 Clinical changes

Clinical changes over one year are summarized in Table 3.A. Patients progressed clinically with worsening EDSS scores ($p=0.02$). There was a non-significant decrease in mean MSFC, with worsening of the TWT and NHPT scores. PASAT scores appeared to improve over one year.

3.1.3.2. Predictive value of baseline MTR

Lower MTR at baseline predicted greater clinical progression on both the EDSS and MSFC over one year after adjusting for age, gender and segmental atrophy (see Table 3.B). Baseline WB MTR (mean $p=0.01$, $r -0.46$) predicted change in EDSS. There was no contribution from lesion MTR, but NAWM MTR parameters predicted EDSS change (mean $p=0.03$, $r -0.39$ and PH $p=0.04$, $r -0.38$). Baseline NAWM mean MTR below 37.0pu (this was chosen as a cut off because it was well below the lowest MTR value in controls, which was 37.68pu) was able to predict worsening on the EDSS over one year with a specificity of 95%, sensitivity of 50%, positive predictive value of 83%, and negative predictive value of 79% (see Table 3.C). The overall accuracy of the test, indicating the proportion of correct predictions, was 80%.

For the MSFC change the most complete predictor was the WB MTR (mean $p=0.001$, $r 0.67$; PH $p=0.001$, $r 0.64$; PL $p=0.006$, $r 0.58$). This prediction emerged largely from the NAWM segment (mean $p<0.001$, $r 0.68$; PH $p<0.001$, $r 0.54$). The grey matter MTR (PL $p=0.02$, $r 0.51$) and the lesion MTR (mean $p=0.047$, $r 0.44$; PL $p=0.01$, $r 0.54$) were weak predictors of MSFC change.

Of the MSFC subtests, change in the zTWT was predicted by baseline NAWM ($p\leq 0.001$ in all cases, mean $r 0.81$, PH $r 0.75$, PL $r 0.64$) and grey matter parameters (PH $p=0.007$, $r 0.55$; PL $p=0.004$, $r 0.58$), and lesion MTR (mean $p=0.01$, $r 0.52$; PL $p=0.009$, $r 0.53$). zPASAT was weakly predicted by WB (mean and PH) and by lesion MTR (PL $p=0.013$, $r 0.50$). Although there was a group improvement in zPASAT, the positive correlation demonstrated that

Table 3.B Baseline MTR parameters predict clinical change over one year

MTR parameters at baseline		Change in				
		EDSS	MSFC	zPASAT	zNHPT	zTWT
WB	M	0.01 (-0.46)	0.001 (0.67)	0.03 (0.43)	0.18	<0.001 (0.71)
	PH	0.55	0.001 (0.64)	0.03 (0.44)	0.85	0.001 (0.64)
	PL	0.07 (-0.34)	0.006 (0.58)	0.19	0.08	<0.001 (0.70)
NAWM	M	0.03 (-0.39)	0.001 (0.68)	0.06	0.26	<0.001 (0.81)
	PH	0.29	<0.001 (0.54)	0.10	0.83	<0.001 (0.75)
	PL	0.04 (-0.38)	0.68	0.07	0.20	0.001 (0.64)
Grey matter	M	0.65	0.11	0.34	0.60	0.06 (0.40)
	PH	0.72	0.08	0.57	0.97	0.007 (0.55)
	PL	0.73	0.02 (0.51)	0.52	0.190	0.004 (0.58)
Lesion	M	0.18	0.047 (0.44)	0.05 (0.40)	0.69	0.01 (0.52)
	PH	0.12	0.77	0.66	0.93	0.74
	PL	0.33	0.01 (0.54)	0.01 (0.50)	0.82	0.009 (0.53)

P values are shown for each parameter, and significant p values ($p < 0.05$) are shown in bold. They were obtained from multiple linear regression analysis with age, gender and intra-segmental volume as covariates where significant. R values, shown in brackets, were obtained from partial correlation coefficients. *MTR= Magnetization transfer ratio, WB=Whole brain, NAWM=Normal appearing white matter. PH=Peak height, PL=Peak location. EDSS=Expanded disability status scale, MSFC=Multiple sclerosis functional composite, zPASAT=z-score for the Paced auditory serial addition test, zNHPT=z-score for the Nine hole peg test, zTWT= z-score for the Timed walk test.*

Table 3.C Baseline NAWM mean MTR < 37 pu predicts worsening on EDSS over one year

	NAWM mean MTR <37 pu	NAWM mean MTR >=37 pu	TOTAL	
EDSS worsened	5	5	10	Sensitivity 50%
EDSS the same or improved	1	19	20	Specificity 95%
TOTAL	6	24	30	
	Positive predictive value 83 %	Negative predictive value 79%		Overall accuracy 80%

MTR= Magnetization transfer ratio, pu=percent units, NAWM=normal appearing white matter, < less than, >= greater than or equal to

3.1.3.3. MRI changes over one year

All mean MTR values decreased at one year in patients (see Table 3.D), with lesion MTR showing the least significant decrease ($p=0.03$), followed by NAWM ($p=0.01$). All peak location values, except for lesion MTR, decreased significantly (WB $p=0.01$, NAWM $p=0.01$, grey matter $p=0.001$), but only WB showed a significant decrease in peak height ($p=0.03$). In controls, there were no significant longitudinal changes in MTR. Significant differences in MTR change were only identified between patient and control groups in grey matter mean MTR ($p=0.02$).

Table 3.D MTR changes over one year in patients and controls

MTR Parameter			Baseline mean MTR (SD)	One year mean MTR (SD)	P value	95% Confidence Interval		Pts vs cont (p value)	
						Lower	Upper		
PATIENTS	WB	M	33.51 (1.43)	33.20 (1.57)	<0.001	-0.45	-0.17	-	
		PH	0.98 (0.01)	0.96 (0.01)	0.03	-0.0003	-0.004	-	
		PL	36.51 (1.23)	36.13 (1.37)	0.01	-1.81	-0.23	-	
	NAWM	M	37.48 (1.46)	37.24 (1.57)	0.01	-0.41	-0.06	0.5	
		PH	0.19 (0.03)	0.18 (0.03)	0.15	-0.002	0.013	0.6	
		PL	37.77 (1.03)	37.56 (1.11)	0.01	-0.38	-0.05	0.3	
	Grey matter	M	31.31 (0.98)	31.04 (1.03)	<0.001	-0.40	-0.14	0.02	
		PH	0.11 (0.01)	0.10 (0.02)	0.50	-0.002	0.004	0.4	
		PL	32.64 (0.85)	32.24 (0.91)	0.001	-0.62	-0.18	0.1	
	Lesion	M	31.38 (2.30)	31.05 (2.38)	0.03	-0.61	-0.03	-	
		PH	0.11 (0.03)	0.12 (0.04)	0.18	-0.025	0.005	-	
		PL	34.23 (2.28)	33.75 (2.28)	0.09	-1.03	0.08	-	
	CONTROLS	WB	M	34.72 (0.38)	34.72 (0.64)	0.20	-0.25	0.25	-
			PH	0.01 (0.009)	0.01 (0.01)	0.36	-0.002	0.001	-
			PL	37.42 (0.45)	37.09 (0.78)	0.36	-0.70	0.05	-
NWM		M	38.40 (0.40)	38.23 (0.57)	0.99	-0.44	0.10	-	
		PH	0.20 (0.02)	0.20 (0.02)	0.41	-0.003	0.01	-	
		PL	38.51 (0.37)	38.40 (0.53)	0.09	-0.37	0.15	-	
Grey matter		M	32.90 (0.44)	32.28 (0.68)	0.89	-0.27	0.23	-	
		PH	0.12 (0.01)	0.12 (0.02)	0.49	-0.006	0.003	-	
		PL	33.13 (0.56)	33.09 (0.74)	0.73	-0.34	0.24	-	

Mean and Peak location MTR values are in percent units, and Peak height is given in percent volume. *Pts vs cont* = changes in patients compared to controls. Significant p values ($p < 0.05$) are shown in bold, and are derived from paired t-tests for in-group comparisons, and multiple linear regression adjusting for age and gender for between-group comparisons. *MTR*=magnetization transfer ratio, *WB*=whole brain, *NAWM*=normal appearing white matter, *NWM*= normal white matter, *M*=Mean, *PH*=peak height, *PL*=peak location.

3.1.3.4. Correlations between MTR and volume changes

Correlations were found between decrease in WB, grey and NAWM peak height MTR and decrease in corresponding intra-segmental volume ($p=0.01$, $p=0.008$, $p<0.001$ respectively, see Table 3.E). Change in NAWM mean and peak location MTR parameters also correlated significantly with the progression of atrophy in corresponding brain tissues ($p=0.03$ in both cases). There was no significant correlation between the grey matter MTR decrease and change in NAWMF.

Table 3.E Correlation of change in MTR with change in segmental volume over one year

Changing MTR parameter		Correlation with segmental volume change		
		p value	r value	r ²
WB	Mean	0.15	0.3	0.08
	PH	0.01	0.47	0.23
	PL	0.10	0.32	0.10
NAWM	Mean	0.03	0.42	0.18
	PH	0.008**	0.50	0.24
	PL	0.03	0.42	0.17
Grey matter	Mean	0.61	0.10	0.01
	PH	<0.001**	0.67	0.45
	PL	0.21	0.24	0.06

P values are derived from Pearson's test. Significant values at $p<0.05$ are shown in **bold** and at $p<0.01$ with asterisks **. Mean and Peak location MTR values are in percent units, and Peak height is given in percent volume. *MTR=Magnetization transfer ratio, WB=Whole brain, NAWM=Normal appearing white matter. PH=Peak height, PL=Peak location. r= correlation coefficient for Pearson's test.*

3.1.4 Discussion

3.1.4.1 MTR parameters predict clinical change

This study shows, for the first time, that brain MTI is a modest predictor of clinical evolution in PPMS, over a relatively short period. Importantly, predictions survived adjustment for segmental volume, demonstrating that the predictive value of MTI is independent of atrophy. However, over a short study period clinical and imaging changes are necessarily small, and longer follow-up is necessary to investigate the role of MTI as a prognostic indicator (see section 3.2).

Over one year EDSS scores deteriorated significantly, but MSFC decline was not statistically significant. This may be explained by several factors. Firstly, MSFC data was not available on all patients. Secondly, mean zTWT and zNHPT scores declined over one year, but zPASAT scores improved. This was probably due to practice effects and a reduced anxiety, as patients became accustomed to testing (Tombaugh 2006, Solari 2005). Lastly, patients unable to complete the TWT at baseline could not demonstrate further reductions in mobility on the MSFC, whereas their EDSS score increased. Nevertheless, the MSFC may provide useful information in this study. It has been shown to be more accurate than the EDSS for detecting group differences within a sample in cross-sectional studies (Hobart 2004). There is evidence that the two scales do not correlate well, and thus may provide complementary clinical information (Kragt 2008). Indeed, in our study, reduction in zTWT sub-scores was more strongly predicted by imaging parameters than any other clinical test. This emphasizes that decreasing mobility is likely to be a prime indicator of progression in this cohort, in which 23 out of 30 patients presented with a spastic paraparesis.

NAWM MTR parameters appear to be driving the prediction of clinical change. Only NAWM peak height did not predict EDSS change; significance was lost after adjustment for baseline brain volume. We identified the NAWM mean MTR with a cut-off value of 37pu as the best indicator of progression in this sample. The overall sensitivity for predicting progression was 50%, with a specificity of 95%; using a higher cut-off value increased sensitivity, but decreased

specificity. The value provides information at a group level for this cohort. However, in order to validate a specific predictive MTR value for clinical use, to predict disability in individuals with PPMS, much larger studies would be necessary. Such a value would be scanner- and sequence-specific (see section 2.8.2.2).

Regarding the other MTR parameters, lesion MTR also predicted decline in MSFC, but not EDSS. Baseline grey matter MTR was only a weak predictor of MSFC change; possible reasons for this are discussed in section 3.1.4.2.

3.1.4.2 MTR decreases significantly over one year

To our knowledge only one previous study evaluated MTR in longitudinal follow-up of PPMS (Filippi 2000b): no significant change in lesion, WB or NABT MTR was found in nine PPMS patients over one year. Median disease duration in the PPMS group was 8 years, with a range of 3-14 years.

In our patients grey matter MTR decreased significantly, but the decrease in NAWM MTR was less notable. Similar results were obtained in a diffusion tensor study in advanced PPMS (mean disease duration 10 years), which observed marked deterioration in grey matter indices over a year, without significant NAWM change (Rovaris 2005). Furthermore, relatively marked grey matter MTR decline has been identified in early RRMS (Davies 2005), while CIS patients have shown equivalent reduction in grey and white matter MTR (Fernando 2005). In this study, the relatively extensive changes in grey compared to NAWM MTR could be due to grey matter lesion accumulation. Lesions within the cortex and deep grey matter are very extensive in progressive MS (Bruck 2005, Kutzelnigg 2005a, Kidd 1999), and can not be reliably detected on conventional MRI scans even at higher field strengths (Geurts 2005a). The grey matter thus contained an unknown number of lesions, while visible white matter lesions were masked out of the analysis. The role of partial volume effects, as discussed in section 3.1.1, should also be considered when interpreting the decline in grey matter MTR. Grey matter atrophy without significant white matter atrophy is known to have developed in this cohort over one year (Sastre-Garriga 2005a), and as brain volume decreases, there is an increase in the number of outer voxels at the brain/CSF interface. However,

steps were taken to minimize this effect. Two outer voxel erosions were carried out for the white matter, and one for the grey matter, discarding voxels with an MTR value below 10pu. MTR histograms were then normalised for brain volume. Furthermore, when we correlated atrophy and MTR changes, only the grey matter peak height showed a relationship with atrophy. There were no significant correlations with grey matter mean and peak location, where the significant longitudinal MTR reductions occurred.

Finally, although grey matter MTR decreased more than NAWM MTR over the study, NAWM MTR was a better baseline predictor of clinical change. This may suggest an imbalance of changes in each segment prior to the start of the study: if NAWM changes occurred earlier in the disease course, they would initially contribute more to the clinical picture. Davies and colleagues, studying MTR in RRMS patients, extrapolated their findings backward, suggesting that NAWM changes had begun prior to symptom onset (Davies 2005). If NAWM changes preceded grey matter changes in our cohort, we would expect the grey matter changes evident in this study to affect clinical outcome in subsequent years (see section 3.2). This has been demonstrated in a DTI study in established PPMS (mean disease duration 10 years), in which grey matter damage predicted disability at five years (Rovaris 2006). In other MS subtypes, grey matter MTR has predicted long term EDSS progression over 8 years (Agosta 2006).

3.1.4.3 MTR changes and progression of atrophy

Weak to moderate correlations emerged between MTR and volume changes over one year. Decrease in peak height MTR was most strongly associated with the development of segmental atrophy, confirming previous findings (Rovaris 1999, Phillips 1998). An increase in low MTR voxels widens and flattens the normalized histogram (Tofts 2004). Statistically, however, atrophy explained less than 10% of the significant decrease in grey matter MTR, and less than 20% of the decrease in NAWM MTR.

Our results emphasize that there is a modest relationship between atrophy and MTR, and that in patients with PPMS MTR measures must be interpreted in the context of atrophy. However, we have shown that MTR is an independent

marker of pathology. Significant MTR changes were not explained by brain volume changes, and baseline MTR predicted progression independently of atrophy.

3.2 Monitoring and predicting clinical progression over three years in early PPMS

3.2.1 Introduction

It has been demonstrated that MTR reduction in the NABT correlates with disability in early PPMS (Ramio-Torrenta 2006). In section 3.1, we showed that baseline NAWM MTR predicts short-term clinical progression, and that MTR is sensitive to short-term brain tissue changes. This data implies that MTR may be a useful measure not only to improve understanding of disease progression in PPMS, but also to predict and monitor progression in a clinical setting.

A number of clinical challenges stem from the wide variation in the evolution of disability among individuals with PPMS (Tremlett 2005). The absence of predictive markers for clinical outcome has adversely affected clinical trials, such as the glatiramer acetate study in PPMS, which was terminated early because patients did not progress as anticipated (Wolinsky 2007). In addition, robust surrogate markers are needed to detect treatment effects (Johnston 2007). The potential for using MRI surrogate markers in MS was explored by a working group in 1999 (McFarland 2002), and they adopted criteria described by Prentice (Prentice 1989). These state that a *surrogate marker* should predict future clinical disability, and that any intervention must alter both the surrogate marker and clinical outcome by the same mechanism. In establishing these criteria, the requirement that the marker should change concurrently with clinical status was not included. However, this attribute is clearly advantageous because it allows monitoring of contemporaneous, as well as future, treatment effects.

In this study we examined the potential of MTR as a surrogate marker to monitor progression in early PPMS in a medium term study suited to clinical trial design. For this purpose, we compared MTR to conventional MRI markers

which have been more widely used as outcome measures in MS clinical trials: T2 lesion load and atrophy. First, we assessed whether changes over three years in MTR, brain volume or T2 lesion load reflected concurrent clinical changes. Secondly we explored whether baseline MTR was a better predictor of clinical progression compared to the other two MR measures.

3.2.2 Methods

3.2.2.1 Subjects

As described in study 3.1, 50 patients with definite or probable PPMS (Thompson 2000), within five years of symptom onset, were invited for radiological assessment at baseline. Following this, they were assessed six monthly for three years, and at each time-point they were scored on the EDSS. As before, two patients were excluded after baseline: one developed claustrophobia and one withdrew, and a third patient was excluded because all images were of sub-optimal quality (see section 3.2.2.3). The patient who did not complete the baseline protocol and was excluded from study 3.1 attended all other time-points and was therefore retained in this study. Thus the total number of patients was 47 (Table 3.F). Clinical data was obtained in person or by telephone (Lechner-Scott 2003) for patients who became too disabled to undergo scanning during the study, including those with severe ataxia preventing them from lying still, and those who were unwilling to attend the centre (Table 3.G). Two patients died of conditions unrelated to MS during the study and were excluded from subsequent analysis, one withdrew, and one was unwell at the final time-point. Thus 43 patients were assessed at three years (Table 3.G). None of the patients were taking disease modifying medications. One patient had a single course of intravenous (iv) steroids for a deterioration of symptoms, and two patients were taking regular courses of oral steroids every three months.

Eighteen healthy controls (see Table 3.F), a different group from the controls in study 3.1, underwent the same scanning protocol. Adjustments for age and gender differences between the patient and control group were made at each stage of the analysis, as described below.

Table 3.F Baseline clinical and imaging characteristics of patients and controls

		Patients	Controls	p value
Mean age in years (range)		45.1 (19-65)	34.6 (27-52)	<0.001
Gender (male/female)		28/19	8/10	0.08
Median EDSS (range)		4.75 (1.5-7)	-	-
Mean T2 lesion load (ml)		30.3	-	-
Mean grey matter volume (SD; mean PGMF [%])		710.4 (78.6;47.7)	726.4 (70.6;49.7)	0.001
Mean NAWM volume (SD; mean PNAWMF [%])		369.2 (50.5;24.8)	395.5 (38.3;27.0)	<0.001
Grey matter MTR	Mean (SD)	31.8 (1.1)	33.1 (0.4)	<0.001
	PH, mean (SD)	10.0 (1.4)	12.1 (1.0)	<0.001
	PL, mean (SD)	33.3 (0.6)	33.8 (0.5)	0.006
NAWM MTR	Mean (SD)	37.2 (0.9)	38.1 (0.5)	<0.001
	PH, mean (SD)	17.4 (2.7)	20.2 (1.5)	<0.001
	PL, mean (SD)	37.7 (0.8)	38.4 (0.5)	0.001

EDSS= Expanded disability status scale, SD=Standard deviation, PGMF=Percentage grey matter fraction, PNAWMF=Percentage normal appearing white matter fraction, NAWM=Normal appearing white matter, MTR=Magnetization transfer ratio, PH=Peak height, PL=Peak location, pu=Percent units . PH is given in percent volume, and mean and PL in percent units. P values were derived from unpaired 2 tailed t-tests for patient versus control variables.

Table 3.G Numbers of patients assessed at each time-point and reasons for non-attendance

Time-point (months)	0	6	12	18	24	30	36
Total patients assessed:	47	37	36	33	34	30	43
Scan performed	46	34	33	33	30	25	37
Clinical assessment only, done in person	1	3	3	0	3	2	2
Clinical assessment only, done by telephone	0	0	0	0	1	3	4
Patients who did not attend:	0	10	11	14	13	17	4
Withdrew from study	0	0	0	0	0	1	1
Personal commitments	0	7	6	7	5	7	0
Non-MS related illness	0	3	2	3	4	6	1
Upgrade	0	0	2	3	3	2	0
Death	0	0	1	1	1	1	2

Clinical assessment only= Patients too disabled to be scanned, including patients with severe ataxia preventing them from lying still. *Personal commitments*= patient unable to attend within time allocated due to existing commitments. *Upgrade*= time-point missed because scanner was being upgraded.

3.2.2.2 MRI Acquisition

All scans were performed on a 1.5 Tesla scanner (General Electric Co, Milwaukee, Wisconsin, USA). Each time-point was separated by a mean of 26.7

weeks (range 25.3-29.0 weeks). The scanner was upgraded during the study, and the gradient amplifiers, but not the gradient coils, were changed. Maximum gradient strength increased from 22mTm^{-1} (milli-Tesla per metre) to 33mTm^{-1} . The scanner software was upgraded from SIGNA version 5x to version 11x. The upgrade was accounted for at each stage of the statistical analysis (see below).

Subjects underwent brain MTI (Barker 1996), producing inherently co-registered proton density- (PD) and T2-weighted images (see 3.1.2.2); MTI parameters were unchanged after the upgrade. 3D inversion-prepared fast spoiled gradient recall (3D FSPGR) volume sequences of the brain were also acquired (see 3.1.2.2), and the FSPGR repetition time was reduced from 13.3 to 10.9 ms after the upgrade.

3.2.2.3 Post-processing

Images were displayed on a Sun workstation (Sun Microsystems, Mountain View, CA) using Displmage software (Displmage, D. Plummer, Department of Medical Physics and Bioengineering, UCL, UK).

In this study more accurate segmentation was achieved than in study 3.1, using the FSPGR images acquired during the same session as the MT, on which the boundary between grey and white matter was more clearly defined.

Segmentation was carried out in SPM2, using a maximum likelihood algorithm. This assigns voxels to grey matter, white matter, or CSF segments according to spatial prior probabilities, ascertained here by reference to a standard *a priori* tissue probability map, and voxel signal intensity. This time we dealt with the problem of partial volume voxels by introducing a threshold of 0.75 to the NAWM and grey matter segments (Smith 2006), so that only voxels with a 75% or greater likelihood of being situated in each respective segment were included there. This ensured that voxels with any appreciable partial volume were excluded, wherever they were situated. Erosions would have reduced the volume of tissue retained in the analysis, and unnecessarily excluded full volume voxels situated in the eroded layer. This method also kept the segmentation process completely separate from the generation of MTR values, because the MTR value obtained had no relevance in determining the boundaries of the map (Tofts 2004).

The FSPGR was co-registered to the PD MTR image (Mo), and the transformation parameters were applied to grey and white matter probability maps. In patients, T2 lesions were contoured and converted into binary lesion masks, as described in section 3.1.2.3.1 Segmentation was carried out in SPM2, and the lesion masks applied to the FSPGR images to generate grey, NAWM and lesion segment probability maps. The volume of each tissue segment was calculated in SPM2. Raw grey and NAWM brain volumes were normalized by dividing them by the total intracranial volume (the sum of the grey matter, NAWM, lesion and CSF volumes), and multiplying by 100 to produce a percentage grey and NAWM fraction (PGMF and PNAWMF).

The voxel MTR was calculated, and the probability maps applied to produce grey, NAWM and lesion MTR maps as described in section 3.1.2.3.1. One patient demonstrated severe movement artefacts on every MT image, and was excluded from the study. Histograms, normalized to the segment volume (bin width 0.1pu, smoothing window 0.3pu), were generated for the grey and NAWM, and the mean, peak height (PH) and peak location (PL) were obtained. The lesion segment was considered too small to create acceptable histograms, and only mean MTR was measured. In controls, the procedure was the same without the application of a lesion mask.

3.2.2.4 Statistical Analysis

Analysis was carried out using Stata 9.2 (Stata Corporation, Texas, USA).

3.2.2.4.1 Clinical data

Raw EDSS scores at baseline and three years were compared using the Wilcoxon matched-pairs signed-ranks test. Changes in EDSS were converted into steps (see section 3.1.2.4.1). For predictors of clinical outcome, three step change categories were created: stable EDSS, mild progression (EDSS deterioration of 0.5-1.5 steps), and marked progression (deterioration of 2 steps or more).

3.2.2.4.2 Piecewise mixed effect linear regression models

These models are standard linear mixed models, also known as multilevel or hierarchical regression models (Verbeke and Molenberghs 2000, Goldstein H

1995), but we adapted them specifically to adjust for the scanner upgrade. A simple linear regression with time as predictor would ignore the fact that different data points may belong to the same subject, and estimate a single residual variance around one fitted line. In contrast, linear mixed models accommodate the two-level structure of the data by estimating two components of variance: within-subject variation (around individual subject trajectories) and between-subject variation (in intercept and in rate of change with time). In the absence of upgrade the rate of change of the response variable over time is given directly by the coefficient on time. Non-linearity can be examined by fitting an additional quadratic term in time.

To adjust for the upgrade, a modification of the linear mixed model is necessary to make it 'piecewise': instead of one continuous trajectory being fitted, two separate trajectories, with common gradient, are fitted before and after the upgrade, but estimated simultaneously within one model. The assumption of common gradient is tested, and if there is no evidence for a gradient change the common gradient in the piecewise model gives the rate of change adjusting out the discontinuity due to upgrade.

Linear mixed models allow the inclusion of all available data points in the analysis, so that subjects with some data points missing still contribute information. This minimizes bias that could result from the exclusion of these subjects, for example from a method that examined change over just two time points. Another advantage particular to the piecewise adaptation is that both sections of the data, before and after the upgrade, contribute to the estimation of the single underlying adjusted rate of change. Separate regression before and after would not achieve this formally, and would not allow the assumption of a common gradient to be tested.

3.2.2.4.3 Rates of change in brain MTR, volume and T2 lesion load

For the following analyses, except for those predicting EDSS outcome, piecewise mixed effect linear regression models were fitted. The models used random intercept and random time coefficient. The models assume that the changes are linear. We tested for non-linearity in the data by adding a quadratic term in time, and none was found.

To determine mean annual rates of MTR change in patients *versus* controls, mean, PH and PL for grey and NAWM MTR were modelled in turn as response variables. The covariates were: a binary upgrade indicator, time (centred on the upgrade date to adjust for a scanner upgrade effect), a patient/control indicator, patient*time interaction, age and gender. The mean annual rate of lesion MTR change in patients was calculated in the same way, without the patient/control indicator. For brain volume changes, age was a significant covariate so an age*time interaction was added. The model was repeated using PGMF and PNAWMF. In patients, lesion load changes were similarly modelled, with an age*time interaction but without the patient/control indicator. To assess the relationship with change in EDSS in patients, the same MTR and volume variables were modelled in turn as response variables, and clinical change and clinical change*time were additional covariates.

3.2.2.4.4 Baseline MRI predictors of EDSS change

Multiple proportional odds ordinal logistic regression was used. Ordinal categories of EDSS step change were the response variable, and baseline MTR and volume parameters, age and gender were the covariates. Predictors were modelled individually, then the most significant predictor from each modality was selected for each segment (grey, NAWM and lesions). These were then modelled together to identify the best overall predictor. All baseline scans were performed before the upgrade so no adjustment was necessary.

3.2.3 Results

The results are summarized in Table 3.H

3.2.3.1 Changes in EDSS and MRI parameters over three years

Median EDSS scores increased from 4.5 to 6 ($p < 0.001$). Fourteen patients remained stable, 14 demonstrated mild and 15 marked progression. In patients, grey matter mean MTR declined by -0.60pu and NAWM mean MTR by -0.26pu ($p < 0.001$ in both cases). Annual changes in grey and NAWM MTR parameters for patients and controls are shown in Table 3.I. Lesion MTR increased by 0.77pu , at a rate of 0.26pu per year ($p = 0.002$, 95%CI 0.09 to 0.42).

In patients, mean grey matter volume decreased by -12.0ml , at an annual rate of -3.98ml , 0.26% of the original grey matter fraction ($p < 0.001$, 95%CI -5.82 to -2.15). NAWM volume decreased by -0.77ml per year, which was not significant. T2 lesion volume increased annually by 2.80ml , or 9.25% of the original T2 volume ($p < 0.001$, 95%CI 1.87 to 3.74). In controls, there were no significant changes. The rate of change in PGMF (percentage grey matter fraction; $p = 0.005$) but not PNAWMF ($p = 0.47$) was significantly different between patients and controls.

Table 3.H Summary of significant findings for MTR, volume and lesion load measurements in early PPMS

	MTR decrease		Volume decrease		T2 lesion load increase
	Grey matter	NAWM	Grey matter	NAWM	
Longitudinal changes	Yes	Yes	Yes	No	Yes
Rate of change correlates with EDSS changes	Yes	No	No	No	Yes
Baseline measure predicts future clinical progression	Yes**	Yes	Yes	Yes	Yes

NAWM=Normal appearing white matter. MTR=Magnetization transfer ratio. EDSS=Expanded disability status scale. ** Baseline grey matter PH MTR was the strongest predictor of deterioration.

Table 3.I Mean annual rates of change in grey and NAWM MTR in patients and controls

MTR Histogram parameter		PATIENTS		CONTROLS		Patients versus controls
		Yearly rate (p value)	95%CI	Yearly rate (p value)	95%CI	P value
Grey Matter	Mean	- 0.20 (<0.001)	-0.25 to -0.15	0.02 (0.62)	-0.05 to 0.08	<0.001
	PH	- 0.12 (0.03)	-0.23 to -0.01	-0.06 (0.31)	-0.19 to 0.56	0.41
	PL	- 0.10 (0.007)	-0.17 to -0.03	0.02 (0.58)	-0.06 to 0.10	0.01
NAWM	Mean	- 0.09 (<0.001)	-0.12 to -0.05	0.002 (0.90)	-0.34 to 0.40	<0.001
	PH	- 0.17 (0.14)	-0.40 to 0.05	-0.06 (0.63)	-0.29 to 0.18	0.42
	PL	- 0.07 (0.003)	-0.13 to -0.03	-0.0006 (0.98)	-0.56 to 0.55	0.02

MTR=Magnetization transfer ratio, pu=Percent units. 95%CI=95% confidence intervals. PH=Peak height, PL=Peak location. p values derived from piecewise mixed effect linear regression models. PH is given in percent volume, and mean and PL in percent units. MTR changes in controls were not statistically significant.

3.2.3.2 Surrogate MRI markers of clinical change

3.2.3.2.1 Markers of concurrent clinical progression

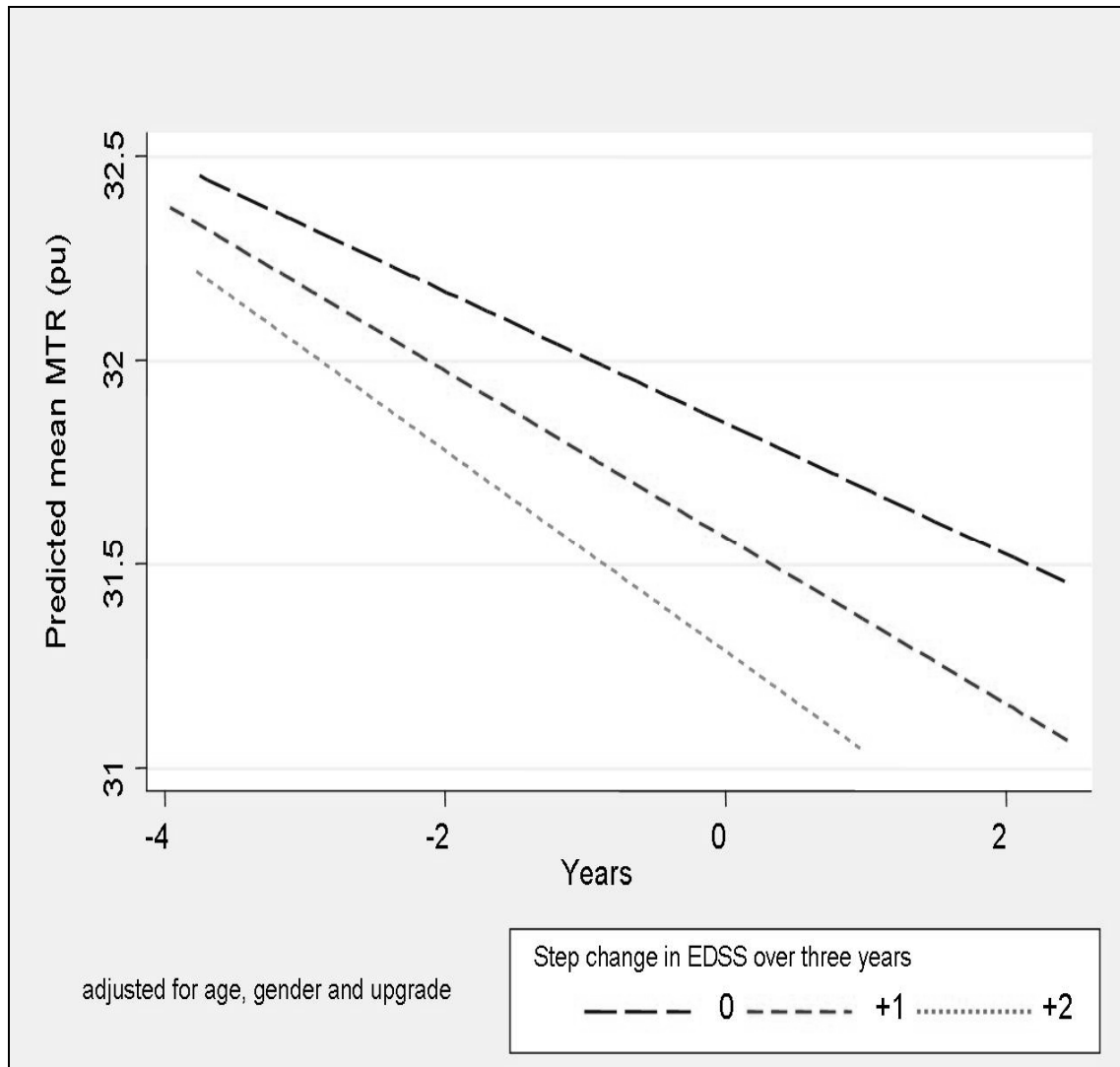
In the grey matter, rapid mean MTR decrease was associated with greater rates of EDSS progression (there was a 0.04pu greater annual MTR decline for each EDSS step deterioration, $p=0.03$, 95%CI -0.82 to -0.003, see Figure 3b), as was PL MTR (0.07pu greater annual MTR decline for each EDSS step deterioration, $p=0.008$, 95%CI -0.01 to -0.2), but not PH MTR decrease. NAWM and lesion changes were not associated with progression rate.

Volume changes in grey and NAWM were not associated with the rate of EDSS change. Greater rate of T2 lesion load increase was associated with faster progression on EDSS (lesion volume increase of 0.70 ml for each EDSS step deterioration, $p=0.02$, 95% CI 0.09 to 1.31).

3.2.3.2.2 Baseline predictors of clinical progression

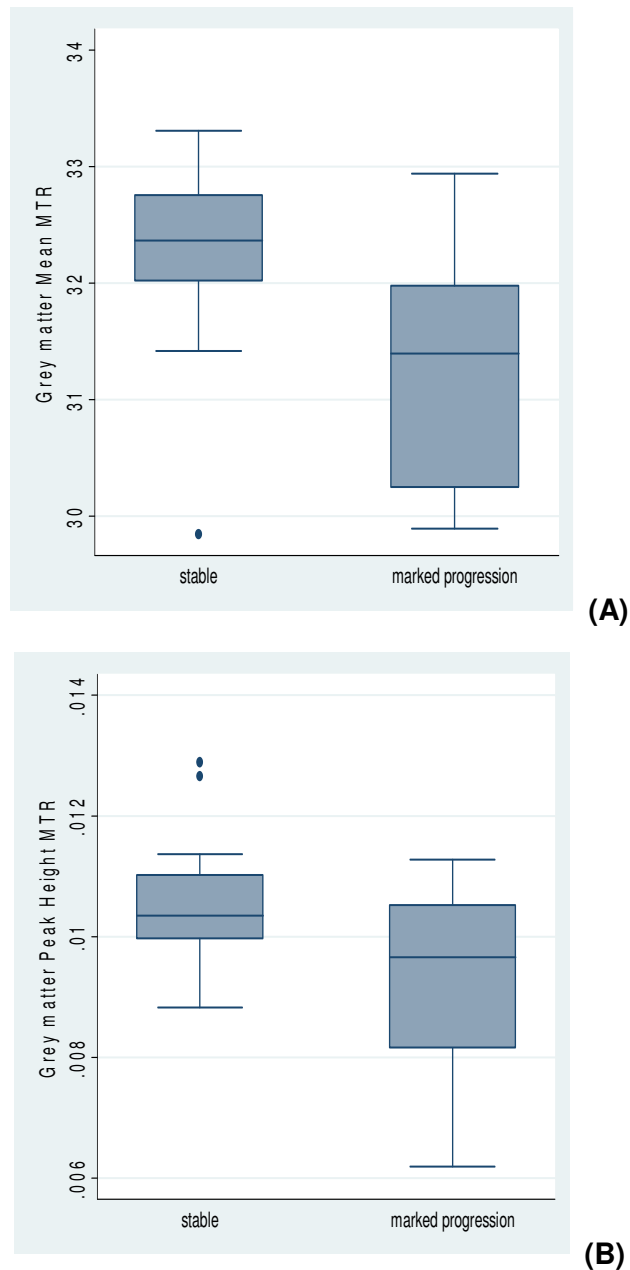
Lower baseline grey matter mean MTR (odds ratio [OR] 2.34, $p=0.02$, 95%CI 1.18 to 4.76; see Figure 3c) and lower grey matter PH MTR (OR 2.43, $p=0.008$, 95%CI 1.27 to 4.65) predicted worse outcome on the EDSS. Grey matter PL MTR showed a trend towards prediction ($p=0.09$). Lower NAWM PL MTR predicted worse outcome on the EDSS (OR=2.5, $p=0.04$, 95%CI 1.04 to 5.88) and NAWM PH MTR showed a trend ($p=0.09$). Lower baseline PGMF (OR 1.42, $p=0.04$, 95%CI 1.01 to 2.00), lower baseline PNAWMF (OR 1.36, $p=0.03$, 95%CI 1.03 to 1.80), and greater T2 lesion load (OR 1.03, $p=0.02$, 95%CI 1.00 to 1.06) were also predictors of worse outcome on EDSS. When the most significant univariate predictors from each modality and segment were modelled together, only grey matter PH MTR remained significant (OR 2.9, $p=0.04$, 95%CI 1.06 to 8.17).

Figure 3b: Grey matter mean MTR decline by EDSS step change over three years



The three lines represent patients who are stable over three years, patients with an overall EDSS step deterioration of 1, and patients with an overall step deterioration of 2 over three years. Those with a more rapid EDSS decline have a faster rate of MTR reduction. The model predicts MTR decline over time centred on the upgrade, at time=0 (see section 3.2.2.4.2 for details); the initial time-point for each patient occurs up to three years earlier. The model is adjusted for age, gender and upgrade. *EDSS=Expanded disability status scale, MTR=Magnetization transfer ratio, pu=Percent units*

Figure 3c Grey matter mean MTR (A) and grey matter PH MTR (B) at baseline, in patients who remained stable and patients who progressed markedly over 3 years



PL showed only a trend to prediction and is therefore not represented. The boxes represent the values between the 25th and 75th centile. The horizontal line within the box represents the median. The vertical lines attached to the box represent adjacent values, and the small circles represent outside values. *MTR*=Magnetization transfer ratio, *PH*=Peak height.

3.2.4 Discussion

We found MTR decline, particularly in the grey matter, grey matter atrophy, and increasing T2 lesion load over three years in early PPMS. The rate of change in grey matter MTR and T2 lesion load, but not grey matter volume, reflected the rate of clinical deterioration. Baseline MTR, brain volume and T2 lesion load predicted clinical progression, and grey matter PH MTR emerged as the strongest predictor.

3.2.4.1 MRI changes

The disproportionate evolution of grey matter damage, measured using MTR and atrophy, was already evident at one year in subgroup of this cohort (see section 3.1, and Sastre-Garriga 2004) and has been identified in other MS subtypes (Horakova 2007, Valsasina 2005). Cortical lesions may account for the majority of this injury. They exhibit demyelination, contain apoptotic neurons (Rovaris 2005, Valsasina 2005, Peterson 2001) and have been associated with axonal transection and loss (Dutta 2007). Wallerian degeneration secondary to axonal damage from white matter inflammation (Brownell 1962) may also reduce grey matter MTR and tissue volume. Conversely, the imaging techniques we used could be less sensitive to processes involved in NAWM damage. For example, inflammatory processes may mask NAWM atrophy (Pirko 2007, Kutzelnigg 2005b). This is less likely in the grey matter, because cortical lesions are less inflammatory (Pirko 2007, Peterson 2001). Notably, the relatively small decline in NAWM MTR is not explained by the removal of the white matter lesions, regarded as the main focus of white matter injury: lesions showed an overall increase in MTR. This is possibly due to remyelination, which has been demonstrated in pathological studies in PPMS of longer disease duration (Patrikios 2006); our results suggest that lesion remyelination may also be a feature in the early phase of PPMS.

3.2.4.2 Predicting progression

From a clinical perspective, grey matter MTR changes were the most relevant. In the sub-group of this cohort studied at one year (see section 3.1), there was a stronger association between NAWM MTR and EDSS change; grey matter MTR predicted timed walk test changes only. In contrast, at three years grey

matter MTR is the stronger predictor of EDSS change. This suggests that the role of NAWM pathology in determining disease progression may be decreasing over time.

Regarding the grey matter MTR histogram parameters, an 8 year follow-up study in different MS subtypes also identified grey matter peak height MTR as a predictor of clinical disability (Agosta 2006). However, the importance of a specific MTR parameter should not be over-emphasized: each one describes only a single point of the histogram (Zhou 2004). In this study, changes in two grey matter parameters (mean and PL MTR) were significantly correlated with the rate of clinical progression, and two predicted disability (baseline mean and PH MTR). This highlights the importance of viewing parameters as a group when evaluating pathological changes and their clinical significance, rather than concentrating on a single measure (see section 2.8.4.2).

3.2.4.3 Monitoring progression

Our findings advocate grey matter MTR as a possible surrogate marker of progression in PPMS. It was the strongest predictor of future disability *and* changed contemporaneously with clinical status. In addition, treatments shown to counteract MTR reduction could be explained as reducing demyelination and axonal loss, the substrates of progression (Pirko 2007, Schmierer 2004), thus addressing a further criterion for a surrogate marker. However, evidence from a single natural history study can only promote grey matter MTR as an un-validated surrogate (McFarland 2002); larger natural history studies exploring MTR changes in PPMS, and more data on the effect of MS therapies on MTR are required (Filippi 2007). Finally, there are practical challenges to implementing MTR as a surrogate marker in multi-centre studies. A standardized MTR sequence applicable to scanners from different manufacturers has been proposed, although it was only reproducible within 2.5 pu between sites (Barker 2005). However, further improvements are possible using dedicated research scanners with careful attention to the flip angle, B1 calibration and patient positioning, and with the use of body coil excitation (Tofts 2004).

Our findings also suggest that T2 lesion load is a potential surrogate, as has been the case in other MS subtypes (Rovaris 2003). To reflect both focal white matter injury and diffuse neurodegenerative change, a combination of grey matter MTR and T2 lesion load may be optimal (Rovaris 2003). However, our combined model suggests that T2 lesion load is a weaker predictor than grey matter MTR in this group. Perhaps surprisingly, a study in other MS subtypes, in a less disabled patient group, also identified grey matter MTR as being a stronger predictor of worsening than T2 lesion load (Agosta 2006). In contrast, developing brain atrophy, regarded as a potential surrogate marker in established PPMS (Fazekas 2007, Simon 2001), did not reflect concurrent clinical change in this group. This may reflect a delay between demyelination and axonal loss, the development of associated atrophy, and the clinical consequences of the tissue loss. Indeed, clinical trials utilizing brain volume as a surrogate have required extensive follow-up to demonstrate treatment effects (Simon 2006), and in advanced PPMS brain atrophy predicted clinical outcome five years later, but not before (Sastre-Garriga 2005b, Ingle 2002).

3.2.4.4 Limitations

The main limitation of this study was incomplete attendance, particularly relating to worsening disability which prevented us from scanning the patients with higher EDSS scores. This is an inevitable problem in longitudinal studies of disabling conditions. We were able to address this by using a statistical model which minimized bias due to drop-out by utilizing *all* available data at each time-point, so that subjects who missed time-points still contributed to the gradient.

The second limitation was the scanner upgrade. After the upgrade, changes to the acquisition parameters were minimized, but one parameter was changed (see 3.2.2.2). Using the piecewise mixed effects model, we were able to take the upgrade into account, and in effect “edit out” discontinuity caused by the upgrade from the trajectory of change, making the longitudinal correlations more robust. In addition, all the changes in patients are described with reference to controls scanned both before and after the upgrade. These approaches address a common problem in longitudinal MR studies, which is particularly relevant for the investigation of quantitative MR measurements.

3.3 Conclusions

MTR histogram analysis is a sensitive measure for detecting change in brain tissues over a relatively short period in PPMS. MTR measures are able to predict short and medium term progression, and grey matter MTR parameters decline concurrently with clinical ability. The evident potential for MTR to satisfy the criteria for a surrogate marker of progression in early PPMS could be investigated in larger studies including natural history observations and therapeutic trials.

Our results suggest that NAWM MTR is more clinically relevant in the early stages in this patient group. As the disease advances, grey matter MTR becomes more closely related to progression, perhaps indicating that grey matter pathology is now driving disability. Lesion MTR loses its clinical relevance over time, perhaps due to lesion heterogeneity and remyelination.

Finally, while grey matter MTR is the strongest clinical predictor at three years, T2 lesion load remains extremely relevant to clinical outcome. This indicates that focal white matter inflammation also plays an important role in determining disability in early PPMS. Further follow-up of this group will be interesting to determine whether the influence of T2 lesion load declines over time, as has been demonstrated previously in established PPMS (Khaleeli 2008). The impact of white matter lesions in PPMS is explored further in Chapter 5.

References

1. Agosta F, Rovaris M, Pagani E, Sormani MP, Comi G, Filippi M. Magnetization transfer MRI metrics predict the accumulation of disability 8 years later in patients with multiple sclerosis. *Brain* 2006; 129: 2620-2627.
2. Ashburner J, Friston KJ. Voxel-based morphometry--the methods. *Neuroimage*. 2000; 11: 805-821.
3. Audoin B, Fernando KT, Swanton JK, Thompson AJ, Plant GT, Miller DH. Selective magnetization transfer ratio decrease in the visual cortex following optic neuritis. *Brain* 2006; 129: 1031-1039.
4. Barker GJ, Schreiber WG, Gass A *et al*. A standardised method for measuring magnetisation transfer ratio on MR imagers from different manufacturers--the EuroMT sequence. *MAGMA*. 2005; 18: 76-80.
5. Barker GJ, Tofts PS, Gass A. An interleaved sequence for accurate and reproducible clinical measurement of magnetization transfer ratio. *Magn Reson.Imaging* 1996; 14: 403-411.
6. Brownell B, Hughes JT. The distribution of plaques in the cerebrum in multiple sclerosis. *J.Neurol.Neurosurg.Psychiatry* 1962; 25: 315-320.
7. Bruck W, Stadelmann C. The spectrum of multiple sclerosis: new lessons from pathology. *Curr.Opin.Neurol*. 2005; 18: 221-224.
8. Chard DT, Griffin CM, Parker GJ, Kapoor R, Thompson AJ, Miller DH. Brain atrophy in clinically early relapsing-remitting multiple sclerosis. *Brain* 2002a; 125: 327-337.
9. Chard DT, Parker GJ, Griffin CM, Thompson AJ, Miller DH. The reproducibility and sensitivity of brain tissue volume measurements derived from an SPM-based segmentation methodology. *J.Magn Reson.Imaging* 2002b; 15: 259-267.
10. Cutter GR, Baier ML, Rudick RA *et al*. Development of a multiple sclerosis functional composite as a clinical trial outcome measure. *Brain* 1999; 122 (Pt 5): 871-882.
11. Davies GR, Altmann DR, Hadjiprocopis A *et al*. Increasing normal-appearing grey and white matter magnetisation transfer ratio abnormality in early relapsing-remitting multiple sclerosis. *J.Neurol*. 2005; 252: 1037-1044.
12. Dehmeshki J, Chard DT, Leary SM *et al*. The normal appearing grey matter in primary progressive multiple sclerosis: a magnetisation transfer imaging study. *J Neurol* 2003; 250: 67-74.
13. Dehmeshki J, Silver NC, Leary SM, Tofts PS, Thompson AJ, Miller DH. Magnetisation transfer ratio histogram analysis of primary progressive and other multiple sclerosis subgroups. *J Neurol Sci* 2001; 185: 11-17.
14. Dutta R, Trapp BD. Pathogenesis of axonal and neuronal damage in multiple sclerosis. *Neurology* 2007; 68: S22-S31.
15. Ellison GW, Myers LW, Leake BD *et al*. Design strategies in multiple sclerosis clinical trials. The Cyclosporine Multiple Sclerosis Study Group. *Ann.Neurol*. 1994; 36 Suppl: S108-S112.
16. Fazekas F, Soelberg-Sorensen P, Comi G, Filippi M. MRI to monitor treatment efficacy in multiple sclerosis. *J.Neuroimaging* 2007; 17 Suppl 1: 50S-55S.

17. Fernando KT, Tozer DJ, Miszkiel KA *et al.* Magnetization transfer histograms in clinically isolated syndromes suggestive of multiple sclerosis. *Brain* 2005; 128: 2911-2925.
18. Filippi M, Bozzali M, Horsfield MA *et al.* A conventional and magnetization transfer MRI study of the cervical cord in patients with MS. *Neurology* 2000a; 54: 207-213.
19. Filippi M, Inglese M, Rovaris M *et al.* Magnetization transfer imaging to monitor the evolution of MS: a 1-year follow-up study. *Neurology* 2000b; 55: 940-946.
20. Filippi M, Rocca MA. Magnetization transfer magnetic resonance imaging of the brain, spinal cord, and optic nerve. *Neurotherapeutics*. 2007; 4: 401-413.
21. Gass A, Barker GJ, Kidd D *et al.* Correlation of magnetization transfer ratio with clinical disability in multiple sclerosis. *Ann.Neurol.* 1994; 36: 62-67.
22. Geurts JJ. Imaging cortical lesions and NAGM at high and standard field strength (4.7T and 1.5T) : combined post-mortem MRI and histopathology. abstract from ECTRIMS conference 2005a; S8, Abstract 40.
23. Geurts JJ, Bo L, Pouwels PJ, Castelijns JA, Polman CH, Barkhof F. Cortical lesions in multiple sclerosis: combined postmortem MR imaging and histopathology. *AJNR Am.J.Neuroradiol.* 2005b; 26: 572-577.
24. Goldstein H. *Multilevel Statistical Models*. New York: Halstead Press, 1995.
25. Greenhalgh T. How to read a paper. Papers that report diagnostic or screening tests. *BMJ* 1997; 315: 540-543.
26. Hobart J, Kalkers N, Barkhof F, Uitdehaag B, Polman C, Thompson A. Outcome measures for multiple sclerosis clinical trials: relative measurement precision of the Expanded Disability Status Scale and Multiple Sclerosis Functional Composite. *Mult.Scler.* 2004; 10: 41-46.
27. Hoogervorst EL, Eikelenboom MJ, Uitdehaag BM, Polman CH. One year changes in disability in multiple sclerosis: neurological examination compared with patient self report. *J.Neurol.Neurosurg.Psychiatry* 2003; 74: 439-442.
28. Hoogervorst EL, Kalkers NF, Uitdehaag BM, Polman CH. A study validating changes in the multiple sclerosis functional composite. *Arch.Neurol.* 2002; 59: 113-116.
29. Horakova D, Cox JL, Havrdova E *et al.* Evolution of different MRI measures in patients with active relapsing-remitting multiple sclerosis over 2 and 5 years. A case control study. *J.Neurol.Neurosurg.Psychiatry* 2007.
30. Ingle GT, Stevenson VL, Miller DH *et al.* Two-year follow-up study of primary and transitional progressive multiple sclerosis. *Mult.Scler.* 2002; 8: 108-114.
31. Johnston SC, Hauser SL. Clinical trials: rising costs limit innovation. *Ann.Neurol.* 2007; 62: A6-A7.
32. Khaleeli Z, Ciccarelli O, Manfredonia F *et al.* Predicting progression in primary progressive multiple sclerosis: A 10-year multicenter study. *Ann Neurol* 2008.
33. Kidd D, Barkhof F, McConnell R, Algra PR, Allen IV, Revesz T. Cortical lesions in multiple sclerosis. *Brain* 1999; 122 (Pt 1): 17-26.
34. Kragt JJ, Thompson AJ, Montalban X *et al.* Responsiveness and predictive value of EDSS and MSFC in primary progressive MS. *Neurology* 2008.
35. Kurtzke JF. Rating neurologic impairment in multiple sclerosis: an expanded disability status scale (EDSS). *Neurology* 1983; 33: 1444-1452.

36. Kutzelnigg A, Lassmann H. Cortical lesions and brain atrophy in MS. *J.Neurol.Sci.* 2005a; 233: 55-59.
37. Kutzelnigg A, Lucchinetti CF, Stadelmann C *et al.* Cortical demyelination and diffuse white matter injury in multiple sclerosis. *Brain* 2005b; 128: 2705-2712.
38. Lechner-Scott J, Kappos L, Hofman M *et al.* Can the Expanded Disability Status Scale be assessed by telephone? *Mult.Scler.* 2003; 9: 154-159.
39. McFarland HF, Barkhof F, Antel J, Miller DH. The role of MRI as a surrogate outcome measure in multiple sclerosis. *Mult.Scler.* 2002; 8: 40-51.
40. Patrikios P, Stadelmann C, Kutzelnigg A *et al.* Remyelination is extensive in a subset of multiple sclerosis patients. *Brain* 2006; 129: 3165-3172.
41. Perneger TV. What's wrong with Bonferroni adjustments. *BMJ* 1998; 316: 1236-1238.
42. Peterson JW, Bo L, Mork S, Chang A, Trapp BD. Transected neurites, apoptotic neurons, and reduced inflammation in cortical multiple sclerosis lesions. *Ann.Neurol.* 2001; 50: 389-400.
43. Phillips MD, Grossman RI, Miki Y *et al.* Comparison of T2 lesion volume and magnetization transfer ratio histogram analysis and of atrophy and measures of lesion burden in patients with multiple sclerosis. *AJNR Am.J.Neurol.* 1998; 19: 1055-1060.
44. Pirko I, Lucchinetti CF, Sriram S, Bakshi R. Gray matter involvement in multiple sclerosis. *Neurology* 2007; 68: 634-642.
45. Plummer D. Dispimage: a display and analysis tool for medical images. *Rev Neuroradiol* 1992; 5: 489-495.
46. Prentice RL. Surrogate endpoints in clinical trials: definition and operational criteria. *Stat.Med.* 1989; 8: 431-440.
47. Ramio-Torrenta L, Sastre-Garriga J, Ingle GT *et al.* Abnormalities in normal appearing tissues in early primary progressive multiple sclerosis and their relation to disability: a tissue specific magnetisation transfer study. *J.Neurol.Neurosurg.Psychiatry* 2006; 77: 40-45.
48. Rovaris M, Agosta F, Sormani MP *et al.* Conventional and magnetization transfer MRI predictors of clinical multiple sclerosis evolution: a medium-term follow-up study. *Brain* 2003; 126: 2323-2332.
49. Rovaris M, Bozzali M, Rodegher M, Tortorella C, Comi G, Filippi M. Brain MRI correlates of magnetization transfer imaging metrics in patients with multiple sclerosis. *J.Neurol.Sci.* 1999; 166: 58-63.
50. Rovaris M, Bozzali M, Santuccio G *et al.* Relative contributions of brain and cervical cord pathology to multiple sclerosis disability: a study with magnetisation transfer ratio histogram analysis. *J.Neurol.Neurosurg.Psychiatry* 2000; 69: 723-727.
51. Rovaris M, Gallo A, Valsasina P *et al.* Short-term accrual of gray matter pathology in patients with progressive multiple sclerosis: an in vivo study using diffusion tensor MRI. *Neuroimage.* 2005; 24: 1139-1146.
52. Rovaris M, Judica E, Gallo A *et al.* Grey matter damage predicts the evolution of primary progressive multiple sclerosis at 5 years. *Brain* 2006.
53. Sastre-Garriga J, Ingle GT, Chard DT *et al.* Grey and white matter volume changes in early primary progressive multiple sclerosis: a longitudinal study. *Brain* 2005a; 128: 1454-1460.

54. Sastre-Garriga J, Ingle GT, Chard DT, Ramio-Torrenta L, Miller DH, Thompson AJ. Grey and white matter atrophy in early clinical stages of primary progressive multiple sclerosis. *Neuroimage*. 2004; 22: 353-359.
55. Sastre-Garriga J, Ingle GT, Rovaris M *et al*. Long-term clinical outcome of primary progressive MS: predictive value of clinical and MRI data. *Neurology* 2005b; 65: 633-635.
56. Schmierer K, Scaravilli F, Altmann DR, Barker GJ, Miller DH. Magnetization transfer ratio and myelin in postmortem multiple sclerosis brain. *Ann.Neurol*. 2004; 56: 407-415.
57. Simon JH. Brain and spinal cord atrophy in multiple sclerosis: role as a surrogate measure of disease progression. *CNS.Drugs* 2001; 15: 427-436.
58. Simon JH. Brain atrophy in multiple sclerosis: what we know and would like to know. *Mult.Scler*. 2006; 12: 679-687.
59. Smith SM, Jenkinson M, Johansen-Berg H *et al*. Tract-based spatial statistics: voxelwise analysis of multi-subject diffusion data. *Neuroimage*. 2006; 31: 1487-1505.
60. Solari A, Radice D, Manneschi L, Motti L, Montanari E. The multiple sclerosis functional composite: different practice effects in the three test components. *J.Neurol.Sci*. 2005; 228: 71-74.
61. Thompson AJ, Montalban X, Barkhof F *et al*. Diagnostic criteria for primary progressive multiple sclerosis: a position paper. *Ann.Neurol*. 2000; 47: 831-835.
62. Tofts P. *Quantitative MRI of the Brain*. Chichester: John Wiley & Sons, 2004.
63. Tombaugh TN. A comprehensive review of the Paced Auditory Serial Addition Test (PASAT). *Arch.Clin.Neuropsychol*. 2006; 21: 53-76.
64. Tremlett H, Paty D, Devonshire V. The natural history of primary progressive MS in British Columbia, Canada. *Neurology* 2005; 65: 1919-1923.
65. Valsasina P, Benedetti B, Rovaris M, Sormani MP, Comi G, Filippi M. Evidence for progressive gray matter loss in patients with relapsing-remitting MS. *Neurology* 2005; 65: 1126-1128.
66. Verbeke and Molenberghs. *Linear Mixed Models for Longitudinal Data*. New York: Springer-Verlag, 2000.
67. Vrenken H, Pouwels PJ, Ropele S *et al*. Magnetization transfer ratio measurement in multiple sclerosis normal-appearing brain tissue: limited differences with controls but relationships with clinical and MR measures of disease. *Mult Scler* 2007; 13: 708-716.
68. Wolinsky JS, Narayana PA, O'Connor P *et al*. Glatiramer acetate in primary progressive multiple sclerosis: results of a multinational, multicenter, double-blind, placebo-controlled trial. *Ann.Neurol*. 2007; 61: 14-24.
69. Zhou LQ, Zhu YM, Grimaud J, Hermier M, Rovaris M, Filippi M. A new method for analyzing histograms of brain magnetization transfer ratios: comparison with existing techniques. *AJNR Am J Neuroradiol* 2004; 25: 1234-1241.

**Localizing tissue injury:
Voxel-based Analysis of MTR and
Atrophy**

CHAPTER 4

4.1 Introduction

In Chapter 3 we demonstrated that damage to the NABT had an impact on clinical progression in PPMS, and could be detected by measuring MTR and atrophy. However, while the MTR histogram and brain segmentation methods described suggest that grey matter damage is particularly relevant in this group, these techniques can not locate the damage more specifically.

In this study, we used a voxel-based methodology, in which all images were spatially normalized into standard space. This allows a voxel-by-voxel statistical comparison between patients and a control group, so that all parts of the grey matter are investigated. The technique avoids the bias introduced when using an *a priori* hypothesis, for example in ROI analysis (see sections 2.8.4.1 and 2.8.4.3). The technique was previously applied to localize grey matter atrophy in a subgroup of our cohort, and thalamic atrophy was identified (Sepulcre 2006). In the present study we implemented methodological improvements to maximize the sensitivity of the technique, and increased the study population, in order to test for atrophy not only in the deep grey matter but also in the cortex.

We aimed to localize both grey matter MTR changes and atrophy, to establish the relationship between the processes reflected by each technique. In addition, we assessed the direct clinical impact of the MTR changes by correlating them with clinical scores for the functional systems relevant to the damaged areas, while taking into account volume loss within the regions of reduced MTR.

4.2 Methods

4.2.1 Subjects

As described in section 3.1.2.1, fifty patients with definite or probable PPMS (Thompson 2000), within five years of symptom onset, were invited for radiological assessment and scored on the EDSS and MSFC. As described previously, one patient did not complete the baseline protocol, and another developed claustrophobia. One patient withdrew after baseline, but was retained in the present study. Two patients were excluded from this study on the basis of their images (see section 4.2.2). Thus a total of 46 patients entered the present study (19 female, 27 male; mean age 43.5 years, range 19 to 65 years; see Table 4.A for patient characteristics), and twenty-three healthy controls were also scanned (12 female, 11 male; mean age 35.1 years, range 23-56 years). The difference in age between patients and controls was adjusted for at each stage of the analysis, as described below.

Table 4.A Characteristics of patients and controls

	Patients (n=46)	Controls (n=23)
Age in years (range)	43.5 (19-65)	35.1 (23 -56)
Gender female/male	19/27	12/11
EDSS median (range)	4.5 (1.5-7)	-
Disease duration in years (range)	3.3 (2-5)	-
T2 lesion load in ml (SD)	13.39 (19.61)	-

SD=Standard deviation, EDSS=Expanded Disability Status Scale, n=number

4.2.2 Image acquisition and post-processing

A 1.5 Tesla GE Signa scanner (General Electric, Milwaukee, Wisconsin, USA) was used to acquire the images. MTI and T1-weighted FSPGR sequences were acquired as described in section 3.1.2.2. The images were transferred to a Sun workstation (Sun Microsystems, Mountain View, CA) for post-processing. MTR maps were calculated from the PD images as described in section 3.1.2.3. The following processing, except the creation of the lesion mask, was done in SPM2 (Wellcome Department of Cognitive Neurology, London, UK).

4.2.2.1 Lesion mask creation

Lesions were contoured on the unsaturated PD images from the MT sequence as described in section 3.1.2.3, and binary lesion masks created for each patient. The lesion mask was smoothed with an 8mm full width at half maximum (FWHM) isotropic Gaussian kernel. Voxels at the lesion boundary with intensity less than one were set to zero, so that any voxel containing lesional and peri-lesional tissue would be included in the mask and therefore excluded from the analysis (see below).

4.2.2.2 Co-registration of MTR and T1-weighted images

PD-weighted scans from the MT sequence were co-registered to the corresponding T1-weighted volume, using normalized mutual information as the cost function (Studholme 1997). The same transformation was then applied to the MTR map and lesion mask, so that all images were in the space of the T1-weighted volume.

4.2.2.3 Segmentation of the T1-weighted images in native space

Segmentation of the T1-weighted volume image was performed in native space in SPM2, as described in Chapter 3 section 3.2.2.3. Lesion masks were applied to patients' scans to remove any lesional tissue erroneously classified as grey or white matter.

4.2.2.4 Normalization of segmented images

The use of lesion masks excluded lesions from the normalization process by assigning them a zero weighting. The grey matter T1 segmented images were normalized into MNI (Montreal Neurological Institute) stereotactic space using a 12 parameter affine transformation, optimized using 16 non-linear warps (Ashburner 1997). Optimized transformation parameters were noted and used again later.

4.2.2.5 Normalization of the original T1-weighted images, lesion masks and MTR maps

The optimum parameters obtained from normalizing the NAGM T1-weighted images as described above were then applied to the original T1-weighted images. This optimized methodology is used because normalization is ideally performed on segmented images, so that structural differences affecting normalization do not influence segmentation; however, segmentation is optimally performed on normalized images corresponding to the *a priori* T1 template (Good 2001). The same transformation parameters were applied to MTR maps and lesion masks.

4.2.2.6 Segmentation in stereotactic space

Normalized T1-weighted images were then segmented in stereotactic space to produce grey matter, white matter, and CSF segments, as explained above. Normalized lesion masks were applied to the grey matter segments to ensure no lesions were included erroneously.

4.2.2.7 Production and application of grey matter mask

A conservative threshold of 0.75 (Smith 2006) was applied to the grey matter segment from the FSPGR image produced in Step 6, as described in section 3.2.2.3. Thus only those voxels with a 75% or more likelihood of being situated in the grey matter were used to compute a binary grey matter mask in SPM2. This mask was then applied to the MTR map, to produce a conservative NAGM MTR map. The voxel size was 1mm³.

4.2.2.8 Smoothing

MTR maps and T1-weighted images were smoothed with a 12mm FWHM Gaussian kernel, which rendered the data more statistically normal for analysis by SPM2, and corrected for errors during normalization.

The post-processing output on each patient was checked at each stage, and two patients were excluded from the study. The first had extensive and severe global atrophy far in excess of the rest of the group, making normalization to the T1 template problematic. The second had an extremely high lesion load causing a segmentation failure in which white matter was incorrectly included in the grey matter segment, as described in section 3.1.2.3.

4.2.3 Location of Regions with abnormal MTR and grey matter volume

Comparisons of grey matter MTR and volume between patients and controls were performed in SPM2 using analysis of covariance adjusted for age, and using a family-wise error correction at $p < 0.01$ for multiple comparisons at voxel level across the whole brain. This produced maps depicting regions where MTR and grey matter volumes were significantly lower in patients. Regions comprising clusters of less than one hundred voxels were excluded from the analysis, which is a relatively conservative threshold (Ceccarelli 2008, Henry 2008). We calculated a mean MTR for each region where MTR was significantly reduced.

To investigate the relationship between abnormal regions in the deep grey matter and cortex, Pearson's correlation were carried out (in SPSS 11.0 [Statistical package for the Social Sciences, Chicago, IL, USA]) between the mean MTR in the thalamic regions and regions in the motor, somato-sensory, temporal and occipital cortex.

4.2.4 Correlations between MTR in abnormal regions and clinical measures

Z-scores (z) for MSFC subtests were calculated using our own sample as reference, and used to obtain the MSFC (Cutter 1999). Correlations between clinical scores and the mean MTR in selected regions with reduced MTR (chosen *a priori*) were carried out in SPSS. From among the regions where patients showed reduced MTR compared to controls, we selected those within the motor network and within areas reported as relevant to PASAT performance. The motor regions were the pre- and post-central gyri, from which the cortico-spinal tract originates (Toyoshima 1982). Mean MTR in these regions was correlated with disability (EDSS) as well as mobility and upper limb function test scores (z TWT and z NHPT respectively). Regions selected as relevant to PASAT performance were: superior and middle frontal cortex, inferior parietal cortices and precuneus, superior temporal, inferior and medial occipital cortices. These regions were reported to activate during PASAT testing in functional MRI (fMRI) experiments in controls and patients with relapsing and remitting MS (RRMS) (Forn 2006, Audoin 2005, Mainero 2004, Audoin 2003). Mean MTR for each of these regions was correlated with the z PASAT score.

We wanted to identify whether MTR was associated with any of the clinical scores collected, so a general linear model was performed separately for each clinical measure using SPM2. Clinical score was the dependent variable and MTR within the selected region was the covariate. As the z TWT scores were not normally distributed, the inverse z TWT score was used as this rendered the data more normal (iz TWT). Models were adjusted for age and gender where they significantly affected the model. R values were obtained using partial correlations adjusted for the same covariates as the general linear model. Since MTR can be affected by partial volume effects in voxels containing CSF or white matter in addition to grey matter, we always adjusted models for the grey matter volume within precisely the same voxels in which the MTR was reduced. To calculate this value we used MRicro software (<http://www.sph.sc.edu/comd/rorden/micro.html>). Abnormal MTR regions were delineated as regions of interest (ROIs), and a separate ROI mask created for each region. The masks were then applied one by one to the

segmented grey matter maps, to extract the grey matter volume for each individual in each region of abnormal MTR (normalized to the voxel size).

4.2.5 *Post hoc* analysis on the region in the left pre-central gyrus

Having co-registered scans from different sequences with different resolutions and then normalized them into standard space, we wanted to be certain that the anatomical location of our abnormal regions was correct, and that the MTR changes identified reflected genuine grey matter abnormalities. We used a *post hoc* analysis similar to that described by Sommer (Sommer 2002). We chose to perform this on the region identified in the left pre-central gyrus, because the MTR reduction in this region in patients was highly significant, and correlated with clinical measures of disability, but the region was sufficiently small to make accurate localization relevant. First, we extracted the transformation parameters used to put the T1-weighted image into standard space using SPM2, and inverted them using the SPM Deformation Toolbox. We applied the inverted transformation parameters of each individual patient's T1-weighted image in turn to the ROI mask for the abnormal region in the left pre-central gyrus (created above). This produced an ROI mask of the abnormal region in the left pre-central gyrus in the space of the native T1-weighted image. We then reversed the rigid body transformation originally used to register the MTR image onto the T1-weighted image, producing an image of the ROI mask in the space of the original MT image. This allowed us to check the location of the region on each original scan in native space, and to obtain the mean MTR for this region from the original images. Finally, we compared the mean MTR in this region between patients and controls (in SPSS) using a general linear model adjusted for age, where MTR was the dependent variable and patient or control status and age were covariates.

4.3 Results

4.3.1 Location of regions of reduced MTR and atrophy

4.3.1.1 Cortical grey matter

In patients, all cortical regions with significantly reduced grey matter volume overlapped with regions with significantly reduced MTR (see Figure 4a and Table 4.B). The largest and most significant ($p < 0.001$) regions of cortical reduction in MTR and grey matter volume were in the right pre-central gyrus (Brodmann area [BA] 4), but regions were also present in the right middle frontal gyrus (BA 44), left post-central gyrus (BA3), and left insula.

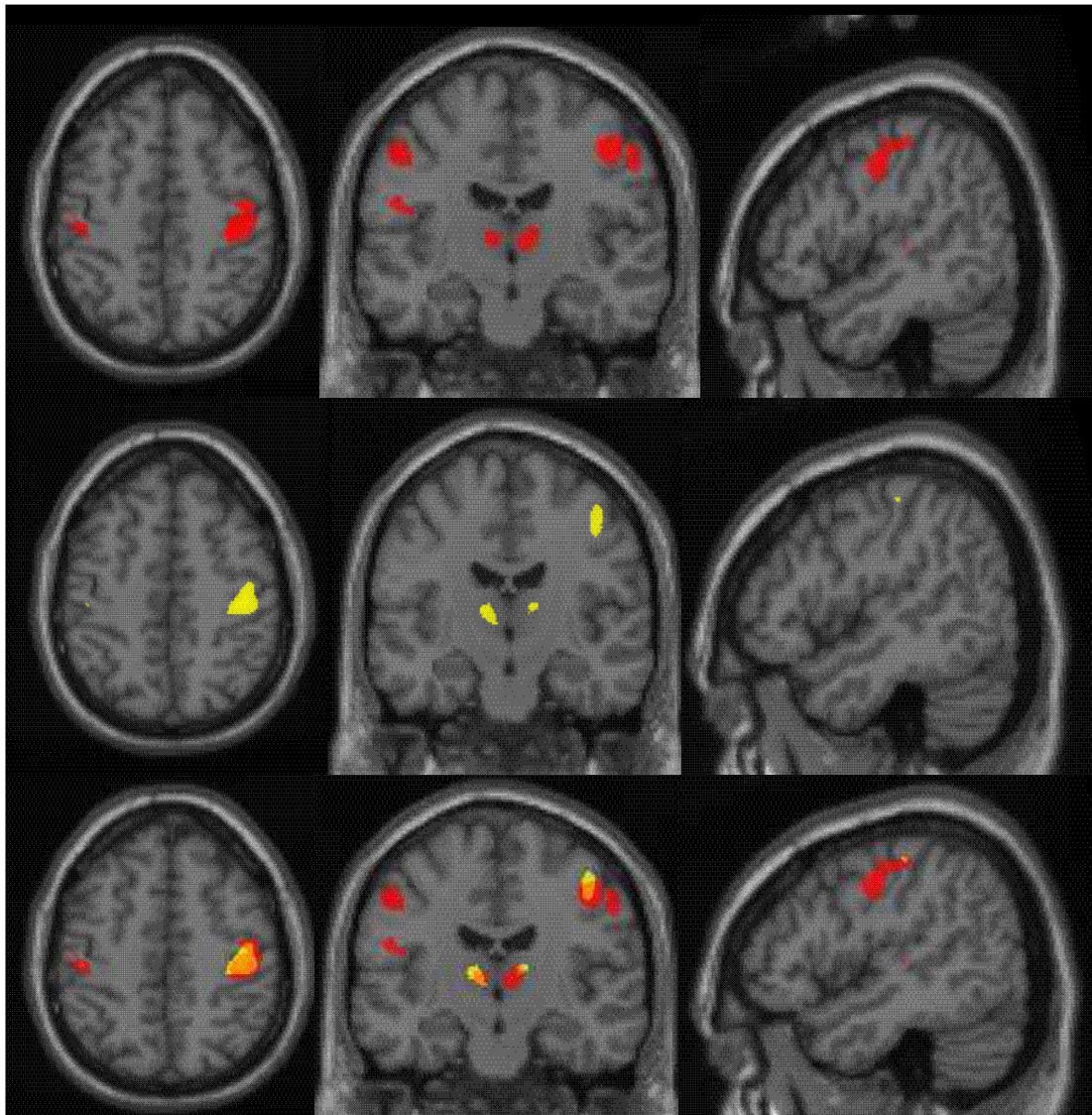
Reduced MTR without significant atrophy was seen in the left superior frontal gyrus (BA 9/46), left pre-central gyrus (BA 4), right inferior parietal cortex and precuneus (BA7), right insula, bilateral superior temporal gyrus (BA 42 and 22), and right medial and bilateral inferior occipital cortex (BA 17 and 18; see Table 4.B).

4.3.1.2 Deep grey matter

In both thalami the region of reduced MTR extended anteriorly, laterally and infero-laterally, encompassing the anterior, ventral anterior, ventral lateral, ventral posterior and lateral geniculate nuclei and pulvinar (see Table 4.B). The right thalamus contained the region with the most significantly reduced MTR in the whole brain ($p < 0.001$).

Moderate correlations were present between the mean MTR in the thalamic regions and in all the regions identified in connected areas of cortex: motor cortex, somato-sensory cortex, temporal and occipital cortex ($p < 0.001$, r value between 0.60 and 0.80 in all cases).

Figure 4a: Regions of significantly reduced MTR and grey matter volume in patients compared to controls



z = 48

y = -14

x = 49.8

The top row shows regions of MTR reduction, in red. The middle row shows regions of atrophy, in yellow. The bottom row shows regions of MTR and atrophy superimposed to demonstrate the degree of overlap, shown in orange.

x, y and z are the Montreal Neurological Institute co-ordinates, in mm. MTR=magnetization transfer ratio

Table 4.B Regions with significantly reduced MTR and grey matter volume in patients compared to controls

Gyrus/portion			BA	MTR			ATROPHY		
				MNI co-ordinates of maxima	Number of voxels	p value*	MNI co-ordinates of maxima	Number of voxels	p value*
Frontal	Superior	L	9/46	-23 49 25	718	0.001	-	-	-
	Middle	R	44	43 10 37	408	<0.001	44 10 37	19	0.004
	Pre-central	R	4	40 -23 50	3916	<0.001	41 -22 52	2520	<0.001
		R	4	-	-	-	56 -9 40	139	<0.001
		L	4	-45 -13 43	1850	<0.001	-	-	-
Parietal	Post-central	L	3	-49 -12 23	1131	<0.001	-47 -19 57	234	<0.001
	Inferior	R	7	34 -62 46	194	0.003	-	-	-
	Precuneus	R	7	10 -56 43	120	0.002	-	-	-
Temporal	Superior	R	22	63 -29 -9	430	0.004	-	-	-
		L	42	-51 -42 17	351	0.001	-	-	-
Occipital	Medial	R	17	15 -67 14	316	0.002	-	-	-
		R	17	10 -82 -1	175	0.002	-	-	-
	Inferior	R	18	28 -90 -9	244	0.002	-	-	-
		L	18	-27 -92 -10	270	<0.001	-	-	-
		L	18	-10 -79 -2	532	<0.001	-	-	-
Insula		R	13	36 3 4	1036	0.002	-	-	-
		L	13	-37 5 1	1190	<0.001	-36 5 0	558	<0.001
Thalami	Anterior, Lateral, Infero-lateral	R	-	20 -28 2	1152	<0.001	21 -26 7	1092	<0.001
	Anterior, Lateral, Infero-lateral	L	-	-8 -12 5	778	<0.001	-10 -10 9	794	<0.001

* p value after family wise error correction of $p < 0.01$ at voxel level

BA=Brodmann area, MTR=magnetization transfer ratio, MNI= Montreal Neurological Institute, R=Right, L=Left

4.3.2 Clinical correlations with MTR in abnormal regions after adjusting for atrophy

4.3.2.1 Motor function

Clinical scores correlated with mean MTR in the regions identified as different to controls within the pre- and post-central gyri (see Table 4.C). Patients with greater disability measured by EDSS, MSFC, NHPT and TWT scores had a lower MTR in these regions.

4.3.2.2 Cognition

zPASAT correlated with mean MTR in the right inferior parietal cortex (BA 7; $p=0.043$, $r=0.30$) and right inferior occipital gyrus (BA 18; $p=0.04$, $r=0.30$). There was a trend to correlation between the zPASAT and mean MTR in the abnormal region identified in the left superior frontal gyrus (BA 9; $p=0.06$, $r=0.28$). In these regions, lower zPASAT scores correlated with lower MTR values. In the remaining regions identified, there were no correlations between zPASAT score and MTR.

4.3.2.3 Post hoc Analysis

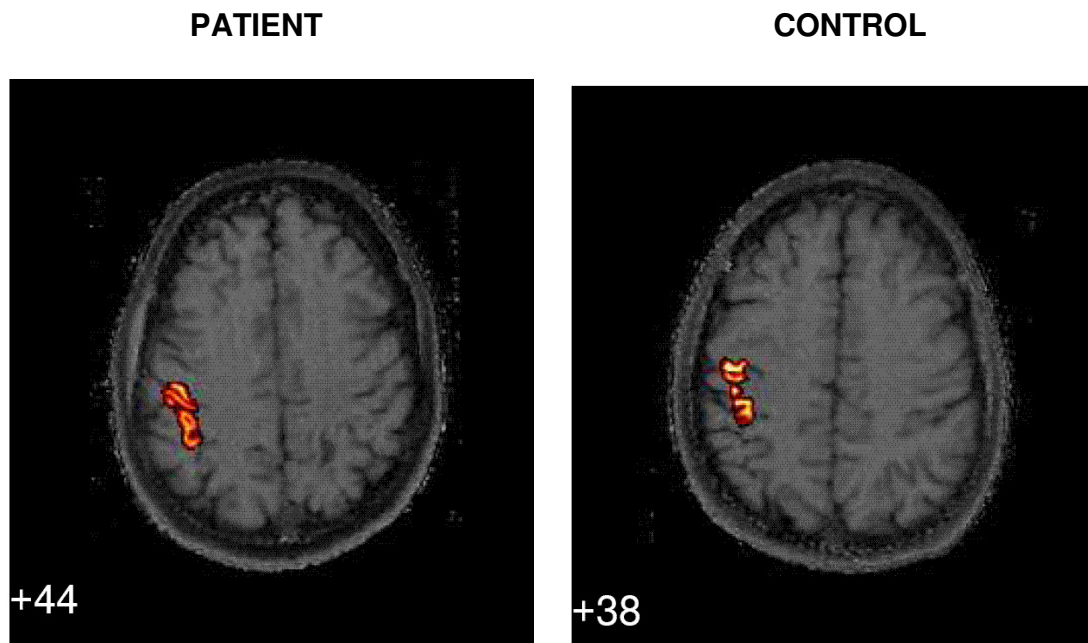
When the abnormal region identified in the left motor cortex was translated back into native space and applied to the original MTR map, the position of the region was shown to be consistent in all subjects (see Figure 4b for examples). The mean MTR obtained in this region from the original MTR map was significantly lower in patients than in controls ($p=0.001$).

Table 4.C Correlation between mean MTR in abnormal regions found within the motor network and clinical measures of disability

			EDSS		zNHPT		izTWT		MSFC	
			p	r	p	r	p	r	p	r
Frontal	Pre-central (BA 4)	R	0.013	-0.37	<0.001	0.49	0.013	0.37	<0.001	0.53
		L	0.004	-0.43	<0.001	0.55	0.001	0.48	0.001	0.49
Parietal	Post-central (BA 3)	L	0.001	-0.50	<0.001	0.56	<0.001	0.53	0.001	0.50

EDSS= Expanded disability status scale, zNHPT= z-score for the nine hole peg test, izTWT= inverse of z-score for the timed walk test, MSFC= Multiple sclerosis functional composite, BA= Brodmann area

Figure 4b: The abnormal region in the left pre-central gyrus translated back into native space and applied to the original PD-weighted MTR images



The number on the left of the image is the slice number

4.4 Discussion

It has been widely accepted that the NABT changes contributing to clinical progression are likely to be diffuse (Filippi 2003). In this study we report for the first time that focal regions of damage occur in the cortex and deep grey matter in early PPMS, as demonstrated by localized regions of MTR reduction and atrophy, and that they contribute to disability.

4.4.1 Regions of reduced MTR and atrophy

4.4.1.1 Cortical Regions

The largest and most significant cortical regions of MTR and volume reduction were in the pre-central gyrus (BA 4), indicating severe damage to the primary motor cortex early in the disease course of PPMS. Reduced MTR and grey matter atrophy were also found in: the post-central gyrus (left somato-sensory cortex, BA 3 in particular); left insula, a highly connected brain area integrating information from a number of functional systems; and the right middle frontal gyrus, which may be involved in the directed forgetting of unwanted memories (Aron 2004). It should be noted that although there was no region with a local maximum in the right post-central gyrus, the pre-central gyrus cluster was very large and extended into the post-central gyrus. MTR reduction alone involved a number of additional areas, including the right somato-sensory association cortex; right insula, bilateral superior temporal gyri, which are involved in lexical-semantic processing (Koeda 2006); and the bilateral visual cortex.

4.4.1.2 Deep Grey Matter Regions

Thalamic damage has been noted from the earliest stages of MS (Mesaros 2008, Derache 2006, Geurts 2006, Audoin 2004), and this was the area that differed most significantly from controls in our cohort. The anterior thalamic centres are connected to the motor and pre-motor cortex, and the infero-lateral areas to the somato-sensory, temporal and occipital cortex (Behrens 2003). Thus the areas of thalamus affected correspond with areas where we found cortical damage, and

indeed there was a moderate correlation between the MTR in the thalamic regions identified and those identified in connected areas of cortex.

It remains uncertain whether the cortical and deep grey matter damage is a primary pathological process, whether it is due to lesions within the grey matter, or whether it is secondary to white matter lesions causing retrograde or Wallerian neuro-axonal degeneration (Brownell 1962). A study in RRMS found a significant relationship between focal thinning in the cortex and white matter lesion load (Charil 2007) in a large cohort, and more recently T2 lesion volume has been shown to correlate strongly with thalamic atrophy in PPMS (Ceccarelli 2008). Recent work suggests that lesions in PPMS may have a predilection for the cortico-spinal tract (Di Perri 2008), but examination of larger cohorts will be necessary to confirm this.

4.4.1.3 Relationship between MTR reduction and Atrophy

As expected, MTR reduction was always present in regions with significant atrophy. The pathological substrate of grey matter MTR reduction remains unclear. However, *post mortem* studies in NAWM suggest that while MTR reduction reflects axonal loss, and thus essentially areas of tissue atrophy, this is probably secondary to its sensitivity to demyelination (Schmierer 2004). This may explain the incomplete overlap in the cortex and the thalamus, where regions of MTR reduction tend to extend beyond regions of atrophy. MTR reduction in these areas may, in addition to axonal loss, also reflect a qualitative change in the atrophied tissues. This is likely to represent demyelination of remaining neuro-axonal tissue (Schmierer 2004), which is a common finding in pathological studies of the grey matter in MS (Geurts 2005), but other reversible processes such as oedema and inflammation may also contribute.

This raises the possibility that regions showing reduced MTR in the absence of atrophy are demonstrating reversible change, where irreversible neuro-axonal loss has not yet occurred. If this were the case, these regions would be vulnerable to atrophy in the future. Indeed, regions showing MTR reduction alone in our study in early PPMS are similar to regions showing atrophy in patients with advanced MS in

other studies (Prinster 2006, Chen 2004, Sailer 2003). Comparisons between heterogeneous studies must, however, be made with caution, and longitudinal studies are necessary to investigate this hypothesis.

4.4.1.4 Methodological considerations

There is debate surrounding the use of voxel-based analysis (Davatzikos 2004, Bookstein 2001), and in particular its application to quantitative data (Smith 2006, Jones 2005). In all voxel-based analyses, normalization of images into standard space necessitates a degree of interpolation, and images are then smoothed to render the data normal for statistical analysis. In addition, we co-registered MT and volume sequences which had different slice thicknesses. These aspects may have influenced our results by compromising accurate localization of abnormal regions, and by increasing the number of partial volume voxels, which contain other tissues along with grey matter, in the image.

In this study, we minimized registration biases by using an optimized technique, so that significant regions identified are clearly attributable to grey matter differences. In addition, we applied a very conservative threshold to our grey matter masks, so that only voxels with greater than 75% likelihood were included. This threshold minimized the effect of partial volume voxels containing CSF or white matter in addition to grey matter (which may alter the MTR measurement; see section 2.8.4.3) on the analysis, while still allowing the detection of atrophy. Although the combination of a conservative threshold (75%) and a relatively large smoothing kernel (12mm) may reduce the overall accuracy of the localization, using the threshold increases the certainty that the abnormal regions are situated in the grey matter. In addition, in order to confirm the anatomical position of the abnormal regions on the original images in native space, and to confirm that our findings were genuine, we performed a *post hoc* analysis on one of the abnormal regions. When the region was translated back into native space and applied to the original image, our results were confirmed; both qualitatively, by assessing the anatomical position of the region, and quantitatively, by confirming *post hoc* the significant difference in mean MTR values between patients and controls.

We used PD-weighted rather than T1-weighted MT sequences because T1 effects are known to affect the MTR (Finelli 1998, Hajnal 1992). However, poor grey-to-white matter contrast in PD-weighted sequences made it necessary to include the additional step of co-registering the MT sequence to the volume images to perform the segmentation accurately. For these images, this method is likely to produce more accurate results than direct normalization of MT images onto a template. Furthermore, in a recent study comparing automated segmentation methods, SPM was shown to have an accuracy advantage over FSL and Freesurfer, although SPM5 was tested rather than SPM2 as used in our study (Klauschen 2009). The intra-subject co-registration was optimized in this study by the use of a voxel-intensity registration measure known to work well for images of different contrasts, namely normalized mutual information (Studholme 1997).

4.4.2 Clinical correlations

4.4.2.1 Motor function

Correlations were present between clinical tests of disability and regions of MTR reduction within the motor network, suggesting that the local MTR reduction identified is contributing to the clinical status of the patient. However, the moderate nature of our associations suggests that damage in other areas, such as the white matter and spinal cord, may also be contributing to functional impairment.

PPMS tends to present with locomotor disability (Sailer 2003), and this was the most common presentation in our cohort. There is some indication that damage to the motor cortex occurs later in other types of MS (Sailer 2003). Localized damage in the somato-sensory, but not the motor, cortex, is apparently greater in SP compared to RRMS, and greater in SP than in PPMS (Ceccarelli 2008). This suggests that differences in symptom prevalence between disease subtypes may, in part, reflect differential patterns of cortical predilection.

4.4.2.2 Cognition

MTR in regions in the right inferior parietal cortex and right inferior occipital gyrus showed a correlation with PASAT scores, suggesting that damage to these areas

reduced ability to perform the task. There was a trend to correlation with MTR in the left superior frontal gyrus (left lateral prefrontal cortex BA9 and BA 46), which has been identified in a number of functional MRI studies as a key functional area for the PASAT test (Forn 2006, Audoin 2005, Mainero 2004). However, damage to other areas known to be active during PASAT testing did not correspond with lower PASAT scores (middle frontal gyrus [BA 44] and superior temporal gyrus [BA 42 and 22], medial occipital cortex [BA 17]). Notably, these areas were identified in patients with RRMS (Forn 2006, Mainero 2004), and specific combined MT and fMRI studies would be necessary to confirm which areas are functionally relevant during PASAT testing in our own cohort. Furthermore, correlations between MTR in these regions and PASAT scores may be weak because damage in other brain areas, such as the white matter, makes an important contribution to cognitive impairment. The findings of a recent study in RRMS, which identified a relationship between localized peri-ventricular atrophy and PASAT performance (Jasperse 2007), lends some support to this hypothesis.

4.5 Conclusions

This study demonstrates that areas of grey matter damage, reflected by MTR reduction and atrophy, can be localized to specific sites of predilection early in the course of PPMS. Localized regions of MT change are more widespread than localized regions of atrophy, and the two measures may provide complementary information. Clinically, localized MT reduction is expressed as disability in the systems related to the damaged areas.

References

1. Aron AR, Robbins TW, Poldrack RA. Inhibition and the right inferior frontal cortex. *Trends Cogn Sci.* 2004; 8: 170-177.
2. Ashburner J, Friston K. Multimodal image coregistration and partitioning--a unified framework. *Neuroimage.* 1997; 6: 209-217.
3. Audoin B, Ibarrola D, Au Duong MV *et al.* Functional MRI study of PASAT in normal subjects. *MAGMA.* 2005; 18: 96-102.
4. Audoin B, Ibarrola D, Ranjeva JP *et al.* Compensatory cortical activation observed by fMRI during a cognitive task at the earliest stage of MS. *Hum.Brain Mapp.* 2003; 20: 51-58.
5. Audoin B, Ranjeva JP, Au Duong MV *et al.* Voxel-based analysis of MTR images: a method to locate gray matter abnormalities in patients at the earliest stage of multiple sclerosis. *J.Magn Reson.Imaging* 2004; 20: 765-771.
6. Behrens TE, Johansen-Berg H, Woolrich MW *et al.* Non-invasive mapping of connections between human thalamus and cortex using diffusion imaging. *Nat.Neurosci.* 2003; 6: 750-757.
7. Bookstein FL. "Voxel-based morphometry" should not be used with imperfectly registered images. *Neuroimage.* 2001; 14: 1454-1462.
8. Brownell B, Hughes JT. The distribution of plaques in the cerebrum in multiple sclerosis. *J.Neurol.Neurosurg.Psychiatry* 1962; 25: 315-320.
9. Ceccarelli A, Rocca MA, Pagani E *et al.* A voxel-based morphometry study of grey matter loss in MS patients with different clinical phenotypes. *Neuroimage* 2008; 42: 315-322.
10. Charil A, Dagher A, Lerch JP, Zijdenbos AP, Worsley KJ, Evans AC. Focal cortical atrophy in multiple sclerosis: Relation to lesion load and disability. *Neuroimage.* 2007; 34: 509-517.
11. Chen JT, Narayanan S, Collins DL, Smith SM, Matthews PM, Arnold DL. Relating neocortical pathology to disability progression in multiple sclerosis using MRI. *Neuroimage.* 2004; 23: 1168-1175.
12. Cutter GR, Baier ML, Rudick RA *et al.* Development of a multiple sclerosis functional composite as a clinical trial outcome measure. *Brain* 1999; 122 (Pt 5): 871-882.
13. Davatzikos C. Why voxel-based morphometric analysis should be used with great caution when characterizing group differences. *Neuroimage.* 2004; 23: 17-20.
14. Derache N, Marie RM, Constans JM, Defer GL. Reduced thalamic and cerebellar rest metabolism in relapsing-remitting multiple sclerosis, a positron emission tomography study: correlations to lesion load. *J.Neurol.Sci.* 2006; 245: 103-109.
15. Di Perri C, Battaglini M, Stromillo ML *et al.* Voxel-based assessment of differences in damage and distribution of white matter lesions between patients with primary progressive and relapsing-remitting multiple sclerosis. *Arch Neurol* 2008; 65: 236-243.
16. Filippi M. MRI-clinical correlations in the primary progressive course of MS: new insights into the disease pathophysiology from the application of magnetization transfer, diffusion tensor, and functional MRI. *J Neurol Sci* 2003; 206: 157-164.

17. Finelli DA, Reed DR. Flip angle dependence of experimentally determined T1sat and apparent magnetization transfer rate constants. *J.Magn Reson.Imaging* 1998; 8: 548-553.
18. Forn C, Barros-Loscertales A, Escudero J *et al.* Cortical reorganization during PASAT task in MS patients with preserved working memory functions. *Neuroimage*. 2006; 31: 686-691.
19. Geurts JJ, Bo L, Pouwels PJ, Castelijns JA, Polman CH, Barkhof F. Cortical lesions in multiple sclerosis: combined postmortem MR imaging and histopathology. *AJNR Am.J.Neuroradiol.* 2005; 26: 572-577.
20. Geurts JJ, Reuling IE, Vrenken H *et al.* MR spectroscopic evidence for thalamic and hippocampal, but not cortical, damage in multiple sclerosis. *Magn Reson.Med.* 2006; 55: 478-483.
21. Good CD, Johnsrude IS, Ashburner J, Henson RN, Friston KJ, Frackowiak RS. A voxel-based morphometric study of ageing in 465 normal adult human brains. *Neuroimage*. 2001; 14: 21-36.
22. Hajnal JV, Baudouin CJ, Oatridge A, Young IR, Bydder GM. Design and implementation of magnetization transfer pulse sequences for clinical use. *J.Comput.Assist.Tomogr.* 1992; 16: 7-18.
23. Henry RG, Shieh M, Okuda DT, Evangelista A, Gorno-Tempini ML, Pelletier D. Regional grey matter atrophy in clinically isolated syndromes at presentation. *J.Neurol.Neurosurg.Psychiatry* 2008; 79: 1236-1244.
24. Jasperse B, Vrenken H, Sanz-Arigita E *et al.* Regional brain atrophy development is related to specific aspects of clinical dysfunction in multiple sclerosis. *Neuroimage* 2007; 38: 529-537.
25. Jones DK, Symms MR, Cercignani M, Howard RJ. The effect of filter size on VBM analyses of DT-MRI data. *Neuroimage*. 2005; 26: 546-554.
26. Klauschen F, Goldman A, Barra V, Meyer-Lindenberg A, Lundervold A. Evaluation of automated brain MR image segmentation and volumetry methods. *Hum.Brain Mapp.* 2009; 30: 1310-1327.
27. Koeda M, Takahashi H, Yahata N, Asai K, Okubo Y, Tanaka H. A functional MRI study: cerebral laterality for lexical-semantic processing and human voice perception. *AJNR Am.J.Neuroradiol.* 2006; 27: 1472-1479.
28. Mainero C, Caramia F, Pozzilli C *et al.* fMRI evidence of brain reorganization during attention and memory tasks in multiple sclerosis. *Neuroimage*. 2004; 21: 858-867.
29. Mesaros S, Rocca MA, Absinta M *et al.* Evidence of thalamic gray matter loss in pediatric multiple sclerosis. *Neurology* 2008; 70: 1107-1112.
30. Prinster A, Quarantelli M, Orefice G *et al.* Grey matter loss in relapsing-remitting multiple sclerosis: a voxel-based morphometry study. *Neuroimage*. 2006; 29: 859-867.
31. Sailer M, Fischl B, Salat D *et al.* Focal thinning of the cerebral cortex in multiple sclerosis. *Brain* 2003; 126: 1734-1744.
32. Schmierer K, Scaravilli F, Altmann DR, Barker GJ, Miller DH. Magnetization transfer ratio and myelin in postmortem multiple sclerosis brain. *Ann.Neurol.* 2004; 56: 407-415.
33. Sepulcre J, Sastre-Garriga J, Cercignani M, Ingle GT, Miller DH, Thompson AJ. Regional gray matter atrophy in early primary progressive multiple sclerosis: a voxel-based morphometry study. *Arch Neurol* 2006; 63: 1175-1180.

34. Smith SM, Jenkinson M, Johansen-Berg H *et al.* Tract-based spatial statistics: voxelwise analysis of multi-subject diffusion data. *Neuroimage*. 2006; 31: 1487-1505.
35. Sommer M, Koch MA, Paulus W, Weiller C, Buchel C. Disconnection of speech-relevant brain areas in persistent developmental stuttering. *Lancet* 2002; 360: 380-383.
36. Studholme C, Hill DL, Hawkes DJ. Automated three-dimensional registration of magnetic resonance and positron emission tomography brain images by multiresolution optimization of voxel similarity measures. *Med.Phys.* 1997; 24: 25-35.
37. Thompson AJ, Montalban X, Barkhof F *et al.* Diagnostic criteria for primary progressive multiple sclerosis: a position paper. *Ann.Neurol.* 2000; 47: 831-835.
38. Toyoshima K, Sakai H. Exact cortical extent of the origin of the corticospinal tract (CST) and the quantitative contribution to the CST in different cytoarchitectonic areas. A study with horseradish peroxidase in the monkey. *J.Hirnforsch.* 1982; 23: 257-269.

**Enhancing Lesions:
The role of inflammation in early PPMS**

CHAPTER 5

5.1 Introduction

The concept that primary progressive multiple sclerosis (PPMS) may be pathologically distinct from other MS subtypes gained momentum in the late 1980's, when its characteristic MRI features were first described (Thompson 1990). Fewer and smaller lesions, demonstrating relatively little enhancement with gadolinium-DTPA (gadolinium-diethylenetriaminepentaacetic acid) were seen in PPMS (Thompson 1991). *Post-mortem* investigations have since confirmed a relative paucity of inflammation in PPMS lesions. In comparison to SPMS, fewer perivascular cuffs, reduced parenchymal cellularity (Revesz 1994), and a relative reduction in T and B cell infiltrates have been described (Magliozzi 2007, Lucchinetti 2004). Furthermore, there are relatively few active lesions in PPMS; instead established lesions show a tendency to radial expansion (Kutzelnigg, Prineas Annals 2001). Radiological studies have demonstrated that this expansion is largely responsible for increases in T2 lesion load (Stevenson 2002).

It was therefore somewhat surprising that, in a subgroup of our cohort with early PPMS, 42% had at least one enhancing lesion at baseline after administration of triple dose (0.3mmol/kg) gadolinium (Ingle 2005). This is three times the percentage of patients demonstrating enhancement in the PROMiSe trial (Wolinsky 2004), although single dose gadolinium was used in the latter study. This raised the possibility of an early enhancing phase in PPMS, a finding which may have therapeutic implications. In addition, the patients with enhancement were more disabled, with a higher T2 lesion load and reduced partial brain volume, compared to those without enhancing lesions. This raises the possibility that enhancement is a poor prognostic feature.

In this study we followed patients with early PPMS over five years, to investigate whether they continued to show the same level of enhancement. We also investigated whether enhancement influenced clinical progression, or correlated with changes in MRI markers over this period.

5.2 Methods

5.2.1 Subjects

As described in section 3.1.2.1, fifty patients fulfilling the diagnostic criteria for definite or probable PPMS (Thompson 2000), within five years of symptom onset, were invited to attend for clinical assessment and scanning every six months for three years, and again at five years. The clinical assessment involved neurological examination and scoring on Kurtzke's Expanded Disability Status Scale (EDSS) (Kurtzke 1983) and multiple sclerosis functional composite (MSFC) (Cutter 1999) at each time-point. The scanning protocol is described below. Five patients were excluded from the study: two patients declined gadolinium injections, two patients were taking regular courses of oral steroids prescribed by their GPs, and one patient died during the first year of the study. Thus 45 patients were included in this study (28 male, 17 female, mean age 44.2 years, range 19-65 years). Median EDSS was 4.5 (range 1.5-7) at the start of the study, with mean disease duration of 3.4 years (range 2-5 years). The number of patients attending each study time-point is given in Table 5.A. During the study some patients became too disabled to undergo scanning or no longer felt able to attend our centre, and one became claustrophobic. In addition, three patients were unable to undergo gadolinium injections because the normality of their renal function could not be established prior to the scan. In these cases we obtained EDSS data in person if possible, or using a telephone interview (Lechner-Scott 2003). Patients taking short courses of disease modifying or anti-inflammatory medications were excluded from the analysis at that time-point (see Table 5.A). A total of 38 patients (24 male, 14 female, mean age 44.4 years, range 19-63) completed the study.

Table 5A Patients attending at each time-point

Time-point (months)	0	6	12	18	24	30	36	60
Total patients assessed:	45	38	34	33	34	29	40	38
Patients given gadolinium	45	37	32	31	28	25	30	19
Patients with clinical assessment only	0	1	2	2	6	4	10	19
Patients who did not attend:	0	7	11	12	11	16	5	7
Withdrew from study	0	1	1	1	1	2	2	2
Personal commitments	0	5	7	7	7	8	0	0
Non-MS related illness	0	1	2	3	3	5	1	1
Upgrade	0	0	1	1	0	0	0	0
Death	0	0	0	0	0	0	1	1
Could not be contacted	0	0	0	0	0	1	0	2
Drugs	0	0	0	0	0	0	1	1

Personal Commitments= patients were unable to arrange an appointment during the six month period due to personal commitments, eg work, holiday and family commitments. *Upgrade*= scanner undergoing upgrade during this time-point. *Drugs*= patients taking drugs which affect gadolinium enhancing lesions (the patient excluded at 36 months had intra-venous steroids within 6 weeks of the scan, the patient excluded at 60 months was being treated with mitoxantrone for rapid clinical deterioration with superimposed relapses unresponsive to steroids). Patients had a clinical assessment only if they were unable to attend the centre, or if their renal function was not proven to be normal.

5.2.2 MRI Acquisition

All scans were performed on a 1.5 Tesla GE Signa scanner (General Electric Co, Milwaukee, Wisconsin, USA). The mean and median times between scans for each six-month time-point were 26.7 and 26.5 weeks respectively (range 25.3-29.0 weeks), and between the three and five year time point were 101.2 and 100 weeks (range 46.7 to 166.3 weeks). The scanner was upgraded during the study, and the gradient amplifiers, but not the gradient coils, were changed. Maximum gradient strength increased from 22mTm^{-1} to 33mTm^{-1} . The scanner software was upgraded from SIGNA version 5x to version 11x. At each time-point imaging of the brain and spinal cord was carried out as follows:

1. Axial T1-weighted spin echo sequences of the brain were acquired before and after injection of triple dose gadolinium-DTPA (0.3mmol/kg). The acquisition comprised 28 contiguous slices of 5mm thickness, with a repetition time (TR) of 540ms, and an echo time (TE) of 20ms, field of view (FOV) 240 x 240, number of excitations (NEX)=1. Sagittal T1-weighted spin echo images of the spine were also acquired before and after gadolinium injection, with a slice thickness of 3mm TE of 18ms, TR of 500ms, FOV 48x24, NEX=3. Parameters were not changed after the upgrade.
2. T2-weighted images were acquired as described in section 3.2.2.2, as part of the MTI sequence (Barker 1996). Parameters were not changed after the upgrade.
3. 3D inversion-prepared fast spoiled gradient recall (3D FSPGR) sequence of the brain was acquired as described in section 3.2.2.2. After the upgrade the TR was reduced to 10.9 ms.

5.2.3 MRI post-processing

Gadolinium enhancing lesions were identified, marked and counted on hard copies of the T1 -weighted images, by an experienced neuro-radiologist blinded to the clinical details of the patients.

Images were displayed on a Sun workstation (Sun Microsystems, Mountain View, CA) using Displmage software (Plummer 1992). Calculation of the T2-weighted lesion load and segmentation of the FSPGR images was carried out as described in section 3.2.2.3, for images from baseline to three years.

5.2.4 Statistical Analysis

Analysis was carried out using Stata (<http://www.stata.com>).

Statistical significance is reported at the 5% level.

5.2.4.1 Clinical data

We converted the change in EDSS scores into step changes as described in section 3.1.2.4.1. Z-scores (z) were derived for the MSFC subtests using our own baseline sample as reference, and used to calculate the MSFC. Patients who were too disabled to complete the TWT and NHPT were initially given a score for the maximum time allowed (see section 3.1.2.4.1) but the statistical models were invalidated because the data was no longer normally distributed. They were therefore excluded from the analysis, and full details of this subgroup are given in Table 5.B.

5.2.4.2 Gadolinium measures

As in the PROMiSe trial (Wolinsky 2007), we examined the number of gadolinium enhancing lesions rather than the gadolinium lesion load, a measure easily applicable in a clinical setting. In PPMS lesions tend to be smaller (Thompson 1991) and the lesion number is likely to reflect lesion load. We formulated the following measures, which were entered one by one into the models described below: Baseline measures (number of enhancing lesions, binary enhancement

status measure [ie. enhancing/non-enhancing], categories of enhancement [0, 1-3, or > 3 enhancing lesions]); Early changes (change in number of enhancing lesions from baseline to six months, change in number of enhancing lesions from baseline to one year); Overall changes at three and five years (total number of enhancing lesions, overall binary enhancement status [enhancing/non-enhancing], categories of enhancement [<3, 3-9 or >9 enhancing lesions], percentage of time-points with enhancing lesions for each subject).

5.2.4.3 Changes in MRI parameters over five years

To model the change in the percentage of patients with enhancing lesions at each study time-point, we used a mixed effect logistic model with the binary enhancement variable as the response variable and months from study entry as predictor. This allows estimation of the reduction in odds of enhancement per month. We included a quadratic term in time to assess the linearity of the data. To ensure that the upgrade had not altered the detection of enhancing lesions we compared the number of enhancing lesions in pre- and post- upgrade groups at each time-point using unpaired 2-tailed t-tests. The calculation of volume and T2 lesion changes over three years, using piecewise mixed effect linear regression models adjusting for the upgrade, are described in detail in section 3.2.2.4.2.

5.2.4.4 Predicting clinical changes over three and five years

We compared clinical outcome between patients with spinal cord and other presentations using Mann-Whitney U tests (for EDSS changes) and t-tests (for the MSFC and subtests). First we examined clinical changes over three years, and then over five years. To identify predictors of EDSS change over three and five years, ordinal logistic regression was carried out with EDSS change as the response variable. Each enhancing lesion parameter was tested as a covariate in turn, and the model was adjusted for age and T2 lesion volume at baseline. For changes in MSFC and its subtests, a multiple linear regression was carried out with the change in the MSFC and each subtest in turn as the dependent variable, using the same covariates as for the EDSS.

5.2.4.5 Correlates of MRI change over three years

Using multiple linear regression, changes in grey and NAWM volume were modeled in turn as the response variable. The enhancing lesion parameters were introduced in turn, with age, upgrade, T2 lesion load and interaction terms with time as covariates, in order to investigate their effect on the rate of volume change. As described in section 3.2.2.4, this model adjusts for any gradient discontinuity due to the upgrade. The model was repeated with T2 lesion load as the response variable rather than a covariate.

The analyses were run using data on enhancing lesions in the brain only, then rerun using data on both the brain and spinal cord.

5.3 Results

5.3.1 Clinical progression

Clinical progression was evident over three and five years on the EDSS, TWT and NHPT (see Table 5.2). The PASAT test showed significant improvement, probably due to practice effects, which affected the MSFC (section 3.1.4.1). For this reason the PASAT and MSFC data were considered flawed. However, we present results on the NHPT and TWT subtests. There was no difference in progression between the 35 patients presenting with a spinal cord syndrome, and the 10 presenting with deficits in other systems.

Table 5.B Clinical tests at baseline, three and five years, with separate data on the subgroup completing all tests and study time-points

Clinical test		Baseline	3 years	p*	5years	p**
Median EDSS (range)	All	4.5 (1.5-7) n=45	6 (1.5-9) n=41	<0.001	6.5 (2-9) n=38	<0.001
	Pts with 5 year EDSS data	4.25 (1.5-7) n=38	6 (1.5-9) n=38	<0.001	6.5 (2-9) n=38	<0.001
Mean MSFC (SD)	All	0.02 (0.7) n=42	0.14 (0.8) n=30	0.52	0.001 (1.2) n=18	0.11
	Pts with 5 year data able to complete all MSFC subtests	0.51 (0.4) n=14	0.60 (0.3) n=14	0.34	0.56(0.4) n=14	0.55
Mean TWT in seconds (SD)	All	20.2 (37.8) n=44	35.8 (61.1) n=34	0.02	57.6(77.3) n=22	0.06
	Pts with 5 year data able to complete TWT	7.0 (2.1) n=16	8.6(4.7) n=16	0.05	11.7(11.1) n=16	0.28
Mean NHPT in seconds (SD)	All	38.0 (33.4) n=45	53.9 (63.5) n=34	0.01	50.1(64.6) n=21	0.01
	Pts with 5 year data able to complete NHPT	25.9 (5.4) n=20	33.7 (30.9) n=19	0.28	37.6(30.6) n=20	0.01
Mean PASAT score (SD)	All	41.6 (13.2) n=43	46.8 (14.2) n=32	0.06	47.2(16.6) n=21	0.90
	Pts with 5 year PASAT data	43.1 (12.3) n=21	49.4 (12.1) n=20	0.002	47.2(16.6) n=21	0.90

Pts with 5 year data= the subgroup of patients who attended at five years. *Pts with 5 year data able to complete test*= the subgroup of patients who attended at five years and were not too disabled to complete the test. *EDSS*= *expanded disability status scale*, obtained in person or by telephone, *NHPT*= *Nine Hole Peg Test*, *TWT*= *Timed Walk Test*, *PASAT*= *Paced Auditory Serial Addition Test* (maximum score=60). *SD*= *standard deviation*. p*= p value from Mann-Whitney U (EDSS) and t-tests comparing baseline and three year scores. p**= p value from Mann-Whitney U (EDSS) and t-tests comparing three year and five year scores

5.3.2 The proportion of patients with enhancing lesions decreased over five years

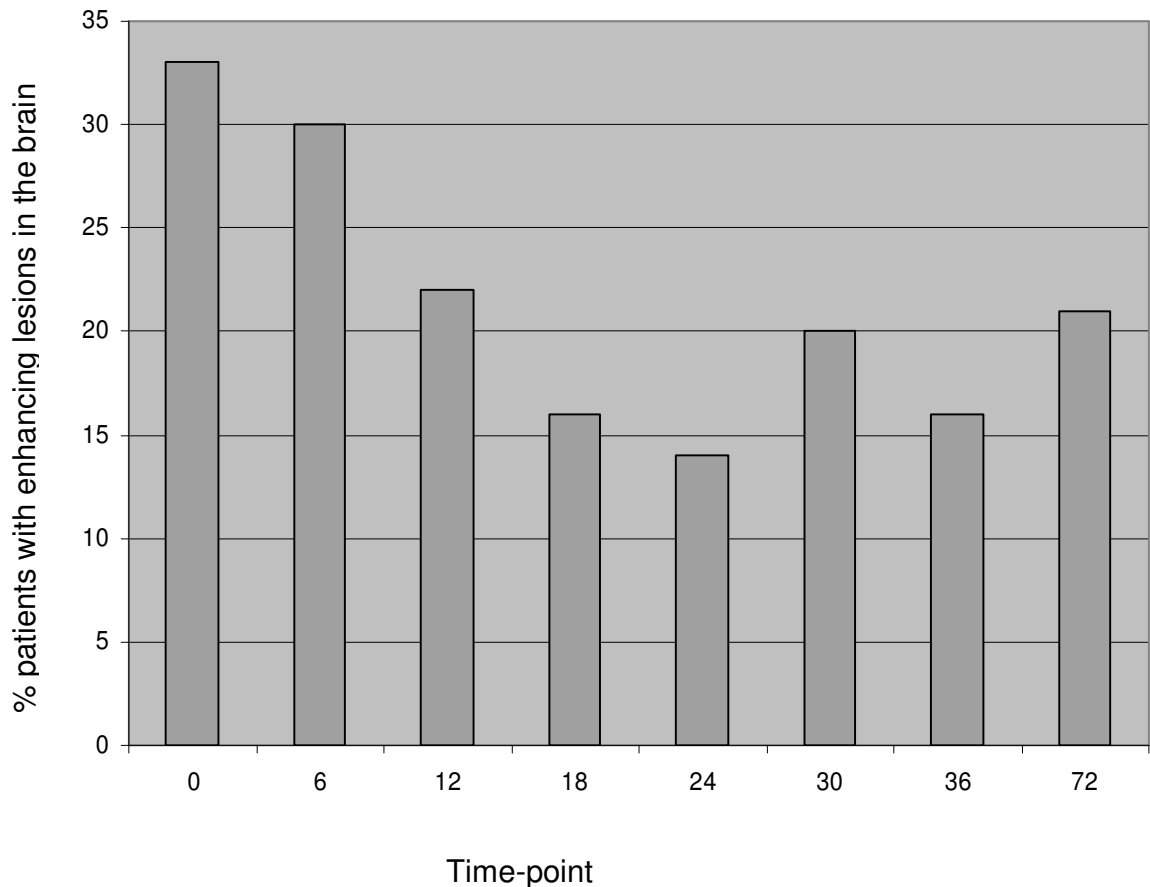
In the group as a whole over five years, the *percentage* of patients with enhancing lesions in the brain and spinal cord declined significantly over five years ($p=0.03$). The significant quadratic term in time ($p=0.046$) suggests that most of this decline occurred early on; a decreasing decline over time, with eventual leveling off, is demonstrated (see Figure 5a). However, in individual patients, both increases and decreases were observed in the number of enhancing lesions at each time-point (see Table 5C).

In total, 24 patients demonstrated enhancement in either the brain or cord at one or more time-points (see Table 5C for the number of patients with enhancing lesions at each time-point), and 21 patients (47%) had no enhancing lesions. Five patients showed enhancing lesions in the brain or spinal cord for the first time at six months, one at twelve months, two at eighteen months, two at three years, and one at five years. Out of a total of 369 enhancing lesions seen over five years, only 19 were spinal cord lesions, seen in eight different patients. The inclusion of the spinal cord lesions in the statistics did not alter the results, and as this additional parameter conferred no benefit we present the results using enhancing brain lesion parameters only. The number of enhancing lesions detected was not affected by the upgrade.

Table 5.C The frequency of each number of enhancing lesions identified in the brain and spinal cord at each time-point

Number of Enhancing Lesions	Time-point							
	0	6	12	18	24	30	36	60
0	30	23	24	25	24	20	24	14
1	4	7	3	4	0	2	3	3
2	4	2	0	0	1	0	1	0
3	1	0	0	0	0	0	0	1
4	2	1	0	0	2	1	0	0
5	0	0	1	1	0	0	0	0
6	2	1	1	0	0	1	0	0
7	1	0	1	0	0	0	0	0
8	0	0	0	0	1	0	1	0
9	0	0	1	0	0	0	0	0
10	0	1	0	0	0	1	0	0
11	0	0	0	0	0	0	1	0
14	1	0	0	0	0	0	0	0
22	0	1	0	0	0	0	0	1
26	0	1	0	0	0	0	0	0
43	0	0	0	1	0	0	0	0
60	0	0	1	0	0	0	0	0
Total with enhancement	15	14	8	6	4	5	6	5
Total imaged	45	37	32	31	28	25	30	19

Figure 5a: Percentage of patients with gadolinium enhancing lesions at each time-point



5.3.3 Enhancing lesions were modestly related to clinical progression

Progression on the EDSS over three years was predicted by the number of gadolinium enhancing lesions at baseline ($p=0.01$, OR 1.32, 95%CI 1.06-1.64), and greater increase in the number of enhancing lesions over the first year ($p=0.047$, OR 1.08, 95%CI 1.00-1.16) but this did not survive adjustment for T2 lesion load. Progression on the EDSS over five years was predicted by the number of gadolinium enhancing lesions at baseline ($p=0.02$, OR 1.28, 95%CI 1.04-1.58), but this did not survive adjustment for T2 lesion load. EDSS increase over three

and five years correlated inversely with age ($p < 0.05$), and positively with T2 lesion load at baseline ($p = 0.008$).

Changes in NHPT score over three and five years, and in TWT score over three years, were not predicted by enhancing lesion parameters. Reducing mobility on the TWT over five years was predicted by the number of enhancing lesions at baseline ($p = 0.02$, coefficient 0.03, 95%CI 0.006 to 0.05, $r^2 = 0.64$), and increase in enhancing lesion number at 6 months ($p = 0.02$, coefficient 0.004, 95%CI 0.0008 to 0.008, $r^2 = 0.64$) and one year ($p = 0.046$, coefficient 0.02, 95%CI 0.0004 to 0.04, $r^2 = 0.70$), after correction for age and T2 lesion load. There was an inverse correlation with age ($p = 0.04$).

5.3.4 Enhancing lesions were related to T2 lesion load increase but not atrophy

Increase in T2 lesion load over three years correlated with an increase in the number of enhancing lesions over one year after adjusting for age ($p = 0.048$, coefficient 2.18 95%CI 0.024 to 4.34, $r^2 = 0.21$). Grey and NAWM volume decrease was not associated with clinical presentation, age or enhancing lesion parameters.

5.5 Discussion

We report a decline of the initially substantial level of lesion enhancement in patients with early PPMS over five years. The level of enhancement towards the end of the study (16-21%) is very slightly higher than that found in patients with longer disease duration using single dose gadolinium (14%) (Wolinsky 2004). This may suggest that there is an early inflammatory phase in a subgroup of patients with PPMS. Conversely, almost half of our cohort never showed enhancement, and few patients developed enhancement during the study. This may reflect a spectrum of activity in PPMS, in which reported cases of 'pure' PPMS – clinically progressive patients without focal lesions (Zwemmer 2008)- lie at one extreme. Alternatively, the non-enhancing patients in our study may have demonstrated enhancement if scanned more frequently (Tortorella 1999) or earlier; lesion activity may occur long before symptom onset in PPMS (McDonnell 2003). Furthermore, advancing age

may have influenced the reduction in lesion activity in our cohort, as observed in RRMS (Tortorella 2005). Indeed, we found more gradual disability accumulation and T2 lesion load increase in older patients.

Active inflammation had only a small impact on future disability in this group. The concept of an early inflammatory phase in PPMS raises the possibility of benefit from disease modifying treatments in a subgroup, if given early enough in the disease course. In the interferon and mitoxantrone studies in PPMS, gadolinium was not administered (Montalban 2004, Stuve 2004, Leary 2003). In the glatiramer acetate study, treated patients showed a reduction in gadolinium enhancing lesions in the first year, but this was not sustained over three years and did not affect progression. Mean disease duration in this study was double that in our cohort (Wolinsky 2007), but data from other MS subtypes also cautions against over-anticipating the long term benefits of treatments targeting inflammation. Even in RRMS, where enhancement levels correlate more directly with clinical activity (Kappos 1999, Barkhof 1992), natural history studies suggest that disability accrual is 'amnesic' and disregards early relapse history (Confavreux 2006). Furthermore, treatments which limit relapse activity and the development of enhancing lesions have not affected the progression of disability in SPMS (Giovannoni 2004).

Regarding brain atrophy, suppression of gadolinium enhancing lesions in clinical trials has also had minimal impact on this measure (Inglese 2004). In our study, the level of lesion enhancement failed to predict atrophy, as it has in other MS subtypes (Rashid 2007, Inglese 2005, Zivadinov 2002). However, it may also be the case that the relationship between focal lesion activity and eventual brain atrophy becomes apparent only after lengthy follow-up.

It should be noted when interpreting this data that triple dose gadolinium was administered. RRMS studies suggest that additional lesions detected with triple dose gadolinium are less destructive than those already visible with single dose (Rovaris 1999), and it may be that the detection of 'extra' lesions complicates the relationship between enhancement and disability. The relevance of this remains unclear in PPMS, because the increased sensitivity using triple dose gadolinium

has not been consistently demonstrated. A study involving ten patients with PPMS (Filippi 1995) identified four enhancing lesions in two patients; following a triple dose of gadolinium in the same group, 13 enhancing lesions were seen in five patients. The patients had a mean disease duration of 6.5 years. In contrast, in 16 patients with PPMS examined as part of a larger group, no increase in enhancing lesion number was found using triple rather than single dose gadolinium (Silver 1997). Of note, only two enhancing lesions were identified in these patients, who had a mean disease duration of nine years. Both studies were small, and it is difficult to draw firm conclusions from them. Furthermore, gadolinium enhancement may be a more non-specific and less sensitive measure of blood-brain-barrier (BBB) breakdown than previously appreciated. A study measuring T1-relaxation time in post contrast scans in patients with RR and SPMS, found gadolinium leakage in chronic inactive non-enhancing lesions, particularly smaller lesions and those which persisted as T1 black holes (Soon 2007). Pathological studies have reported ongoing BBB leakage in inactive plaques in PPMS, suggestive of defective repair. Interestingly, persistent endothelial abnormalities in grey and NAWM have also been demonstrated in PPMS (Leech 2007). Newer MRI techniques, such as the ultra-small iron oxide particle (USPIO) enhancement, a putative marker of cellular infiltration, may provide complementary information not available from gadolinium images (Vellinga 2008, Dousset 2006). These findings indicate that BBB dysfunction is more extensive and complicated than previously appreciated, and may partly explain the poor correlation between gadolinium enhancement and irreversible disability.

The clinical correlations identified in this group were weak. While the TWT in the subgroup still walking at five years was predicted by early gadolinium enhancement independently of T2 lesion volume, this was not yet evident at three years. Progression on the EDSS was predicted by early enhancing lesion parameters, but this effect did not survive adjustment for T2 lesion load. Nonetheless, this does indicate that enhancing lesion parameters give some prediction of EDSS outcome, and enhancing lesion numbers may be a more useful clinical tool than overall T2 lesion volume. Furthermore, as enhancing lesions are a

subset of T2 lesions, adjusting the analysis for T2 lesion volume may have introduced considerable Type II error.

This study was limited by the number of patients unable to undergo gadolinium injection at later time-points, particularly as they were the most disabled patients. This may have caused a selection bias by artificially reducing the proportion of patients demonstrating enhancement later in the study, and results should be interpreted with caution. However, these considerations did not affect the predictive part of the analysis, as clinical data was obtained on most patients at five years.

5.6 Conclusions

Our findings indicate a decline in active lesions over five years, suggesting that there is an early inflammatory phase in a subgroup of patients with early PPMS. Lesion activity has some influence on clinical progression in the medium term.

References

1. Barker GJ, Tofts PS, Gass A. An interleaved sequence for accurate and reproducible clinical measurement of magnetization transfer ratio. *Magn Reson.Imaging* 1996; 14: 403-411.
2. Barkhof F, Scheltens P, Frequin ST *et al.* Relapsing-remitting multiple sclerosis: sequential enhanced MR imaging vs clinical findings in determining disease activity. *AJR Am J Roentgenol* 1992; 159: 1041-1047.
3. Confavreux C, Vukusic S. Accumulation of irreversible disability in multiple sclerosis: from epidemiology to treatment. *Clin Neurol Neurosurg* 2006; 108: 327-332.
4. Cutter GR, Baier ML, Rudick RA *et al.* Development of a multiple sclerosis functional composite as a clinical trial outcome measure. *Brain* 1999; 122 (Pt 5): 871-882.
5. Dousset V, Brochet B, Deloire MS *et al.* MR imaging of relapsing multiple sclerosis patients using ultra-small-particle iron oxide and compared with gadolinium. *AJNR Am J Neuroradiol* 2006; 27: 1000-1005.
6. Filippi M, Campi A, Martinelli V *et al.* Comparison of triple dose versus standard dose gadolinium-DTPA for detection of MRI enhancing lesions in patients with primary progressive multiple sclerosis. *J Neurol Neurosurg Psychiatry* 1995; 59: 540-544.
7. Giovannoni G. Management of secondary-progressive multiple sclerosis. *CNS.Drugs* 2004; 18: 653-669.
8. Ingle GT, Sastre-Garriga J, Miller DH, Thompson AJ. Is inflammation important in early PPMS? a longitudinal MRI study. *J.Neurol.Neurosurg.Psychiatry* 2005; 76: 1255-1258.
9. Inglese M, Benedetti B, Filippi M. The relation between MRI measures of inflammation and neurodegeneration in multiple sclerosis. *J Neurol Sci* 2005; 233: 15-19.
10. Inglese M, Mancardi GL, Pagani E *et al.* Brain tissue loss occurs after suppression of enhancement in patients with multiple sclerosis treated with autologous haematopoietic stem cell transplantation. *J Neurol Neurosurg Psychiatry* 2004; 75: 643-644.
11. Kappos L, Moeri D, Radue EW *et al.* Predictive value of gadolinium-enhanced magnetic resonance imaging for relapse rate and changes in disability or impairment in multiple sclerosis: a meta-analysis. *Gadolinium MRI Meta-analysis Group. Lancet* 1999; 353: 964-969.
12. Kurtzke JF. Rating neurologic impairment in multiple sclerosis: an expanded disability status scale (EDSS). *Neurology* 1983; 33: 1444-1452.
13. Leary SM, Miller DH, Stevenson VL, Brex PA, Chard DT, Thompson AJ. Interferon beta-1a in primary progressive MS: an exploratory, randomized, controlled trial. *Neurology* 2003; 60: 44-51.
14. Lechner-Scott J, Kappos L, Hofman M *et al.* Can the Expanded Disability Status Scale be assessed by telephone? *Mult.Scler.* 2003; 9: 154-159.
15. Leech S, Kirk J, Plumb J, McQuaid S. Persistent endothelial abnormalities and blood-brain barrier leak in primary and secondary progressive multiple sclerosis. *Neuropathol Appl.Neurobiol.* 2007; 33: 86-98.
16. Lucchinetti C, Bruck W. The pathology of primary progressive multiple sclerosis. *Mult.Scler.* 2004; 10 Suppl 1: S23-S30.

17. Magliozzi R, Howell O, Vora A *et al.* Meningeal B-cell follicles in secondary progressive multiple sclerosis associate with early onset of disease and severe cortical pathology. *Brain* 2007; 130: 1089-1104.
18. McDonnell GV, Cabrera-Gomez J, Calne DB, Li DK, Oger J. Clinical presentation of primary progressive multiple sclerosis 10 years after the incidental finding of typical magnetic resonance imaging brain lesions: the subclinical stage of primary progressive multiple sclerosis may last 10 years. *Mult Scler* 2003; 9: 204-209.
19. Montalban X. Overview of European pilot study of interferon beta-1b in primary progressive multiple sclerosis. *Mult Scler* 2004; 10 Suppl 1: S62-S64.
20. Plummer D. Dispimage: a display and analysis tool for medical images. *Rev Neuroradiol* 1992; 5: 489-95.
21. Rashid W, Davies GR, Chard DT *et al.* Relationship of triple dose contrast enhanced lesions with clinical measures and brain atrophy in early relapsing-remitting multiple sclerosis: a two-year longitudinal study. *Mult Scler* 2007; 13: 178-185.
22. Revesz T, Kidd D, Thompson AJ, Barnard RO, McDonald WI. A comparison of the pathology of primary and secondary progressive multiple sclerosis. *Brain* 1994; 117 (Pt 4): 759-765.
23. Rovaris M, Mastrorlando G, Prandini F, Bastianello S, Comi G, Filippi M. Short-term evolution of new multiple sclerosis lesions enhancing on standard and triple dose gadolinium-enhanced brain MRI scans. *J Neurol Sci* 1999; 164: 148-152.
24. Silver NC, Good CD, Barker GJ *et al.* Sensitivity of contrast enhanced MRI in multiple sclerosis. Effects of gadolinium dose, magnetization transfer contrast and delayed imaging. *Brain* 1997; 120 (Pt 7): 1149-1161.
25. Soon D, Tozer DJ, Altmann DR, Tofts PS, Miller DH. Quantification of subtle blood-brain barrier disruption in non-enhancing lesions in multiple sclerosis: a study of disease and lesion subtypes. *Mult Scler* 2007; 13: 884-894.
26. Stevenson VL, Smith SM, Matthews PM, Miller DH, Thompson AJ. Monitoring disease activity and progression in primary progressive multiple sclerosis using MRI: sub-voxel registration to identify lesion changes and to detect cerebral atrophy. *J.Neurol.* 2002; 249: 171-177.
27. Stuve O, Kita M, Pelletier D *et al.* Mitoxantrone as a potential therapy for primary progressive multiple sclerosis. *Mult Scler* 2004; 10 Suppl 1: S58-S61.
28. Thompson AJ, Kermode AG, MacManus DG *et al.* Patterns of disease activity in multiple sclerosis: clinical and magnetic resonance imaging study. *BMJ* 1990; 300: 631-634.
29. Thompson AJ, Kermode AG, Wicks D *et al.* Major differences in the dynamics of primary and secondary progressive multiple sclerosis. *Ann.Neurol.* 1991; 29: 53-62.
30. Thompson AJ, Montalban X, Barkhof F *et al.* Diagnostic criteria for primary progressive multiple sclerosis: a position paper. *Ann.Neurol.* 2000; 47: 831-835.
31. Tortorella C, Bellacosa A, Paolicelli D *et al.* Age-related gadolinium-enhancement of MRI brain lesions in multiple sclerosis. *J Neurol Sci* 2005; 239: 95-99.
32. Tortorella C, Codella M, Rocca MA *et al.* Disease activity in multiple sclerosis studied by weekly triple-dose magnetic resonance imaging. *J Neurol* 1999; 246: 689-692.
33. Vellinga MM, Oude Engberink RD, Seewann A *et al.* Pluriformity of inflammation in multiple sclerosis shown by ultra-small iron oxide particle enhancement. *Brain* 2008; 131: 800-807.

34. Wolinsky JS. The PROMiSe trial: baseline data review and progress report. *Mult Scler* 2004; 10 Suppl 1: S65-S71.
35. Wolinsky JS, Narayana PA, O'Connor P *et al*. Glatiramer acetate in primary progressive multiple sclerosis: results of a multinational, multicenter, double-blind, placebo-controlled trial. *Ann.Neurol.* 2007; 61: 14-24.
36. Zivadinov R, Zorzon M. Is gadolinium enhancement predictive of the development of brain atrophy in multiple sclerosis? A review of the literature. *J Neuroimaging* 2002; 12: 302-309.
37. Zwemmer J, Bot J, Jelles B, Barkhof F, Polman C. At the heart of primary progressive multiple sclerosis: three cases with diffuse MRI abnormalities only. *Mult Scler* 2008; 14: 428-430.

Conclusions and Future Directions

Mechanisms and measures of progression

The mechanisms underlying clinical progression in PPMS are not clearly established. Our studies examine the evolution of brain injury in the early phase of PPMS *in vivo*, by measuring changes in brain volume, lesions and magnetization transfer ratio (MTR) over time. Our findings suggest that normal appearing white matter (NAWM) injury is already established, but remains relatively stable in early PPMS. Grey matter injury is evolving more quickly, and appears to be driving clinical progression in the medium term. Focal lesions and the level of lesion activity in the white matter continue to play a role in determining disability accrual.

These findings are relevant to inform therapeutic approaches, and suggest that the identification of neuro-protective agents is a priority. In addition, they provide data for clinical trials in PPMS, which have been limited by the uncertain evolution of the condition. Our results suggest that MTR, particularly in the grey matter, is a sensitive and responsive measure of brain injury in early PPMS, and that it is associated with clinical progression. Therefore, grey matter MTR may be a useful measure for selecting and monitoring patients for study in clinical trials in early PPMS, possibly in combination with T2 lesion measures. At present our MTR findings are applicable only to groups, and can not guide the care of individual patients. Studies in larger cohorts will be necessary to confirm our results, and to identify clinically applicable thresholds. Future work on our own cohort will aim to establish whether grey matter injury, reflected by MTR, continues to drive clinical progression over five years; whether irreversible grey matter damage, reflected by atrophy, becomes more closely related to concurrent clinical progression, and whether the clinical relevance of white matter damage declines over five years.

Spinal Cord Studies

Spinal cord pathology is likely to play an important role in disease progression in PPMS. In our study, the level of lesion activity in the spinal cord did not contribute significantly to progression, but the number of lesions observed was small. Measures of spinal cord atrophy may be a more suitable way to examine the impact of spinal cord injury on progression in early PPMS, and will be examined in a future study. Technical difficulties have previously hindered MRI studies in the spinal cord, but recent improvements in receiver coils and imaging speed have allowed the introduction of more sophisticated techniques (Bakshi 2008). Grey matter MTR has been used to detect clinically relevant cervical cord damage in patients with RRMS, in the absence of atrophy (Agosta 2007). Application of this technique in PPMS poses challenges, due to the presence of atrophy and partial volume effects, but a combination of MTR and atrophy measures in the grey matter could help to elucidate the mechanisms underlying progressive spastic paraparesis in early PPMS. High field *post mortem* MRI studies in the spinal cord have indicated that grey matter lesions are more readily detectable in the cord (Gilmore 2009). As high field MR becomes more widely applicable *in vivo*, the spinal cord may become a prime location for comparing the clinical relevance of grey matter lesions with changes in the normal appearing grey matter.

Understanding grey matter injury

Having demonstrated the importance of grey matter injury for progression in Chapter 3, in Chapter 4 we went on to identify sites of predilection for cortical and deep grey matter injury in early PPMS, for the first time. We developed a voxel-based technique which demonstrated that regions of localized MTR reduction were more widespread than regions of atrophy, but that significant atrophy was not present in the absence of MTR reduction. The focus of future work in this area will be on expanding our understanding of the processes evolving in this compartment over time, in terms of location, quantity and quality. We will apply voxel-based techniques longitudinally, to investigate the following questions: (1) Do potentially

reversible changes, reflected by MTR reduction, precede irreversible changes, reflected by tissue atrophy? To answer this question, it will be necessary to develop a technique which ensures accurate longitudinal intra-subject registration, but allows the detection of subtle changes in tissue MTR and volume over time (2) Are differences in early symptom prevalence between disease subtypes explained by different areas of cortical predilection? This will be investigated by comparing patients with early PPMS and early RRMS (3) Do longitudinal changes in specific localized areas of damage correlate more closely with clinical progression? If progression is found to be associated with damage in specific areas, it may help to explain the wide inter-subject variation in clinical course.

In order for this information to be fully exploited, better understanding of the pathological basis of grey matter MTR changes is needed. *Post mortem* studies combining imaging and histopathology are the best way to explore this further (Schmierer 2004), although the advanced disease duration of *post mortem* cases limits the relevance of these findings for early PPMS. *In vivo*, more specific analysis of the macromolecular proton pool is now possible using quantitative MT indices, which allow assessment of myelin content without the confounding T1 effects inherent in MTR measurements (Schmierer 2007). This may elucidate whether the grey matter changes we identified are primarily attributable to cortical demyelination. Our studies could be further enhanced by incorporating 3D double inversion recovery (DIR) sequences, which greatly improve cortical lesion detection, and may allow the segmentation of cortical lesions from relatively normal appearing areas of grey matter (Geurts 2008).

Finally, spectroscopic imaging allows the direct measurement of metabolites which act as markers for pathological processes. Comparing and combining spectroscopic and MTR measures within our cohort may help us to understand the balance between demyelination, axonal loss and gliosis occurring within the grey matter areas where MTR is reduced. In addition, combining these techniques with atrophy, T2 and T1 lesion measures within one cohort could guide us as to the

most useful MRI parameters, or combinations of parameters, for studying clinical progression (Mainero 2001).

Cognition

In assessing the impact of grey matter injury on progression, our studies have focussed on measures of physical disability. However, grey matter changes are likely to play a pivotal role in cognitive decline in MS, as evidenced by recent case reports describing a purely cortical form of MS, presenting with neurobehavioural symptoms (Zarei 2006). We would like to extend our studies to examine the relationship between MRI changes in our cohort and cognitive function, specifically whether grey matter parameters at baseline, or the gradient of their decline over three years, can determine cognitive outcomes.

Understanding White matter injury

Although the work presented in this thesis emphasizes the role of grey matter injury in progression, white matter injury was important early on in the study, and clearly maintained some influence on long term outcome. Recent studies have suggested that the position of white matter lesions may have an influence on clinical outcomes independent of lesion burden, and may vary between disease subtypes (Di Perri 2008). This would be an interesting area to explore in our cohort, as variation in lesion position may explain some of the wide inter-individual variability in outcome. Qualitative assessment of lesions using a combination of T1 and T2-weighted imaging with MTR may also provide a more comprehensive picture of the way in which pathological heterogeneity within white matter lesions affects disability (Fisher 2007). Damage to specific white matter tracts outside of lesions can be studied using tractography; given that we have identified areas of predilection for cortical damage, it would be fascinating to examine the white matter tracts directly associated with these areas, for example the cortico-spinal tracts. In addition, areas of NAWM damage can now be identified in the absence of an *a priori* hypothesis, using tract based spatial statistics (TBSS), which directly

complements our localization of grey matter damage using VBM. Combining grey and white matter techniques in this way would allow us to explore the longitudinal relationship between damage in the two compartments in PPMS.

References

1. Agosta F, Pagani E, Caputo D, Filippi M. Associations between cervical cord gray matter damage and disability in patients with multiple sclerosis. *Arch.Neurol.* 2007; 64: 1302-1305.
2. Bakshi R, Thompson AJ, Rocca MA *et al.* MRI in multiple sclerosis: current status and future prospects. *Lancet Neurol.* 2008; 7: 615-625.
3. Di Perri C, Battaglini M, Stromillo ML *et al.* Voxel-based assessment of differences in damage and distribution of white matter lesions between patients with primary progressive and relapsing-remitting multiple sclerosis. *Arch Neurol* 2008; 65: 236-243.
4. Fisher E, Chang A, Fox RJ *et al.* Imaging correlates of axonal swelling in chronic multiple sclerosis brains. *Ann.Neurol.* 2007; 62: 219-228.
5. Geurts JJ, Barkhof F. Grey matter pathology in multiple sclerosis. *Lancet Neurol.* 2008; 7: 841-851.
6. Gilmore C, Geurts J, Evangelou N *et al.* Spinal cord grey matter lesions in multiple sclerosis detected by post-mortem high field MR imaging. *Mult.Scler.* 2009; 15: 180-188.
7. Mainero C, De SN, Iannucci G *et al.* Correlates of MS disability assessed in vivo using aggregates of MR quantities. *Neurology* 2001; 56: 1331-1334.
8. Schmierer K, Scaravilli F, Altmann DR, Barker GJ, Miller DH. Magnetization transfer ratio and myelin in postmortem multiple sclerosis brain. *Ann.Neurol.* 2004; 56: 407-415.
9. Schmierer K, Tozer DJ, Scaravilli F *et al.* Quantitative magnetization transfer imaging in postmortem multiple sclerosis brain. *J.Magn Reson.Imaging* 2007; 26: 41-51.
10. Zarei M. Clinical characteristics of cortical multiple sclerosis. *J.Neurol.Sci.* 2006; 245: 53-58.